

2009

Salvinorin A: Fragment Synthesis and Modeling Studies

Donna McGovern

Virginia Commonwealth University

Follow this and additional works at: <http://scholarscompass.vcu.edu/etd>

 Part of the [Chemicals and Drugs Commons](#)

© The Author

Downloaded from

<http://scholarscompass.vcu.edu/etd/1862>

This Dissertation is brought to you for free and open access by the Graduate School at VCU Scholars Compass. It has been accepted for inclusion in Theses and Dissertations by an authorized administrator of VCU Scholars Compass. For more information, please contact libcompass@vcu.edu.

© Donna Lue McGovern 2009

All Rights Reserved

SALVINORIN A: FRAGMENT SYNTHESIS AND MODELING STUDIES

A dissertation submitted in partial fulfillment of the requirements for the degree of
Doctor of Philosophy at Virginia Commonwealth University.

by

DONNA LUE MCGOVERN

Bachelor of Science in Chemistry, Northern Michigan University, 1976
Master of Science in Organic Chemistry, Old Dominion University, 1978

Director: RICHARD B. WESTKAEMPER
PROFESSOR, DEPARTMENT OF MEDICINAL CHEMISTRY

Virginia Commonwealth University
Richmond, Virginia
August, 2009

Acknowledgements

I would like to thank my parents, Robert and Jeanne Crepeau, who supported me in my decision to pursue my PhD at this point in my life. I would also like to thank Dr. Srinivas Peddi for all his help in organic chemistry and Dr. Philip Mosier for all the time he spent mentoring me in molecular modeling techniques and reviewing my papers. Special thanks go to my fellow graduate student, Jitesh Shah, who encouraged me and who made life interesting in the lab. Lastly, I would like to thank my advisor, Dr. Richard Westkaemper, for supporting my work with tuition grants and for his guidance. Without his support, attainment of this degree would not have been possible.

Table of Contents

	Page
Acknowledgements.....	ii
List of Tables	v
List of Figures.....	vii
List of Schemes.....	ix
List of Abbreviations	x
Abstract.....	xii
Chapter	
1. Introduction.....	1
1.1 Background	1
1.2 Opioids and Opioid Receptors	5
1.3 Opioid Selectivity.....	13
1.4 General Concepts in Selectivity	13
1.5 Binding Energies	18
1.6 Structure-Affinity Relationships (SAFIR) of Salvinorin A Analogs	21
2. Salvinorin A Fragment Synthesis	25
2.1 Introduction	25
2.2 Experimental	31
2.3 Conclusion.....	34

3.	Homology Modeling of Opioid Receptors	35
3.1	Models Based on Bovine Rhodopsin	35
3.1.1.	Experimental	35
3.2.	Models Based on the β_2 Adrenergic Receptor.....	46
3.2.1.	Experimental	46
3.3	MODELLER Models	50
3.3.1.	Experimental	50
3.4	Determining Best Models for Ligand Docking.....	53
3.4.1.	Experimental	53
3.4.2.	Results	55
4.	Comparative Molecular Field Analysis (CoMFA).....	57
4.1	Introduction	57
4.2	Experimental Methods	72
4.3	Results and Discussion.....	78
5.	Conclusions	123
	List of References	126

List of Tables

	Page
Table 1: Non-conserved residues in the binding pocket.....	16
Table 2: Comparison of selective compounds.....	17
Table 3: Average intrinsic binding energies.....	19
Table 4: Free binding energies for morphine and salvinorin A (kcal/mol).....	20
Table 5: Compounds docked into the nine models of opioid receptors and their K _i values.....	54
Table 6: Top-ranking GOLD scores.....	54
Table 7: C-2 position analogs.....	59
Table 8: C-4 position analogs.....	66
Table 9: Furan analogs.....	68
Table 10: Miscellaneous analogs.....	70
Table 11: Model 1 dataset of 34 compounds using [¹²⁵ I] IOXY as the assay radioligand (receptor-docked alignment).....	84
Table 12: Model 1 CoMFA statistics for the receptor-docked alignment.....	89
Table 13: Model 1 dataset of 34 compounds using [¹²⁵ I] IOXY as the assay radioligand (FlexS alignment).....	93
Table 14: Model 1 CoMFA statistics for the FlexS alignment.....	96
Table 15: Model 1 dataset of 34 compounds using [¹²⁵ I] IOXY as the assay radioligand (realignment).....	97

List of Tables (cont.)

	Page
Table 16: Model 1 CoMFA statistics for the realignment.	100
Table 17: Model 2 dataset using [³ H] diprenorphine as the assay radioligand (receptor-docked alignment).....	102
Table 18: Model 2 CoMFA statistics for the receptor-docked alignment.	107
Table 19: Model 2 dataset using [³ H] diprenorphine as the assay radioligand (FlexS alignment)	114
Table 20: Model 2 CoMFA statistics for the FlexS alignment.	118
Table 21: Model 2 dataset using [³ H] diprenorphine as the assay radioligand (realignment).....	119
Table 22: Model 2 CoMFA statistics for the realignment.	122

List of Figures

	Page
Figure 1: The structures of salvinorin A (a) and salvinorin B (b)	4
Figure 2: Opium alkaloids	6
Figure 3: Opioid derivatives	7
Figure 4: Opioid derivative examples.....	8
Figure 5: The endogenous opioid peptides	11
Figure 6: Precursor proteins (rectangles).....	12
Figure 7: Examples of the “message – address” concept	15
Figure 8: Structure-activity relationships of salvinorin A analogs	23
Figure 9: Salvinorin A fragment (red)	27
Figure 10: Alignment of the opioid receptor sequences with bovine rhodopsin	36
Figure 11: Opioid receptor models based on inactive bovine rhodopsin 1F88 crystal structure.....	39
Figure 12: Superimposed bovine rhodopsin 1F88 crystal structure with opioid receptor models.....	40
Figure 13: Opioid receptor models based on inactive bovine rhodopsin 1U19 crystal structure.....	42
Figure 14: Superimposed bovine rhodopsin 1U19 crystal structure with opioid receptor models.....	43

List of Figures (cont.)

	Page
Figure 15: Opioid receptor models based on light-activated bovine rhodopsin 2I37 crystal structure.....	44
Figure 16: Superimposed bovine rhodopsin 2I37 crystal structure and the opioid receptor models.....	45
Figure 17: Opioid receptor models based on the β_2 adrenergic receptor 2RH1 crystal structure.....	48
Figure 18: Superimposed β_2 -adrenergic receptor 2RH1 crystal structure and opioids receptor models.....	49
Figure 19: KOR model number 36 of the MODELLER-generated receptors.....	52
Figure 20: FlexS template molecule	75
Figure 21: Stereo view of salvinorin A docked in the kappa opioid receptor	81
Figure 22: Model 1 dataset alignments.....	88
Figure 23: Model 1 linear regression plots	90
Figure 24: Model 1 CoMFA contour maps	91
Figure 25: Model 2 dataset alignments.....	106
Figure 26: Model 2 linear regression plots	108
Figure 27: Model 2 CoMFA contour maps	109
Figure 28: The β - <i>N</i> -isopropylamine analog of salvinorin A.....	111
Figure 29: Stereo view of the β - <i>N</i> -isopropylamine analog of salvinorin A docked in the KOR	112

List of Schemes

	Page
Scheme 1: Two-step synthesis	25
Scheme 2: Synthesis of methyl-4-oxocyclohexane carboxylate (2).....	26
Scheme 3: Synthesis of methyl -3-acetoxy-4-oxocyclohexanecarboxylate (3).....	30

List of Abbreviations

3D-QSAR	3-dimensional quantitative structure-activity relationship
AM1	Austin Model 1
AR-DOR	active rhodopsin-based δ -opioid receptor
AR-KOR	active rhodopsin-based κ -opioid receptor
AR-MOR	active rhodopsin-based μ -opioid receptor
B-DOR	β_2 adrenergic-based δ -opioid receptor
B-KOR	β_2 adrenergic-based κ -opioid receptor
B-MOR	β_2 adrenergic-based μ -opioid receptor
BNTX	benzylidenenaltrexone
CoMFA	comparative molecular field analysis
DOR	δ -opioid receptor
EL	extracellular loop
GNTI	guanidinylnaltrindole
GOLD	Genetic Optimization for Ligand Docking
GPCR	G protein-coupled receptor
IL	intracellular loop
IR-DOR	inactive rhodopsin-based δ -opioid receptor
IR-KOR	inactive rhodopsin-based κ -opioid receptor
IR-MOR	inactive rhodopsin-based μ -opioid receptor

IOXY	6 β -iodo-3,14-dihydroxy-17-cyclopropylmethyl-4,5 α - epoxymorphinan
KOR	κ -opioid receptor
LOO	leave-one-out
MOR	μ -opioid receptor
MOPAC	Molecular Orbital Package
NOP	nociceptin/orphanin FQ opioid receptor
norBNI	norbinaltorphimine
ORL1	opioid receptor-like
PC	principal components
PDB	Protein Data Bank
PLS	partial least squares
PSET	prediction set
RMSD	root mean square deviation
SAR	structure-activity relationship
SCAM	substituted cysteine accessibility method
SEE	standard error of the estimate
SIOM	spiroindanyloxomorphone
TLC	thin-layer chromatography
TM	trans-membrane
TSET	training set

Abstract

SALVINORIN A: FRAGMENT SYNTHESIS AND MODELING STUDIES

By Donna Lue McGovern, Ph.D.

A dissertation submitted in partial fulfillment of the requirements for the degree of
Doctor of Philosophy at Virginia Commonwealth University.

Virginia Commonwealth University, 2009

Major Director: Richard B. Westkaemper, Ph.D
Professor, Department of Medicinal Chemistry

Salvinorin A is a non-nitrogenous, selective kappa opioid receptor agonist with potent hallucinogenic properties. Because Salvinorin A has no basic nitrogen, it does not readily adhere to the “message-address” concept of selectivity for the opioid receptors. Therefore, a better understanding of how salvinorin A and its analogs interact with the kappa opioid receptor may shed some light on how salvinorin A obtains its potency and selectivity. The structure-affinity relationships (SAFIR) of salvinorin A and its analogs along with a discussion of the selectivity of the opioid receptors, is presented. A fragment of salvinorin A, methyl-3-acetoxy-4-oxocyclohexanecarboxylate, was synthesized to determine if the B, C and D rings are or are not necessary for binding to the opioid receptors. The fragment was found not to bind to the kappa, delta or mu receptor which reinforces the importance of the B, C and D rings in the binding of salvinorin A to the kappa opioid receptor. Homology models of the kappa, delta and mu

opioid receptors were constructed based on inactive bovine rhodopsin, light-activated bovine rhodopsin and the human beta-2 adrenergic receptors. The program MODELLER was also used to construct the kappa opioid receptor. Two comparative molecular field analysis (CoMFA) studies are then presented which compared three different types of alignment methods. The alignment methods employed included a receptor-docked alignment in which the salvinorin A analogs were docked into a model of the kappa opioid receptor using the program GOLD. The docked poses for this alignment were chosen based on their similarity to our postulated model of salvinorin A in the kappa opioid receptor. In our model the furan oxygen forms hydrogen bonds with Q115(2.60) and Y320(7.43), the methoxy oxygen of the C-4 position ester group may form a hydrogen bond with Y312(7.35) and the methyl group of the C-2 position acetoxy moiety forms a hydrophobic interaction with Y313(7.36). These interactions are consistent with mutagenesis studies. The other alignment methods employed were a FlexS alignment and a realignment of the receptor-docked poses using the Fit Atoms function within SYBYL. Only the receptor-docked alignment method resulted in robust and predictive CoMFA models which indicates that the analogs may bind to the kappa opioid receptor in a similar but non-identical way. In addition, information from the CoMFA models based on the receptor-docked alignment led to a postulated binding mode for a set of amine analogs of salvinorin A which were not part of the original data set. Docking studies have the positively charged C-2 position amine group interacting with E209(XL2.49) while the furan oxygen and C-4 position ester group interacts with the same residues as in our model of salvinorin A in the kappa opioid receptor. The studies presented here not

only support our postulated model of salvinorin A binding to the kappa opioid receptor but may also explain the trend of the beta epimers of the amine analogs to have a higher affinity than the corresponding alpha epimers. Site-directed mutagenesis studies could provide data to support or refute the postulated models of the amines docked in the kappa opioid receptor presented here.

1. Introduction

1.1. Background

Salvinorin A, also known as divinorin A, is a non-nitrogenous diterpene from the plant *Salvia divinorum* and is the most potent naturally-occurring hallucinogen known to date. This species of *Salvia* plant, also known as “Ska Maria Pastora” or “Diviner’s Sage”, was first cataloged by Wasson and Hoffman in 1962 and is indigenous to the Sierra Mazateca mountains in Oaxaca, a small region in Mexico.¹ The plant is found today growing in wide-spread locations and is also sold by nurseries. *Salvia divinorum* and its extracts have been used for centuries by the Mazatec Indians of Mexico in their curing and divination rituals to produce visions and enlightenment and to treat a number of ailments such as diarrhea, headache, rheumatism, and anemia.² The plant leaves can be chewed, extracted into a tea or infusion, or dried and smoked to produce the hallucinogenic effect which lasts from 20 minutes to two hours, depending on the route of administration. Effects are rapid with inhalation and occur within seconds. With buccal absorption, effects are seen within minutes. Little or no effects are seen with ingestion possibly due to esterases in the blood or first-pass metabolism, hydrolyzing the ester at the C-2 position to the alcohol Salvinorin B (see Figure 1), which is known to be inactive. Although short-lived, the hallucinogenic effect of salvinorin A has been described as more intense than LSD with frequent reports of mind-body dissociations and confusion of identity described as becoming an object.³ Because of its hallucinogenic

effect, ready availability, and legality, *Salvia divinorum* products have gained popularity as a “legal high” and can be found being sold in shops world-wide and via the Internet.⁴ As of yet, *Salvia divinorum* products have not been classified as a controlled substance by the Food and Drug Administration and Drug Enforcement Administration, although it is designated as a drug of concern. Several states in the United States and some countries have adopted legislation banning the use of salvinorin A and *Salvia divinorum* products.

Salvinorin A was first isolated from the plant *Salvia divinorum* and its structure elucidated in 1982⁵ by Alfred Ortega. The same compound was later isolated from *Salvia divinorum* by Leander Valdes in 1984⁶ who reported its psychoactive properties. Contrary to other hallucinogens which exert their effect by binding to the serotonergic receptor 5-HT_{2A}, salvinorin A is a potent, selective kappa-opioid receptor (KOR) agonist.⁷ Along with its being a hallucinogen, salvinorin A also exhibits the analgesic^{8, 9}, sedative¹⁰, and depressive¹¹ effects typical of opioid receptor substrates.

This dissertation initially presents a discussion of opioid selectivity, the binding energies of morphine and salvinorin A and the structure-affinity relationships of salvinorin A. This is followed by the synthesis of a fragment of the salvinorin A molecule which includes the A ring and its functional groups. This was done in order to ascertain if the B, C and D rings were necessary for binding to the kappa opioid receptor. Homology models of the kappa, delta and mu opioid receptors were then constructed based on the crystal structures of inactive bovine rhodopsin, light-activated bovine rhodopsin and the β_2 -adrenergic receptor. Docking of selective ligands for these

receptors resulted in the light-activated bovine rhodopsin-based kappa, delta and mu receptor models emerging as the apparent best receptor models for additional studies.

Two Comparative Molecular Field Analysis (CoMFA) studies are then presented in which a receptor-docked alignment method was used. Salvinorin A analogs were docked into the light-activated bovine rhodopsin-based kappa opioid receptor model using the program GOLD. Chosen docked poses of each compound in the receptor provided an alignment that resulted in highly predictive and robust CoMFA statistics. This alignment was compared to a FlexS alignment and a realignment of the docked poses using SYBYL Fit Atoms function. The latter two alignments gave poor results.

Also presented is a postulated binding model of a series of amine analogs of salvinorin A in the kappa opioid receptor. This binding model was developed using information from the CoMFA models.

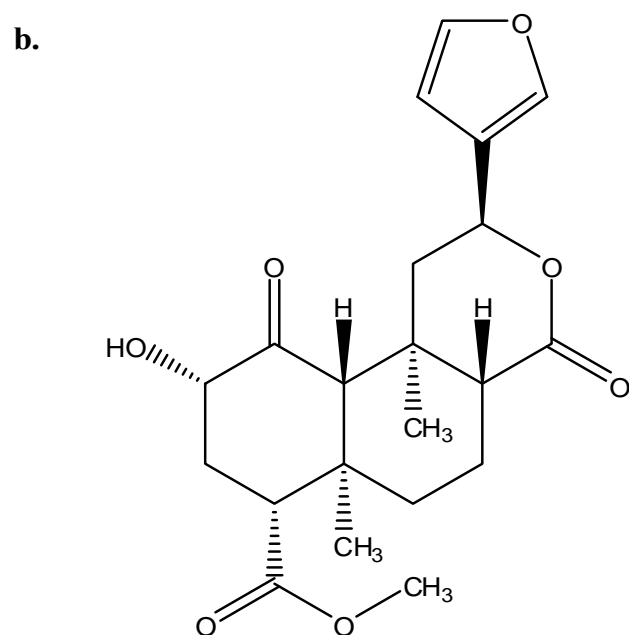
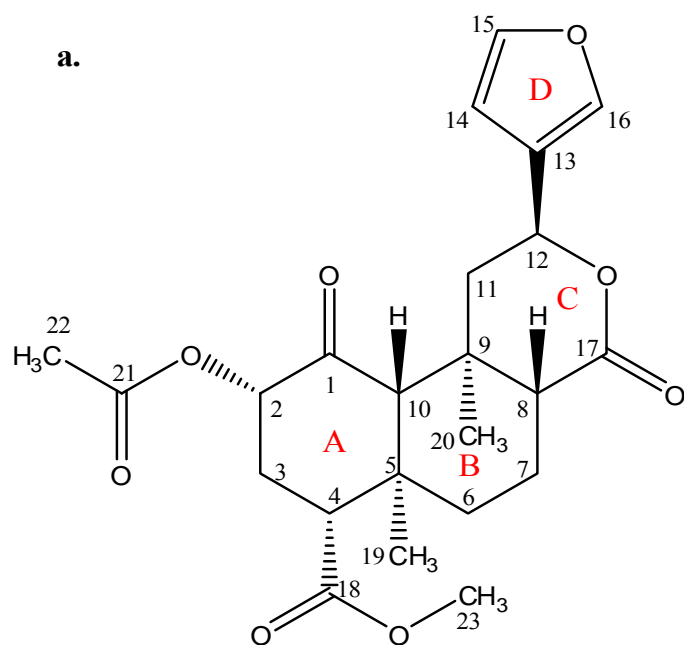
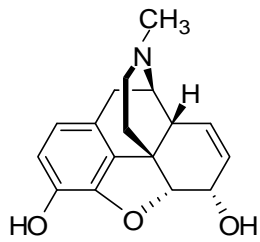


Figure 1. The structures of salvinorin A (a) and salvinorin B (b).

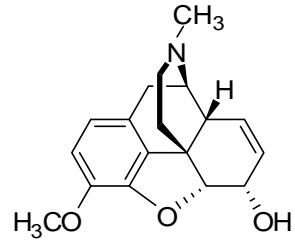
1.2. Opioids and Opioid Receptors

The alkaloids contained in the juice from the seed pod of the poppy *Papaver somniferum* (opium) have been used medicinally for thousands of years. The most abundant alkaloid in opium is morphine, named after the Greek god of dreams, Morpheus. Other medicinally important opium alkaloids include codeine, thebaine, papaverine and noscapine (see Figure 2). Morphine and codeine are analgesics, with codeine also having antitussive (cough suppressing) effects. Thebaine has a stimulating effect and is not used therapeutically but is used industrially as a starting compound for conversion into semisynthetic analgesics such as oxycodone, oxymorphone, and etorphine. The antagonists naloxone and naltrexone and the partial agonist/antagonist buprenorphine also are semisynthetic derivatives of thebaine. Papaverine is an antispasmodic and noscapine is an antitussive.

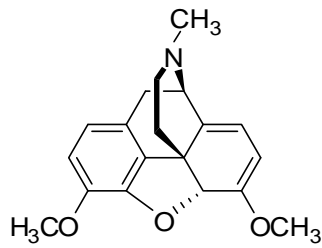
With morphine being the prototypical analgesic, a large number of morphine derivatives¹² have been synthesized. Many of these were derived from a simplified morphine skeleton (see Figures 3 and 4). In a 1955 study by Braenden, et al.¹³ it was observed that all known morphine-like analgesics contained the following features: “(a) a tertiary nitrogen, the group on the nitrogen being relatively small; (b) a central carbon atom none of whose valences are connected with a hydrogen; (c) a phenyl group or a group isosteric with phenyl, which is connected to the central carbon atom; and (d) maximum activity is obtained when the central carbon atom is connected to the nitrogen by a two-carbon chain.” All of the examples shown in Figure 4 adhere to these four features except the 4-anilinopiperidines of which fentanyl is a representative member.



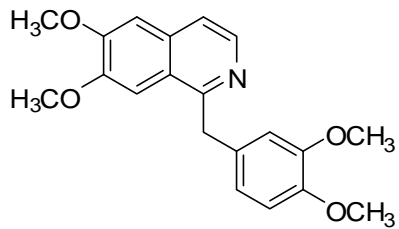
Morphine



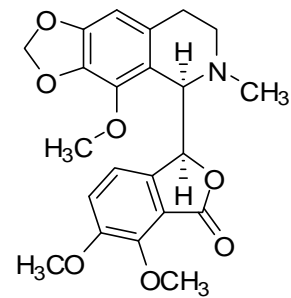
Codeine



Thebaine



Papaverine



Noscapine

Figure 2. Opium alkaloids.

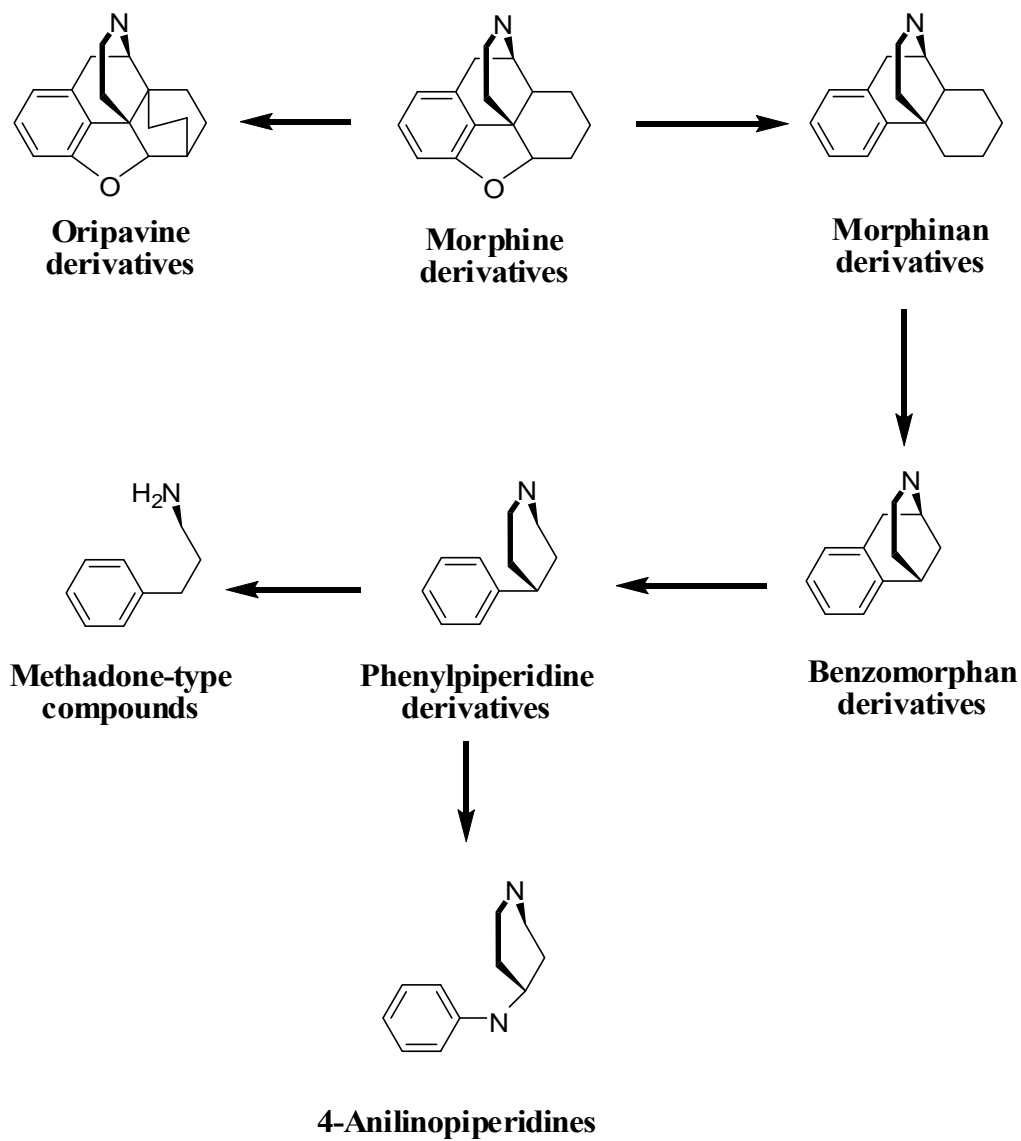
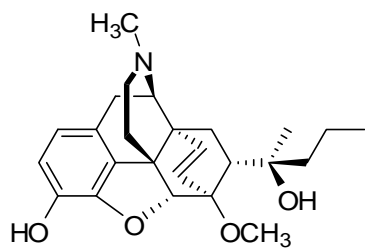
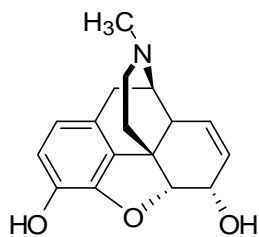


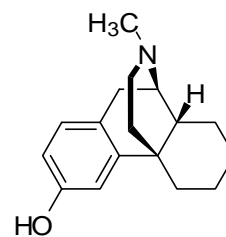
Figure 3. Opioid derivatives.



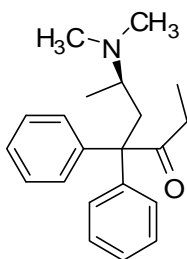
Etorphine



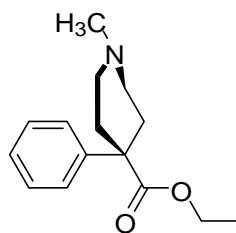
Morphine



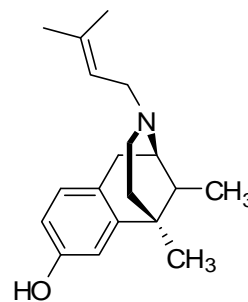
Levorphanol



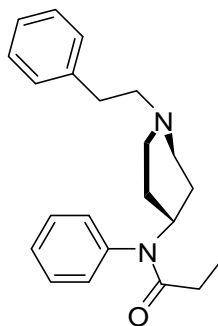
Methadone



Meperidine



Pentazocine



Fentanyl

Figure 4. Opioid derivative examples.

When comparing the opioid derivatives to the structure of salvinorin A, only one of these four features of the opioid analgesics is seen, that being an aromatic ring (furan). Morphine-like compounds have a T-shaped conformation of the polycyclic core while the salvinorin A polycyclic core, aside from ring puckering, is relatively flat. Yet, salvinorin A has analgesic properties^{8,14} at the kappa opioid receptor without having the other features, most notably the basic nitrogen.

In 1954, long before the discovery of the opioid receptors, Beckett and Casy¹⁵ proposed three features to be necessary for proper fit of the opioid analgesic to the receptor surface. These were: “(1) a flat portion allowing van de Waals’ forces binding the aromatic ring of the analgesic drug; (2) an anionic site and (3) a cavity suitably oriented with (between) sites 1 and 2”. This hypothesis held for a number of years until certain analgesics were found not to contain some of these features. Salvinorin A does not fit this hypothesis as an analgesic.

In 1973, Pert and Snyder¹⁶ reported the first evidence of an opioid receptor. The opioid receptors belong to the superfamily of G protein-coupled receptors (GPCRs). GPCRs are proteins that consist of seven trans-membrane (7TM) spanning helices which when activated interact with the trimeric (α , β , and γ) subunits of G proteins to elicit a response. Four types of opioid receptors are known at the present time. These are the μ (mu, for morphine) and κ (kappa, for ketocyclazocine), named for the drugs used in a 1976 study by Martin and colleagues¹⁷, and the δ (delta, for deferens) from a 1977 study in which the mouse vas deferens was used.¹⁸ Only two years after the discovery of the opioid receptors, Hughes et al.¹⁹ isolated and identified two pentapeptides as endogenous

opioids and named them enkephalins after the Greek word “Kaphale” meaning “from the head”. Since this discovery a number of endogenous peptides for the opioid receptors have been identified (see Figure 5) along with their precursor proteins (see Figure 6). The endogenous ligands are associated with the opioid receptors as follows: the enkephalins¹⁹ (delta and mu), β -endorphin²⁰ (delta and mu), dynorphins²¹ (kappa) and α -neoendorphin²¹ (kappa). Another set of endogenous ligands which are agonists at the mu opioid receptor are endomorphin-1 and endomorphin-2²², although their endogenous source or precursor protein has yet to be found. The fourth type of opioid receptor was discovered in 1994 and termed ORL1²³ (for opioid receptor-like) or LC132.²⁴ Two groups independently and simultaneously identified the endogenous peptide that activates this receptor and named it nociceptin²⁵ and orphanin FQ²⁶ (“orphanin” refers to its association with an orphan receptor and “FQ” refers to the terminal residues of the peptide). Today, this receptor is termed NOP-R (for nociceptin/orphanin FQ opioid receptor). Subtypes of the delta (δ_1 and δ_2), kappa (κ_1 , κ_2 and κ_3) and mu (μ_{1A-1X}) have been suggested. However, only in mu have splice variants been identified. Only one cDNA clone has been reported for delta and for kappa receptors and no variants have been identified to date. It is likely that the subtypes arise from interaction of these receptors with other proteins or receptors (i.e. hetero-oligomerization) and not mRNA variants. The opioid receptor subfamily can be divided into two main branches. One branch includes the delta, kappa, and mu receptors at which naloxone acts as an antagonist and the second branch includes the NOP receptor which has a negligible affinity for naloxone.

Met-Enkephalin:	Tyr-Gly-Gly-Phe-Met
Leu-Enkephalin:	Tyr-Gly-Gly-Phe-Leu
β-Endorphin:	Tyr-Gly-Gly-Phe-Met-Thr-Ser-Glu-Lys-Ser¹⁰-Gln-Thr- Pro-Leu-Val-Thr-Leu-Phe-Lys-Asn²⁰-Ala-Ile-Ile-Lys- Asn-Ala-Tyr-Lys-Lys-Gly-GluOH³¹
Dynorphin (dyn¹⁻¹⁷):	Tyr-Gly-Gly-Phe-Leu-Arg-Arg-Ile-Arg-Pro-Lys-Leu- Lys-Trp-Asp-Asn-Gln
Dynorphin (dyn¹⁻⁸):	Tyr-Gly-Gly-Phe-Leu-Arg-Arg-Ile
Dynorphin (dyn¹⁻¹³):	Tyr-Gly-Gly-Phe-Leu-Arg-Arg-Ile-Arg-Pro-Lys-Leu- Lys
α-Neoendorphin:	Tyr-Gly-Gly-Phe-Leu-Arg-Lys-Tyr-Pro-Lys
β-Neoendorphin:	Tyr-Gly-Gly-Phe-Leu-Arg-Lys-Tyr-Pro
Nociceptin:	Phe-Gly-Gly-Phe-Thr-Gly-Ala-Arg-Lys-Ser-Ala-Arg- Lys-Leu-Ala-Asn-Gln
Endomorphin-1:	Tyr-Pro-Trp-Phe-NH₂
Endomorphin-2:	Tyr-Pro-Phe-Phe-NH₂

Figure 5. The endogenous opioid peptides.

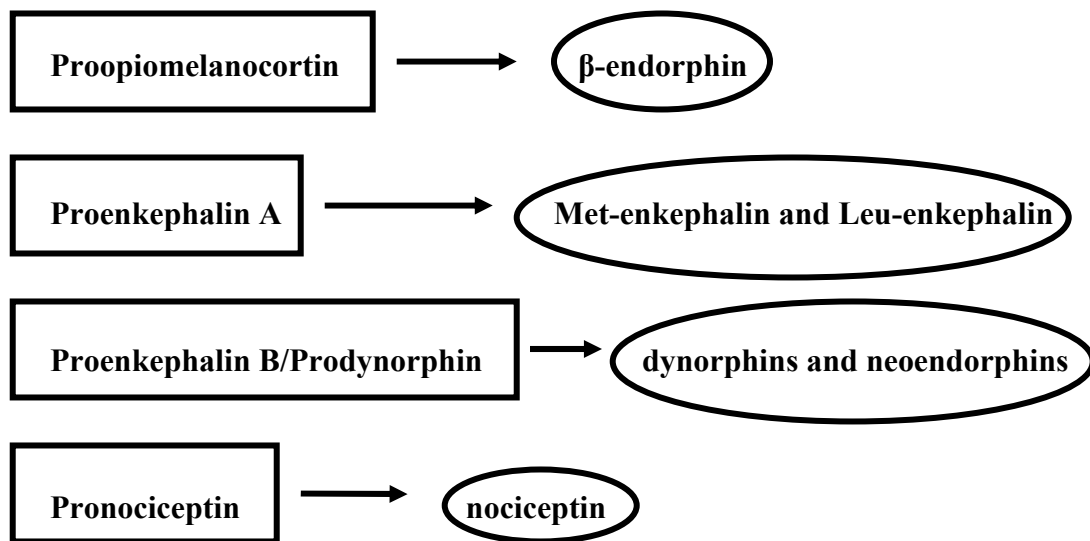


Figure 6. Precursor proteins (rectangles). The endogenous peptide contained in each precursor protein is outlined in ovals.

1.3. Opioid Selectivity

Most of the relevant work on selectivity of the opioid receptors began with the cloning of the kappa, delta and mu opioid receptors in the early 1990s²⁷ using a combination of SAR, chimeric studies, and site-directed mutagenesis. When the first high-resolution crystal structure of the inactive form of bovine rhodopsin became available²⁸ in 2000, molecular modeling docking studies and computational methods became important in determining those residues responsible for conferring selectivity among the opioid receptors. Prior to 2000 opioid receptor models were constructed using the non-homologous bacteriorhodopsin²⁹⁻³¹ or low resolution electron diffraction maps^{32,33} of rhodopsin. Most recent published studies have concentrated on the selectivity of individual ligands, their binding modes, and improvement of potency and affinity for selective agonist and antagonist ligands.

1.4. General Concepts in Selectivity

The kappa, delta and mu opioid receptors share an overall sequence identity in the helical and loop regions of ~60%. However, the sequence identity varies according to which regions of the receptor that are being analyzed. The intracellular loop regions have a high sequence identity of ~90% while the N-terminus, EL2, EL3 and the C-terminus show little to no similarity. Approximately 75% sequence identity is seen in TM2, TM3 and TM7 whereas the identity between TM4, TM5 and TM6 is much less.

Classical opiate ligands and some of the other opioid ligands adhere to the “message – address” concept^{34,35}, the “message” being the shared or universal portion of

the molecule which interacts with the receptor and confers affinity and the “address” being that unique portion of the molecule which interacts with the receptor to confer selectivity. Non-selective opiate ligands have no “address” moiety. For opiates, the tyramine (4-hydroxy-phenylethylamine) constitutes the message moiety while large substituents on the C ring provide the address or selectivity of the molecule (see Figure 7).

The “message” interactions take place with conserved binding site residues. These interactions include D(3.32) and the ligand amine, H(6.52) and the phenolic OH, and a mutagenesis study by Befort, et.al.³⁶ suggests that the conserved residues W(4.50), F(5.47) and W(6.48) form the scaffold stabilizing hydrophobic interaction in all three receptors. Salvinorin A, being non-nitrogenous, does not appear to conform to the “message – address” model. However, if one had to assign a “message” region of the molecule it would most likely be the furan ring which interacts with the conserved residues Q(2.60) and Y(7.43). The “address” moiety would likely be the C-2 position acetate group which interacts with the non-conserved Y313(7.36). The C-2 position benzoate analog of salvinorin A (herkinorin) is μ -selective indicating a lack of bulk tolerance or a need for a H-bonding moiety in that position for the ligand to bind selectively to the KOR.

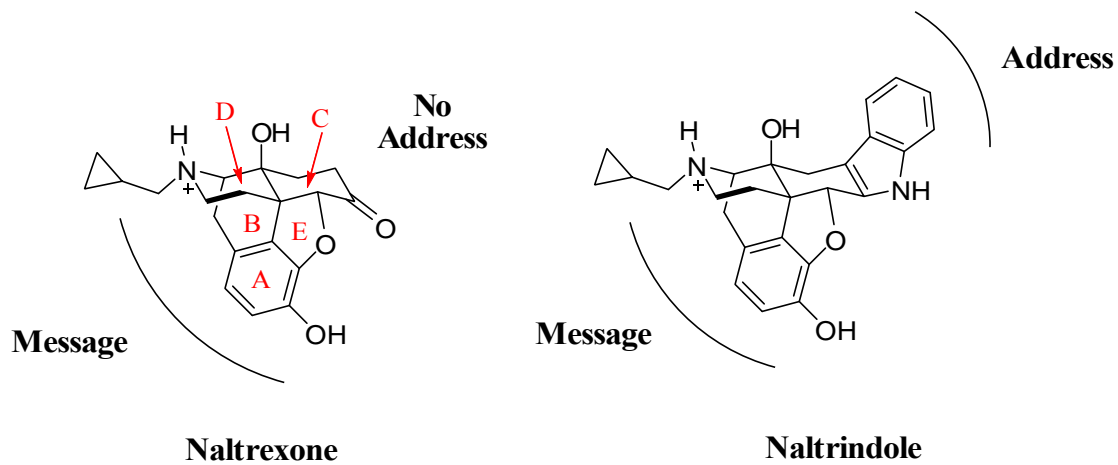


Figure 7. Examples of the “message – address” concept. Shown is the non-selective opiate naltrexone and delta-selective opiate naltrindole.

Conserved residues in the binding pocket include T(2.54), Q(2.60), Y(2.64) in TM2; W(XL1.50) in EL1; D(3.32), Y(3.33), M(3.36) in TM3; W(4.50) in TM4; L(XL2.52) and F(XL2.54) in EL2; K(5.39), F(5.43), F(5.47) in TM5; W(6.48), I(6.51) in TM6 and I(7.39), Y(7.43) in TM7.

Table 1. Non-conserved residues in the binding pocket. Residues underlined are thought to be the most important residues for conferring selectivity of the opiates.

	Kappa	Delta	Mu
TM2 (2.63)	V118	K108	N129
TM3 (3.29)	I135	L125	I146
EL2 (XL2.49)	E209	V197	D218
TM6 (6.55)	I294	V281	V302
TM6 (6.58)	<u>E297</u>	<u>W284</u>	<u>K305</u>
TM7 (7.32)	<u>L309</u>	<u>V297</u>	<u>T317</u>
TM7 (7.35)	Y312	L300	W320
TM7 (7.36)	Y313	H301	H321

Models constructed from site-directed mutation models³⁶ suggested that two residues at the extracellular ends of TM6 and TM7 confer opiate and opiate-like ligand selectivity. The following residues are non-conserved and oriented for ligand binding: kappa - E297(6.58), Y312(7.35); delta - W284(6.58), L300(7.35); and mu - K303(6.58), W318(7.35).

Selectivity arises from two mechanisms: a) mutual attraction and b) steric exclusion. Mutual attraction occurs when the ligand is attracted to a complementary residue on the receptor (e.g. ionic interaction, hydrophobic interaction, etc.) and leads to stabilization and increased binding. Steric exclusion occurs when a residue or residues on the receptor do not allow mutual attraction to occur resulting in decreased binding. The selective opiate and opiate-like compounds achieve their selectivity from a combination of these two mechanisms.

The selectivity of Salvinorin A for the kappa opioid receptor is compared to a number of selective compounds in Table 2. It can be seen that salvinorin A has both

Table 2. Comparison of selective compounds.

Compound	K _i (nM)			Reference
	delta	kappa	mu	
salvinorin A	5790	1.9	>1000	37
morphine	140	46.9	1.1	38
DAMGO	190	1300	0.34	22
U50488	>10,000	0.2	290	38
TRK-820	1200	3.5	53	39
ethylketocyclazocine	3.4	0.1	0.3	38
bremazocine	0.9	0.03	0.2	38
endomorphin-1	1506	5428	0.36	22
endomorphin-2	9233	5240	0.69	22
β-endorphin	2.4	96	2.1	22
Met-enkephalin	0.91	4442	9.5	22
dynorphin (1-17)	42.7	1.7	7.7	38

high affinity and selectivity for the kappa opioid receptor. Only the endogenous endomorphins with their high affinity and selectivity for the mu receptor rival salvinorin A. Salvinorin A has been tested for binding at over fifty receptors and has been found to bind only to the kappa opioid receptor.

1.5. Binding Energies

In 1984, Andrews et al.⁴⁰ proposed a method of calculating binding energies for a molecule by summing the intrinsic binding energies for 10 common functional groups and subtracting two entropy-related terms. The difference between the observed binding energy and the calculated binding energy determines the goodness of fit of a drug to its receptor. The free energy of drug-receptor binding is calculated using the following equation:

$$\Delta G = T\Delta S_{rt} + n_{DOF}E_{DOF} + \sum n_X E_X \quad (1)$$

In equation (1), $T\Delta S_{rt}$ is the loss of overall rotational and translational entropy of the bound drug molecule, n_{DOF} is the number of internal degrees of conformational freedom in the molecule, E_{DOF} is the energy associated with the change in entropy resulting from the loss of each degree of freedom upon binding of the drug to the receptor, and E_X is the intrinsic binding energy associated with each functional group X of which there are n_X such functional groups in the molecule. In order to obtain the E_{DOF} and E_X values, Andrews used data from 200 drugs and enzyme inhibitors and ran regression analyses using the equation:

$$\Delta G = -RT\ln K \quad (2)$$

with experimentally obtained K_i or K_D values to calculate the free binding energies used in the regression analyses. The average intrinsic binding energy values for ten common functional groups and the entropy term coefficient for the loss of degrees of freedom are shown in Table 3.

Table 3. Average intrinsic binding energies.

Group	Energy (kcal/mol)
C(sp ²)	0.7
C(sp ³)	0.8
N ⁺	11.5
N	1.2
CO ₂ ⁻	8.2
OPO ₃ ²⁻	10.0
OH	2.5
C=O	3.4
O, S	1.1
Halogen	1.3
DOF ^a	-0.7

^aDegrees of internal conformational freedom.

The allowance for the loss of overall rotational and translational entropy was calculated to be 14 kcal/mol based on the 1977 work of Page.⁴¹ In its final form, the following equation can be used to obtain the calculated free energy of binding for any molecule:

$$\Delta G = -14 - 0.7n_{\text{DOF}} + 0.7n_{\text{C(sp}^2\text{)}} + 0.8n_{\text{C(sp}^3\text{)}} + 11.5n_{\text{N}^+} + 1.2n_{\text{N}} + 8.2n_{\text{CO}_2^-} + 10.0n_{\text{PO}_4^{2-}} + 2.5n_{\text{OH}} + 3.4n_{\text{C=O}} + 1.1n_{\text{O,S}} + 1.3n_{\text{Hal}} \quad (3)$$

The observed free binding energy minus the calculated (average) free binding energy results in either a positive number indicating a better than average binding, or a negative number indicating a weaker binding than average. According to Andrews, a large positive number would indicate that most or all of the functional groups are involved in binding resulting in a higher affinity at the receptor and would be a good drug candidate as a lead compound for further modification. In his work, morphine was used as an example and the ΔG_{OBS} and ΔG_{AVG} for this compound were calculated using equations (2) and (3), respectively. Table 4 shows the free binding energies for morphine and salvinorin A.

Table 4. Free binding energies for morphine and salvinorin A (kcal/mol).

Group	Coefficient	Morphine	Salvinorin A
$T\Delta S_{\text{rt}}$	-14	-14	-14
DOF	-0.7	-1.4	-3.5
C(sp ²)	0.7	5.6	5.6
C(sp ³)	0.8	7.2	12.0
N ⁺	11.5	11.5	
N	1.2		
CO ₂ ⁻	8.2		
PO ₄ ²⁻	10.0		
OH	2.5	5.0	
C=O	3.4		10.2
O,S	1.1	1.1	4.4
Hal	1.3		
ΔG_{AVG}		15.0	20.5
ΔG_{OBS}		11.2	11.9
$\Delta G_{\text{OBS}} - \Delta G_{\text{AVG}}$		-3.8	-8.6

Andrews concludes that a negative value for the difference between the observed free binding energy and the average (calculated) free binding energy (-3.8 for morphine) indicates that either not all the functional groups are interacting with the receptor or that the ligand is in a relatively high energy conformation and points out that for morphine a negative value is consistent with the finding that portions of the morphine structure can be removed without significant loss of affinity. Salvinorin A has an even larger negative difference between the two energies (-8.6). Because of the constrained polycyclic structure of salvinorin A, it is unlikely that a high energy conformation is the source of the negativity. However, the structure-activity relationship data indicates that several portions of the salvinorin A structure are not required for high affinity binding.

1.6. Structure-Affinity Relationships (SAFIR) of Salvinorin A Analogs

The SAFIR of salvinorin A analogs is shown in Figure 8. Due to the large number of salvinorin A analogs, it is difficult to formulate an all-inclusive, self-consistent SAFIR by inspection. However, several general remarks can be made. The C-1 carbonyl is not required for high affinity.^{42,43} However, reduction of the C-1 carbonyl to an alcohol increases the K_i 500-fold.^{42,43} The C-2 position acetyl group is required for high affinity. Hydrolysis of the ester to the alcohol (salvinorin B) reduces affinity 100-fold.⁴⁴ A C-2 propanoate ester is optimum⁴⁵ and esters as large as the *n*-hexanoate⁴⁶ are tolerated at C-2. Ethyl or propyl ethers⁴⁷ are tolerated at the C-2 position and methoxymethyl ethers⁴⁷ are optimal. The C-4 position group tolerates very little change. The C-18 carbonyl is required for high affinity. The C-18 deoxo compound shows 350-fold⁴⁸ loss

of affinity. The methyl ester at the C-4 position is required. The C-4 carboxylic acid shows a >5000-fold⁴⁹ loss of affinity. The C-17 carbonyl is not necessary. The C-17 deoxo compound⁴² still retains high affinity and reduction of the C-17 carbonyl to an alcohol is tolerated, reducing the affinity by 25-fold.⁴² The furan ring is required for high affinity. Reduction of the furan ring is well tolerated, but removal of the furan ring reduces the affinity 1500-fold.⁴⁴

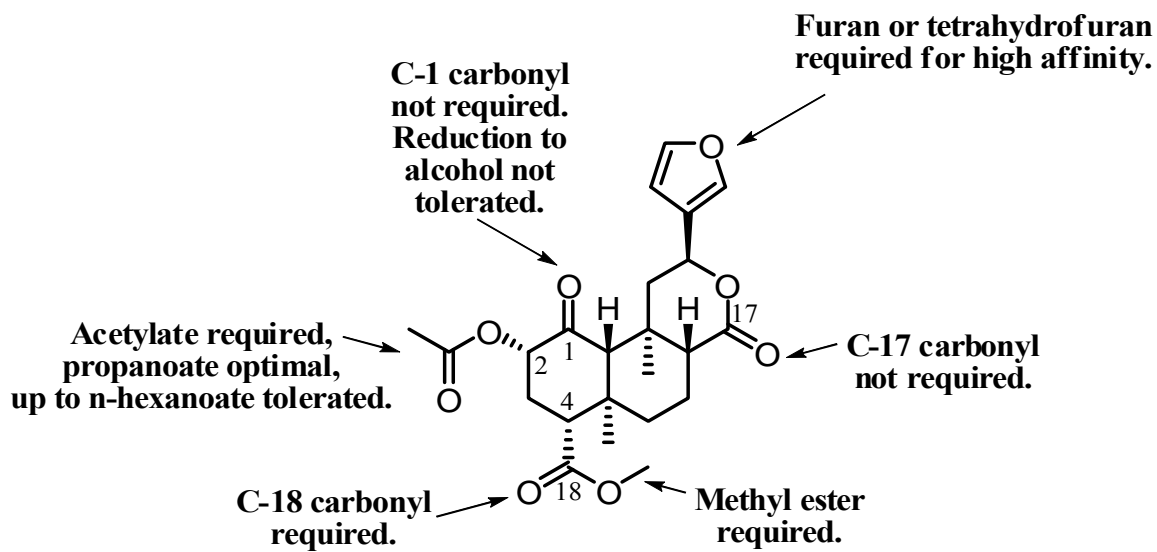


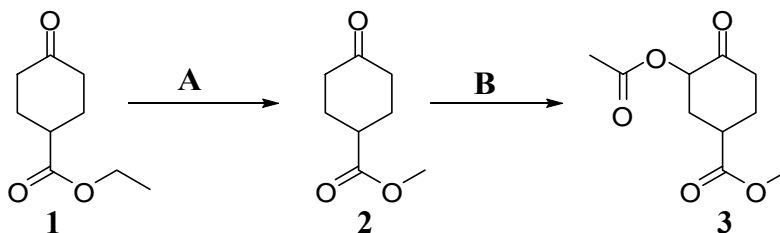
Figure 8. Structure-affinity relationships of salvinorin A analogs.

When looking at the K_i data for the 280 analogs of salvinorin A, the data does not show clear SAFIR trends. It is very difficult to draw any conclusions about why salvinorin A is so extremely selective based on K_i data alone. Salvinorin A has been tested for binding at a myriad of receptors and shows no binding at any receptor other than at the kappa opioid receptor. It does not bind at delta and mu opioid receptors despite the high sequence identity of the opioid receptors. So what makes this compound so selective? Having no basic nitrogen that can be protonated and, therefore, no interaction with the highly conserved D(3.32) as is seen with the aminergic receptors and their ligands, it is fairly easy to see why it does not bind to these receptors in a way that nitrogen-containing substrates do. Salvinorin A has eight possible H-bond acceptor oxygen atoms. From the SAFIR it is suggested that not all of these oxygen acceptor atoms are required for high affinity. Most of the important functional groups for binding reside on the A ring so the first project undertaken in this research was to synthesize the fragment of salvinorin A containing the A ring to see if this fragment would bind to the kappa opioid receptor without the B, C and D rings and possibly shed some light on the binding mode and selectivity of salvinorin A.

2. Salvinorin A Fragment Synthesis

2.1. Introduction

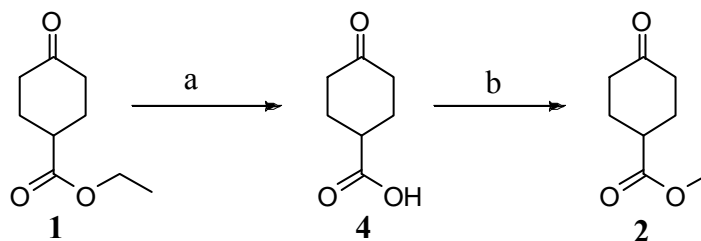
In order to determine the necessity of the B, C and D rings of salvinorin A for binding at the kappa opioid receptor the fragment shown in red in Figure 9 was synthesized. A simple two-step synthesis consisting of a transesterification to the methyl ester at the C-4 position followed by an acetoxylation at the C-2 position was originally planned (see Scheme 1).



Scheme 1. Two step synthesis. A = transesterification, B = acetoxylation.

Three methods of transesterification were attempted. Method 1 (TE1) followed the procedure of Mori, et al.⁵⁰ and used KCN in MeOH, refluxed for 19 hours. Method 2 (TE2) and Method 3 (TE3) used the method of Ranu, et al.⁵¹ TE2 used InI₃ in MeOH, refluxed for 25 hours, whereas TE3 used indium metal and I₂ to form InI₃ *in situ* and was refluxed 30 hours. TE1 produced a small amount of product as indicated by thin layer chromatography (TLC). For all three methods, reaction times were long and little to no

product was formed. Separation of the methyl ester formed from the ethyl ester starting compound was also a problem. These two compounds tended to coelute with column chromatography. After trying several solvent systems for column chromatography with no separation obtained, it was decided to attempt a two-step route to obtain the methyl ester (methyl-4-oxocyclohexane carboxylate). The first step used 10% NaOH in MeOH refluxed for one hour to hydrolyze the ethyl ester to the carboxylic acid followed by a second step of esterification using a catalytic amount of H₂SO₄ in MeOH and refluxed 30 minutes to arrive at the ethyl ester product (see Scheme 2).



Scheme 2. Synthesis of methyl-4-oxocyclohexane carboxylate (**2**). Reagents (a) 10% NaOH in MeOH, (b) H₂SO₄ (cat.) in MeOH.

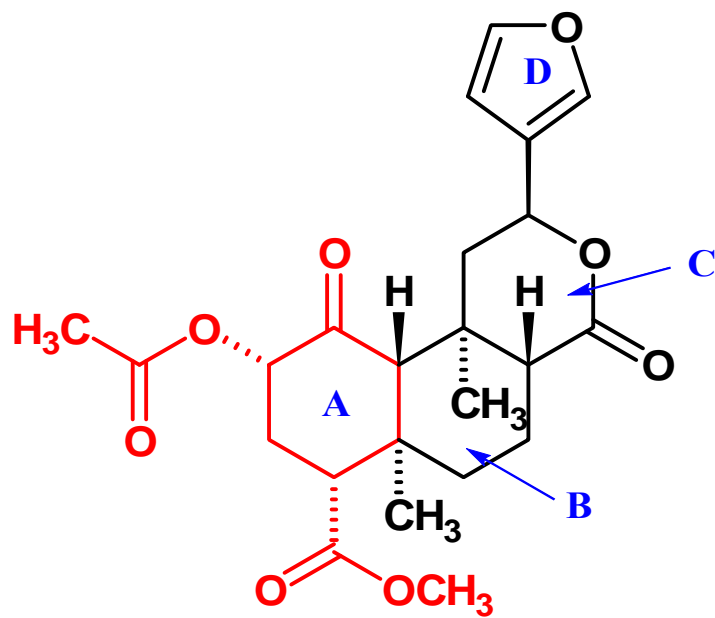


Figure 9. Salvinorin A fragment (red).

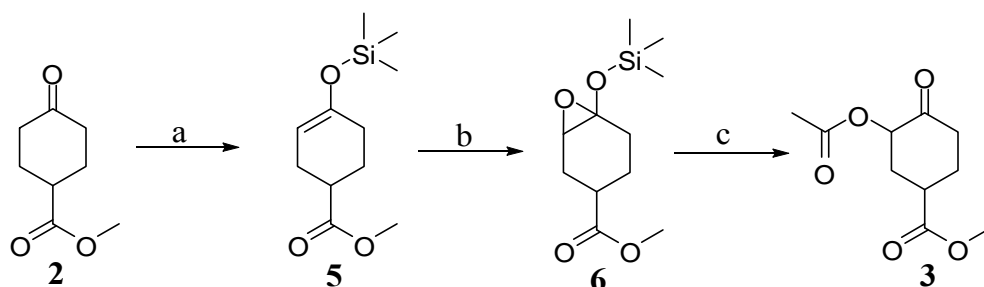
Reaction times were short and yield was good for the methyl ester (92% overall for the two steps). After hydrolysis there was no starting compound left (i.e. 100% yield of the acid **4**) and, therefore, separation from the small amount of impurities was easily achieved using column chromatography.

Acetoxylation of the methyl ester **2** proved to be the more challenging step in the synthesis. Two different methods of direct acetoxylation of **2** were attempted. The first method used was that of Tanyeli, et al.⁵² which used $\text{Pb}(\text{OAc})_4$ in cyclohexane and refluxed 21 hours. This method resulted in very poor yield of product and was very difficult to separate from the starting compound. The second direct method attempted was that of Lee, et al.⁵³ which used $\text{Tl}(\text{OAc})_3$ and $\text{CF}_3\text{SO}_3\text{H}$ in *N,N*-dimethylacetamide (DMAc) at 60 °C followed by H_2O . Yields were very low for this direct acetoxylation method also and, in addition, multiple spots were seen on TLC. An added disadvantage of this method was removal of the DMAc. Because of the high boiling point of DMAc (165° C), it could not be removed by rotary evaporation without losing product. Multiple extractions with water did not remove all the DMAc. Column chromatography was able to separate the residual DMAc; however, multiple spots were detected with TLC of the eluant with much coelution of products.

The next attempt at acetoxylation of the methyl ester **2** was a two-step process starting with α -bromination of **2** followed by acetoxylation of the brominated methyl ester. The bromination procedure was taken from Fleischmann, et al.⁵⁴ and used bromine added to a cooled solution of methyl ester in CH_2Cl_2 . Yields of α -bromo methyl ester compound were good (~80% crude product assumed to be mostly the α -bromo product).

TLC indicated no starting compound and an intense spot at a higher R_f than the methyl ester assumed to be the mono-brominated product and a second, much less intense spot below it which was assumed to be the dibrominated product. The crude bromination product was used without purification in the next acetoxylation step. The acetoxylation procedure was from work done by Lauktien, et al.⁵⁵ and was modified by refluxing the bromo product in glacial acetic acid and adding sodium acetate (the original method used potassium acetate and 2-chlorocyclohexanone). In this procedure the acetic acid was difficult to remove. TLC indicated three spots thought to be starting compound (the α -bromo methyl ester), the desired product **3** and possibly a hydrolysis product of **3**. After column chromatography a sample pure enough for NMR was obtained. DEPT-NMR showed one methyl group instead of two and, therefore, it was concluded to be the hydrolysis product of the desired product **3**. Attempts were made to purify the crude bromo mixture by column chromatography before doing the acetoxylation step. This resulted in a product which had the necessary peaks of the desired product **3**, however, there still remained impurities in the sample.

It was then decided to undertake a three-step synthesis by converting the methyl ester to the silyl enol ether, followed by epoxidation and finally acetoxylation of the epoxide (see Scheme 3).



Scheme 3. Synthesis of methyl-3-acetoxy-4-oxocyclohexane carboxylate (**3**). Reagents: (a) $(\text{CH}_3)_3\text{SiCl}$, Et_3N in DMF or $(\text{CH}_3)_3\text{SiN}(\text{CH}_3)_2$, CH_3I in benzene, (b) MCPBA in CH_2Cl_2 , (c) Et_3NHF , Et_3N in acetic anhydride.

Two different methods were attempted to make the silyl enol ether. The first was a method by House, et al.⁵⁶ that used $(\text{CH}_3)_3\text{SiCl}$ and Et_3N in DMF and refluxing 48 hours. The reaction time was long and no product was obtained with this method. The second method attempted to make the silyl enol ether was a procedure by Yamamoto and Matui⁵⁷ which was modified from the original by using (trimethylsilyl)dimethylamine instead of (trimethylsilyl)diethylamine with methyl iodide in benzene. The reaction time was short (two hours) and the yield (84%) was much better than the first method.

The next step was to convert the silyl enol ether (**5**) to the epoxide (**6**) with *m*-chloroperbenzoic acid (MCPBA) in CH_2Cl_2 followed by acetylation of the epoxide formed using $\text{Et}_3\text{NHF}/\text{Et}_3\text{N}$ in acetic anhydride according to the method by Rubottom and Gruber⁵⁸ to arrive at the desired product (**3**). The crude epoxide was used without purification. Product (**3**) was verified by NMR and GC/MS to be a mixture of two diastereomers and their enantiomers. The product was then sent to the NIMH Psychoactive Drug Screening Program (University of North Carolina, Chapel Hill, NC)

to determine the affinity at the KOR, DOR and MOR. Product (**3**) had a $K_i > 10,000$ nM at all three opioid receptors.

2.2. Experimental

The starting compound (**1**), ethyl-4-oxocyclohexanecarboxylate, was obtained from Aldrich (Sigma-Aldrich, St. Louis MO, catalog number 320825). Melting points were taken on an Optimelt (Stanford Research Systems) melting point apparatus. Proton NMRs were taken on a Varian Mercury-300 MHz spectrometer. The data is being reported as: chemical shifts δ (ppm), multiplicity (s = singlet, d = doublet, t = triplet, q = quadruplet, m = multiplet or unresolved, br = broad signal), coupling constant(s) J (Hz), and integration.

4-oxocyclohexanecarboxylic acid (**4**)

To 5.46 g (0.031 mol) of ethyl-4-oxocyclohexanecarboxylate (**1**) in 10 ml MeOH was added 2.49g (0.062 mol) NaOH dissolved in 10 ml H₂O. The mixture was refluxed 1 hour, cooled and acidified to a pH of 1-2 with 10% aq. HCl followed by extraction with CH₂Cl₂ (50 ml \times 3). Extracts were combined, dried with anhydrous MgSO₄ and filtered. The CH₂Cl₂ was removed by rotary evaporation leaving a white solid (**4**). Yield: 3.90 g (88%, 0.027 mol); mp range = 70 – 72° C, ¹H NMR (CDCl₃): δ 2.02 (m, 4H), 2.35 (m, 4H), 2.85 (m, 1H), 11.43 (br, 1H).

Methyl-4-oxocyclohexanecarboxylate (2)

To 3.90 g (0.027 mol) of 4-oxocyclohexanecarboxylic acid (4) in 10 ml of anhydrous MeOH was added 2 drops of conc. H₂SO₄. The reaction mixture was refluxed 1 – 2 hours. The MeOH was then evaporated to a small volume and 100 ml of CH₂Cl₂ added. The mixture was extracted with H₂O (2 × 100 ml) and the CH₂Cl₂ layer dried with anhydrous MgSO₄, filtered and evaporated to an oil (2). Yield: 4.38 g (100%, 0.28 mol); ¹H NMR (CDCl₃): δ 1.96 (m, 4H), 2.37 (m, 4H), 2.71 (m, 1H), 3.65 (s, 3H).

Methyl-4-(trimethylsilyloxy)cyclohex-3-enecarboxylate (5)

In a three-neck 100 ml round bottom flask set up with a condenser, stopper and septum stopper was added 20 ml anhydrous benzene, 2.2 ml (0.014 mol) trimethylsilyldimethylamine and 1.0 ml (0.16 mol) methyl iodide. The reaction mixture was stirred under N₂ at 50 – 60 °C for one hour. The temperature was raised to 70 – 80 °C after one hour and 1.70 g (0.011 mol) of methyl-4-cyclohexanecarboxylate (2) was added gradually by syringe over a 30-minute period. The mixture was then stirred for one hour longer. The mixture was allowed to cool and 50 ml diethyl ether was added. The amine salt that formed upon the addition of the anhydrous diethyl ether was filtered out. The benzene and diethyl ether were evaporated off leaving 2.37 g of crude (5). The 2.37 g of crude (5) was applied to a 20 cm (40 mm OD) glass column filled with silica gel (60 mesh) which had been pretreated with a 1% solution of Et₃N in ethyl acetate. The elution solvent was 9:1 petroleum ether:ethyl acetate. Yield: 2.10 g (84%, 0.01 mol); ¹H NMR (CDCl₃): δ 0.01 (s, 9H), 1.80 (m, 2H), 1.90 (m, 2H), 2.05 (m, 2H), 2.30 (m, 1H), 3.45 (s, 3H) 4.58 (t, *J*=3.0 Hz, 1H).

Methyl-6-(trimethylsilyloxy)-7-oxabicyclo[4.1.0]heptane-3-carboxylate (6)

To 1.505 g (0.0066 mol) of methyl-4-(trimethylsilyloxy)cyclohex-3-enecarboxylate (**5**) in 5 ml of anhydrous CH_2Cl_2 under N_2 and in a MeOH ice bath (-15 °C) was added 1.680 g (0.0073 mol assuming 75% pure) of *m*-chloroperbenzoic acid (MCPBA) which had been dissolved in anhydrous CH_2Cl_2 . Addition was drop-wise slowly by syringe. After the addition was complete, the mixture was allowed to stir at room temperature for 1 hour. The CH_2Cl_2 was evaporated off and the residue dissolved in 50 ml of hexane. The hexane mixture was extracted with saturated NaHCO_3 (2 × 50 ml). The hexane layer was dried with anhydrous MgSO_4 , filtered and evaporated to dryness. Weight of crude epoxide (**6**) = 0.342 g. The crude residue was used in the next step without purification.

Methyl-3-acetoxy-4-oxocyclohexanecarboxylate (3)

To 0.342 g of crude epoxide (**6**) was added 8 ml of acetic anhydride, 0.7 g of $\text{Et}_3\text{N}\cdot\text{HF}$ and 1.0 ml of Et_3N . The $\text{Et}_3\text{N}\cdot\text{HF}$ was prepared by adding 1.0 g (0.0062 mol) of $\text{Et}_3\text{N}\cdot 3\text{HF}$ to 1.255 g (0.0124 mol) of Et_3N to 10 ml anhydrous acetone. Stir, then evaporate acetone. White crystals form which are very hygroscopic.] The mixture was allowed to stir at room temperature under N_2 for 48 hours. To the reaction mixture was added 75 ml of diethyl ether and then extracted with 50 ml of saturated NaHCO_3 . Additional solid NaHCO_3 was added to hydrolyze the acetic anhydride. The ether layer was then washed successively with 20 ml H_2O , 20 ml 1.2 N HCl and 20 ml saturated NaHCO_3 . The aqueous washes were each extracted with 30 ml diethyl ether, the ether extracts combined, dried with anhydrous MgSO_4 and filtered. The filtrate was

evaporated down to a small volume and loaded on a 15 mm diameter glass column packed with silica gel (mesh 60) to a height of 21 cm. The column was eluted under pressure with 9:1 petroleum ether:ethyl acetate. Fractions containing the desired product were combined and solvent removed under rotary vacuum leaving 85 mg (0.4 mmol) of desired product (**3**). $^1\text{H NMR}$ (CDCl_3): δ 2.15 (s, 6H), 2.5 (m, 6H), 3.0 (m, 1H), 3.70 (s, 3H), 3.80 (s, 3H), 5.25 (dd, $J = 6.0$ Hz, 1H), 5.35 (dd, $J = 6.0$ Hz, 1H); GC/MS: Four peaks appeared on the GC (two diastereomers and their enantiomers). All four had identical mass spectra. m/z : 43 (P), 172, 183. The molecular ion is not seen.

2.3. Conclusion

Failure of the salvinorin A fragment to bind to the kappa opioid receptor indicates that the B, C and D rings are important to the integrity of the molecule for selective binding at the receptor. The next step in this research was to examine the binding modes of salvinorin A and its analogs through molecular modeling studies which may clarify the the observed K_i data and lend some insight into selectivity.

3. Homology Modeling of Opioid Receptors

3.1. Models Based on Bovine Rhodopsin

3.1.1. Experimental

The research presented here will be concerned with only the delta, kappa, and mu opioid receptors. DOR, KOR and MOR will be used throughout this paper to identify the delta opioid receptor, the kappa opioid receptor and the mu opioid receptor, respectively.

The human DOR, KOR and MOR share ~60% sequence similarity in the TM helical and loop regions and they exhibit ~19% sequence similarity with bovine rhodopsin. The crystal structure of bovine rhodopsin in the inactive state²⁸ (PDB access ID = 1F88) at a resolution of 2.80 Å was used as the template to construct models of the opioid receptors. The sequences of human DOR, KOR and MOR were aligned using Clustal X^{59,60} (version 1.83) in the multiple alignment mode, using a gap opening penalty of 15 and BLOSUM⁶¹ 30 protein weight matrix. All other values were left as the default values. The results were then aligned to a previous alignment of six receptors (human acetylcholine muscarinic M₁ receptor, human dopamine D₃ receptor, human vasopressin V_{1a} receptor, human δ -opioid receptor, human β_2 adrenergic receptor and bovine rhodopsin) by Bissantz⁶² et al. using ClustalX in the profile alignment mode (gap opening penalty = 15, BLOSUM Series). The resulting alignment of the opioid receptors with bovine rhodopsin is shown in Figure 10. All but bovine rhodopsin of the Bissantz sequences were removed after alignment for clarity.

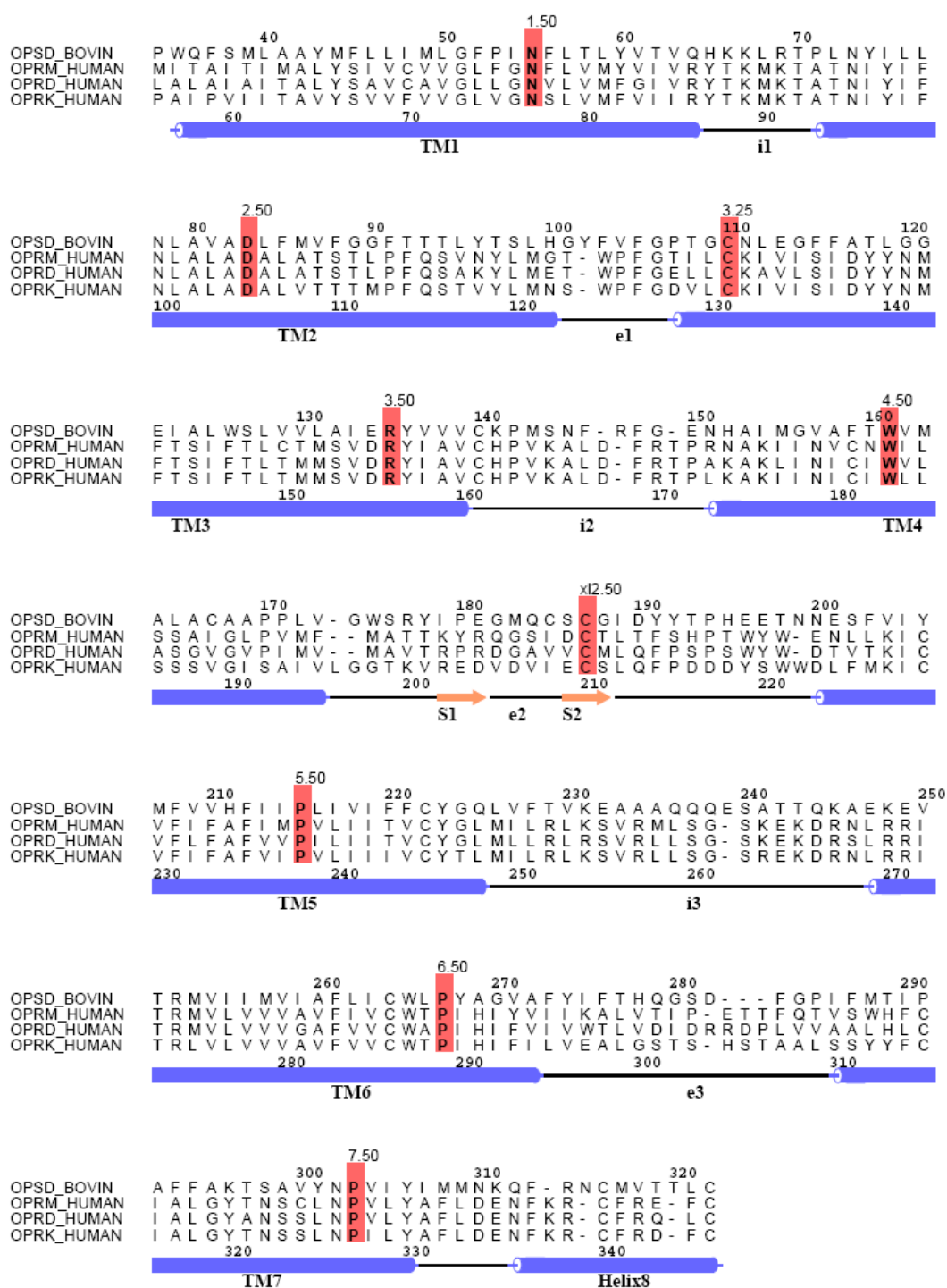


Figure 10. Alignment of the opioid receptors with bovine rhodopsin. Helical regions are in blue. Ballesteros-Weinstein numbering with conserved residues is shown in red. Beta strands are shown with salmon arrows. Sequences are numbered for bovine rhodopsin (top) and kappa opioid receptor (bottom).

Homology modeling of the receptors was performed on a MIPS R14K-based SGI Fuel workstation running SYBYL (version 6.9.2, 2004, Tripos Associates, Inc., St. Louis, MO). The 'A' chain of bovine rhodopsin was used as the template, deleting the ligand retinal, the sugars, ions and waters. The first 33 residues of the N-terminus on the KOR model were removed. These residues have the greatest sequence dissimilarity compared to bovine rhodopsin, are spatially far away from the binding site and are not necessary for small-molecule ligand binding. Residues were mutated individually to the corresponding opioid residues according to the alignment. The appropriate deletions were made. Loop searches were utilized in loop regions to accommodate insertions. Sidechains were added to these loops using SCWRL⁶³ (version 3.0). The receptor was renumbered, hydrogens added, disulfide bridges connected and lone pairs deleted before energy minimization using the Tripos Force Field incorporating Gasteiger-Hückel charges with a distance-dependent dielectric constant = 4 and a nonbonded cutoff = 8 Å to a gradient of 0.05 kcal/(mol × Å).

The substituted cysteine accessibility method (SCAM) provides information on residues which are likely in the binding pocket of GPCRs. SCAM studies of the opioid receptors⁶⁴⁻⁶⁷ have indicated conformational rearrangements in the trans-membrane helices. A helical rotation of trans membrane helix two (TM2) in the opioid receptors has been postulated⁶⁸ based on SCAM studies, chimeric studies and site-directed mutagenesis. Therefore, TM2 was rotated in two parts to prevent distortion within TM2 at the TM2-EL1 loop interface. The first rotation, an axis of rotation was defined by residues 2.41 to 2.53⁶⁹ (Axis 1). Residues 2.57 to 2.66 were then rotated -30° about Axis

1 (counter-clockwise looking down the receptor from the extracellular side). The residues 2.57 to 2.66 defined Axis 2 and these residues were rotated -45° about Axis 2. SCWRL was then used to reassign sidechain conformations on residues 1.29 to 1.47 on TM1 and 2.57 to 2.66 on TM2 followed by energy minimization using the parameters previously described. PROCHECK and PROTABLE (within SYBYL) were then used to identify steric clashes of sidechains and to check backbone geometry and sidechain chirality. Corrections were made and the receptor was again energy-minimized. The structure of inactive bovine rhodopsin crystal (1F88) and the three opioid receptor models constructed from it are shown in Figure 11. The same receptors superimposed are shown in Figure 12.

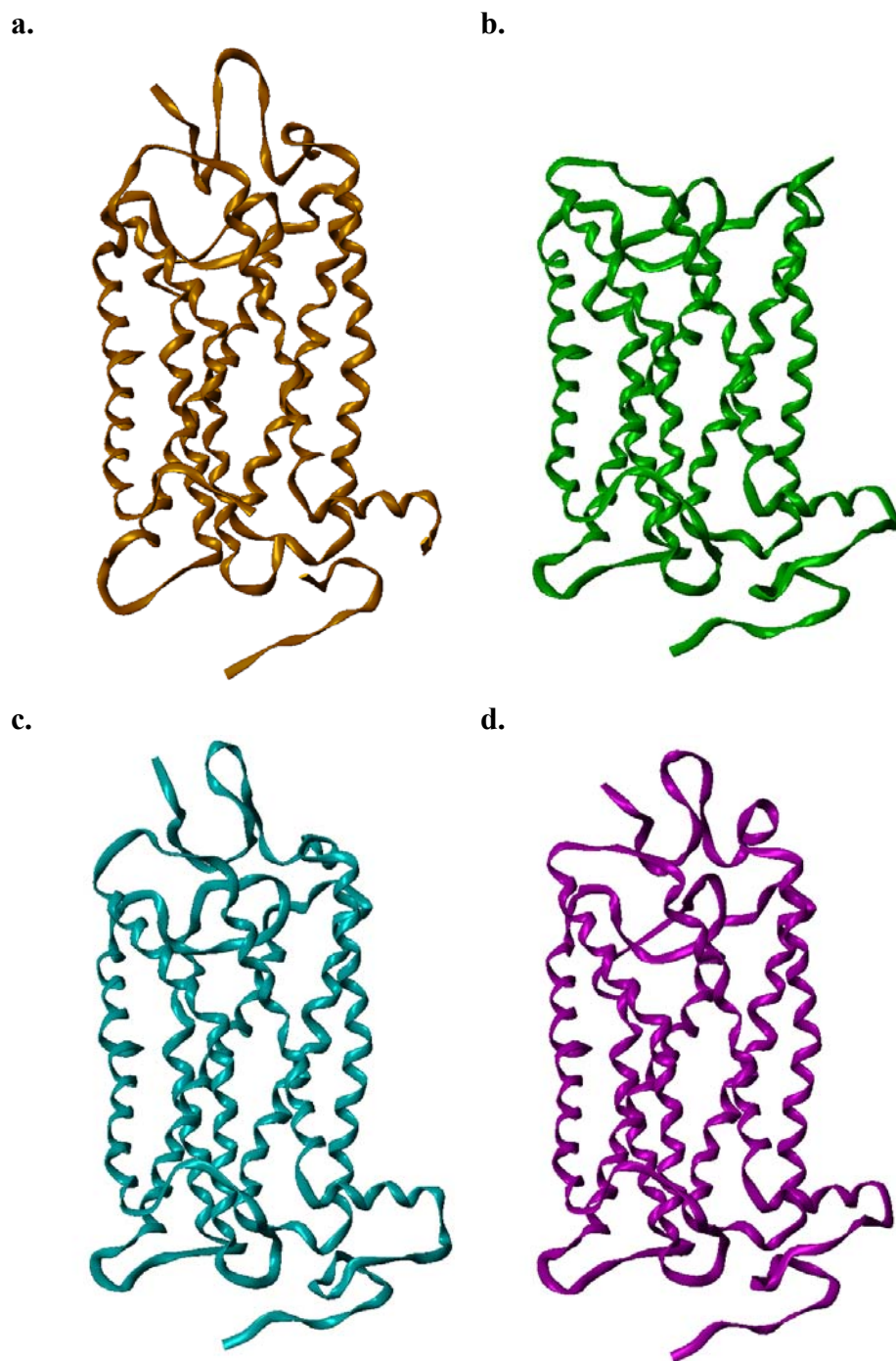


Figure 11. Opioid receptor models based on inactive bovine rhodopsin 1F88 crystal structure. (a) The A chain of bovine rhodopsin template; (b) KOR with N-terminus truncated; (c) DOR; (d) MOR models.

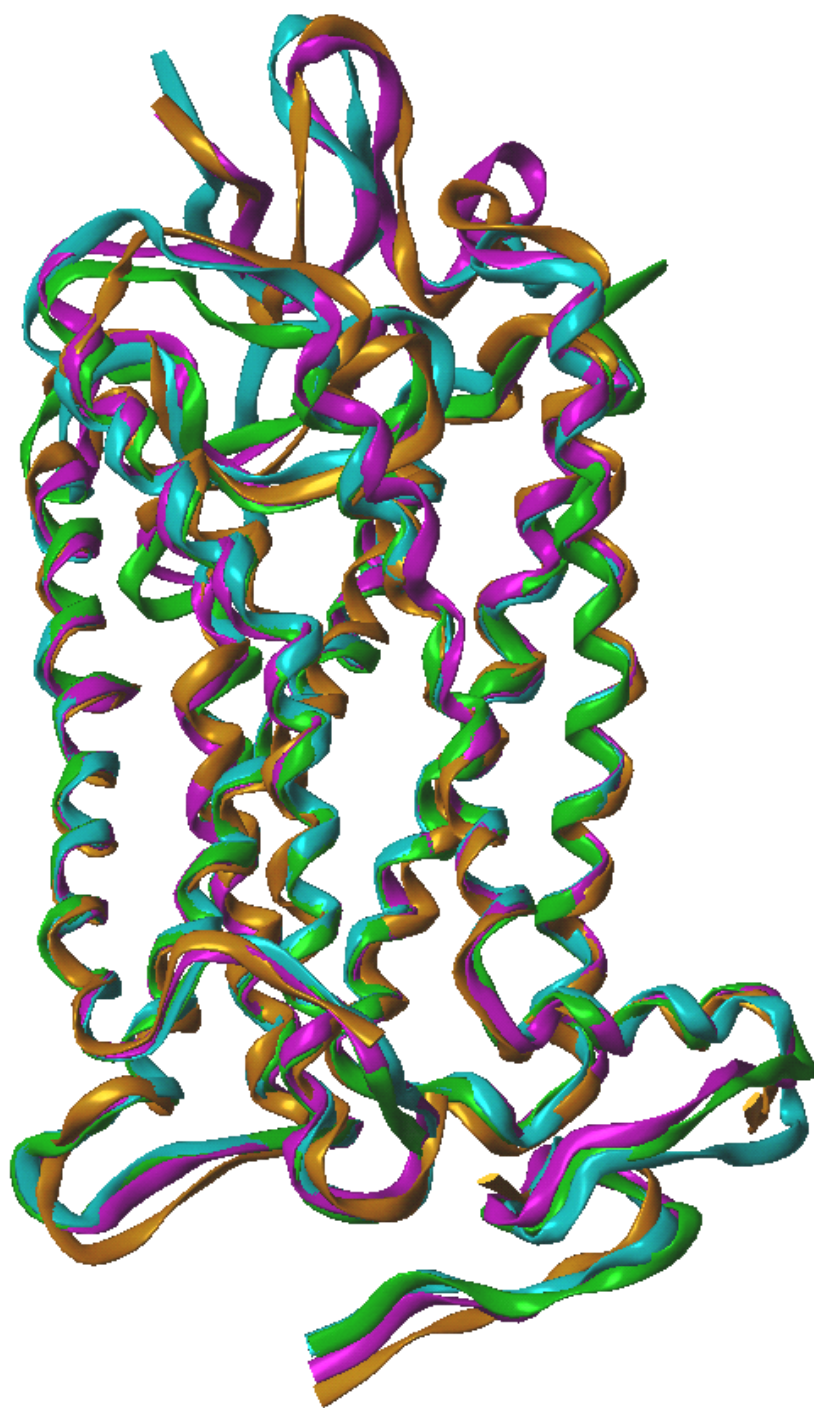


Figure 12. Superimposed bovine rhodopsin 1F88 crystal structure with opioid receptor models. Bovine rhodopsin 1F88 template (yellow); KOR (green); DOR (cyan); MOR (magenta).

Models of the KOR based on the inactive state bovine rhodopsin crystal structure⁷⁰ (PDB ID = 1U19) and the light-activated state bovine rhodopsin crystal structure⁷¹ (PDB ID = 2I37) were kindly provided by Dr. Philip D. Mosier. Details of the building of these two KORs have been described previously.^{68,72,73} The DOR and MOR were then built using the KOR model as a template as described above, except for the rotation of TM2 which was already incorporated into the template KOR models. These six models, three inactive rhodopsin-based models (IR-KOR, IR-DOR and IR-MOR) and three light-activated rhodopsin-based models (AR-KOR, AR-DOR and AR-MOR), were then used in the research presented here. The rhodopsin template and the opioid receptor models constructed from it are shown in Figures 13 and 15. The superimposed models are shown in Figures 14 and 16.

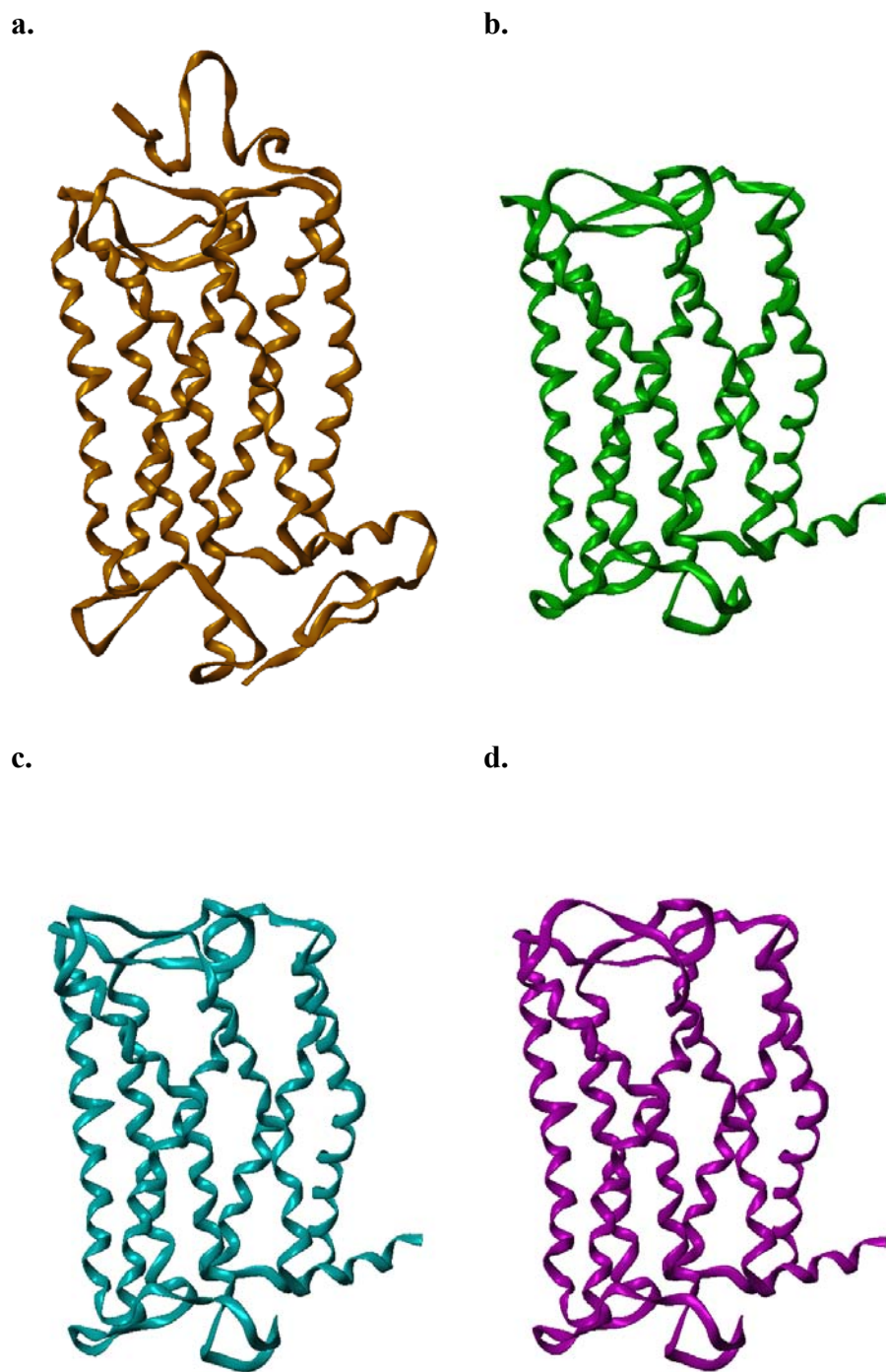


Figure 13. Opioid receptor models based on inactive bovine rhodopsin 1U19 crystal structure. (a) The A chain of bovine rhodopsin template; (b) IR-KOR; (c) IR-DOR; (d) IR-MOR models. The N- and C-termini are truncated in all three opioid models.

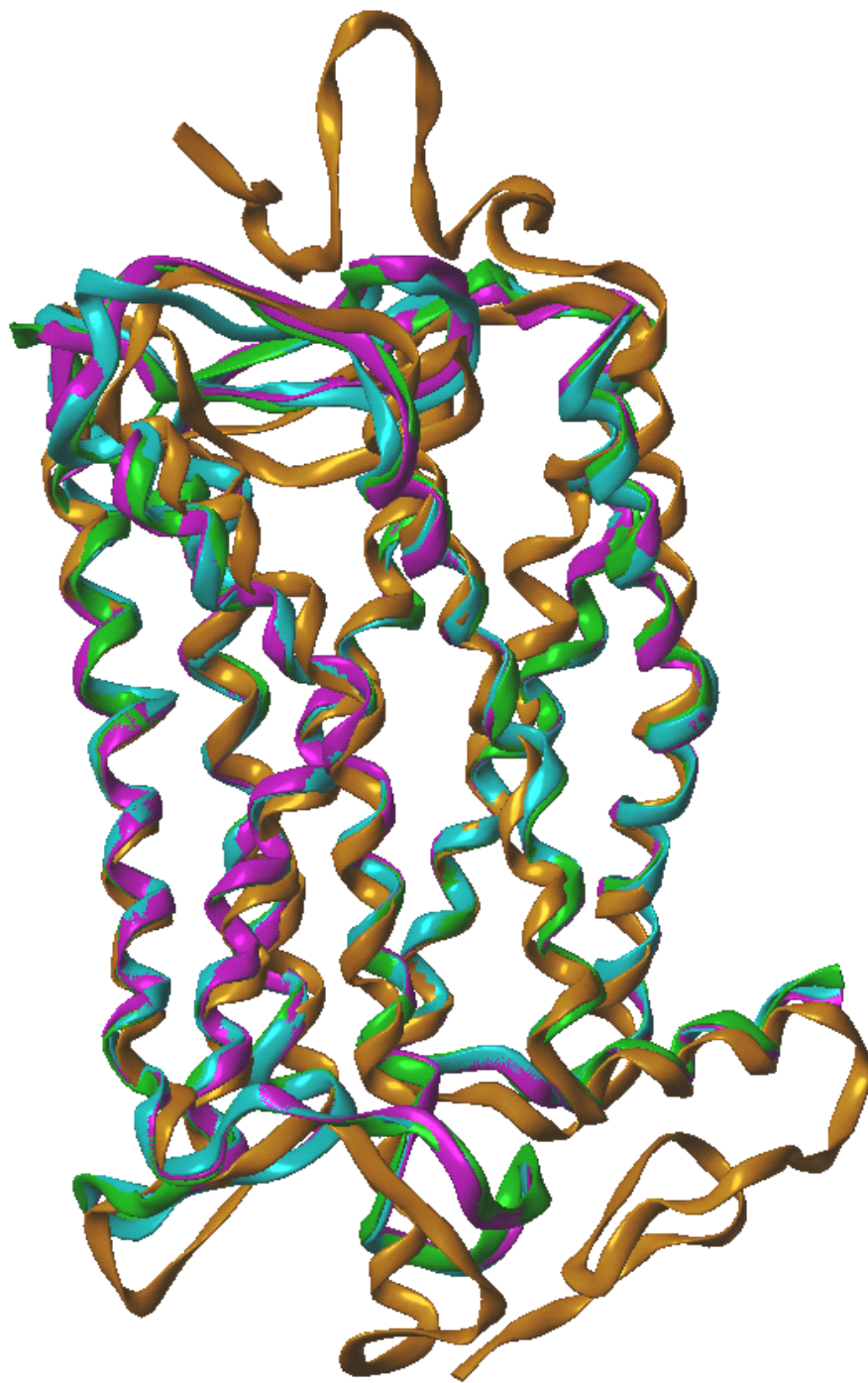


Figure 14. Superimposed bovine rhodopsin 1U19 crystal structure with opioid receptor models. Bovine rhodopsin 1U19 template (yellow); IR-KOR (green); IR-DOR (cyan); IR-MOR (magenta).

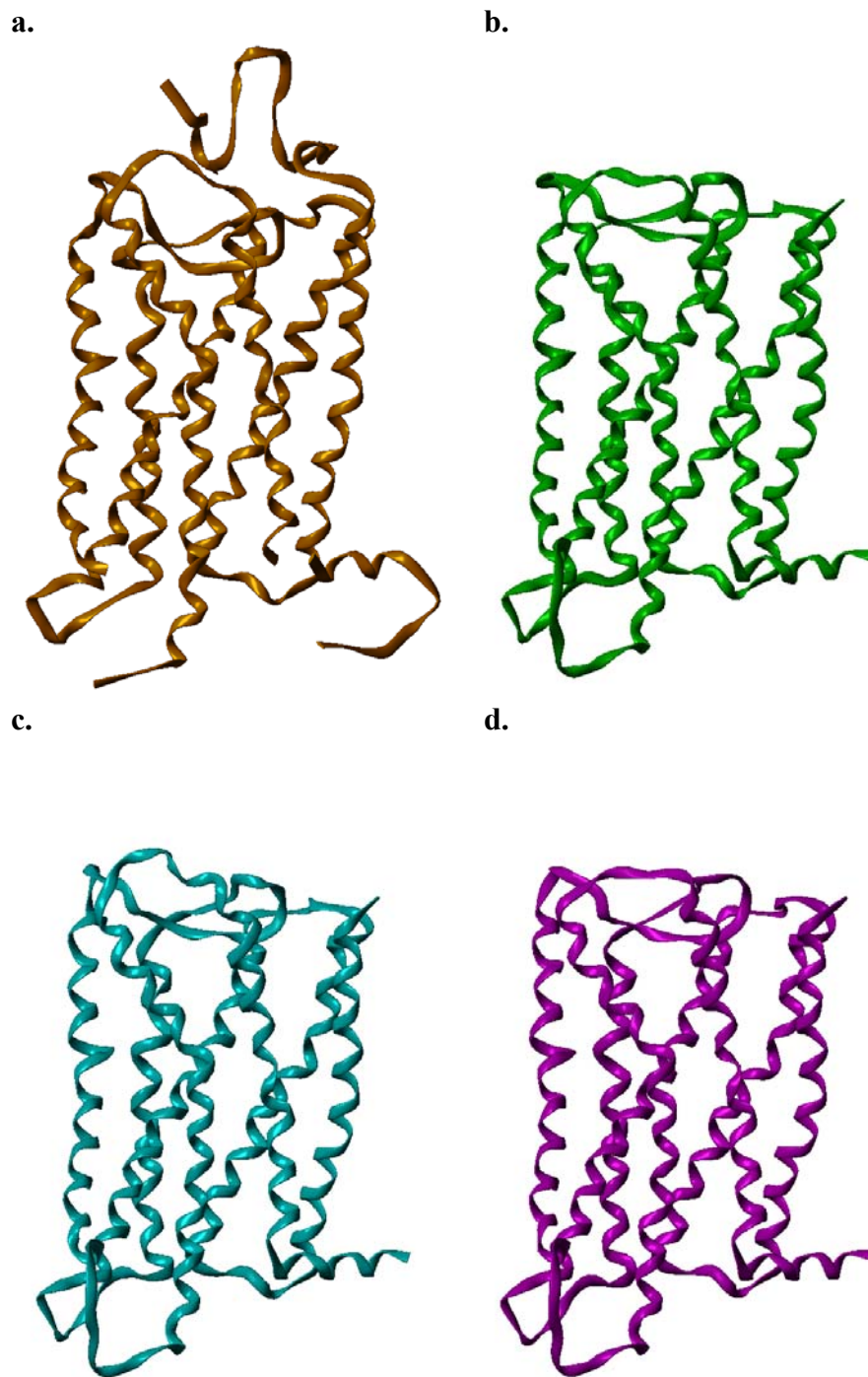


Figure 15. Opioid receptor models based on light-activated bovine rhodopsin 2I37 crystal structure. (a) The A chain of light-activated bovine rhodopsin template; (b) AR-KOR; (c) AR-DOR; (d) AR-MOR models. The N- and C-termini have been truncated in all three opioid models.



Figure 16. Superimposed bovine rhodopsin 2I37 crystal structure and the opioid receptor models. Bovine rhodopsin 2I37 template (yellow); AR-KOR (green); AR-DOR (cyan); AR-MOR (magenta).

3.2. Models Based on the β_2 -Adrenergic Receptor

3.2.1. Experimental

A model of the KOR based on the crystal structure of the β_2 -adrenergic receptor (PDB ID = 2RH1) was also provided by Dr. Philip D. Mosier and was constructed in the following manner:⁷⁴ All molecular modeling was performed using SYBYL 7.3 (Tripos, LLC, St. Louis, MO) except where noted. ClustalX 1.83 was used to align the human KOR and β_2 AR primary amino acid sequences. The hKOR homology model was generated manually using the x-ray crystal structure of the human β_2 AR-T4L fusion protein co-crystallized with carazolol (PDB ID = 2RH1) as the template.⁷⁵ Amino acid residues in the TM regions, IL1, IL2 and Helix 8 were directly mutated to the corresponding hKOR residues. Loop searches were employed to model the remaining loops and to replace the six missing residues of IL3. Like the β_2 -adrenergic receptor, there is evidence⁷⁶ indicating that the EL2 loop segment connecting the extracellular end of TM4 to the EL2-TM3 disulfide bridge in the hKOR is α -helical, and this feature was retained in the present hKOR model. To incorporate the refinement procedures that had previously been applied to successive rhodopsin-based models of the hKOR, the extracellular portion of TM2 was rotated⁶⁸ and the sidechain rotameric states of non-conserved TM helix residues were copied from a previously-described rhodopsin-based activated hKOR model.⁷² The W287(6.48) “toggle” χ_1 torsion angle was set to the “active” (*trans*) conformation.⁷⁷ The N-terminus of the KOR model was truncated and

N-acetylated at P56(1.30), the C-terminus was truncated and *O*-methylated at P347, and the C345 sidechain was palmitoylated. Water molecules involved in conserved GPCR H-bonding networks were added by transferring the water molecule oxygen atoms from the 2RH1 crystal structure to the hKOR model, then removing those with severe clashes and/or fewer than two H-bonding partners. Similarly, the salvinorin A ligand was transferred from the previously-described activated hKOR model⁷² into the current β_2 AR-based hKOR model; receptor-ligand interactions were retained during this procedure. Finally, the hKOR-salvinorin A complex was energy-minimized (Tripos Force Field; energy-gradient termination at 0.05 kcal/(mol \times Å); Gasteiger-Hückel atomic charges; distance-dependent dielectric constant = 4.0) and the structural integrity of the model was assessed using PROCHECK⁷⁸ and the PROTABLE facility within SYBYL. Using this model as a template, the DOR and MOR were constructed in an analogous manner as the inactive and active rhodopsin-based receptors and will be referred to as B-KOR, B-DOR and B-MOR. The β_2 -adrenergic receptor template and the opioid models constructed from it are shown in Figure 17. Superimposed models are shown in Figure 18.

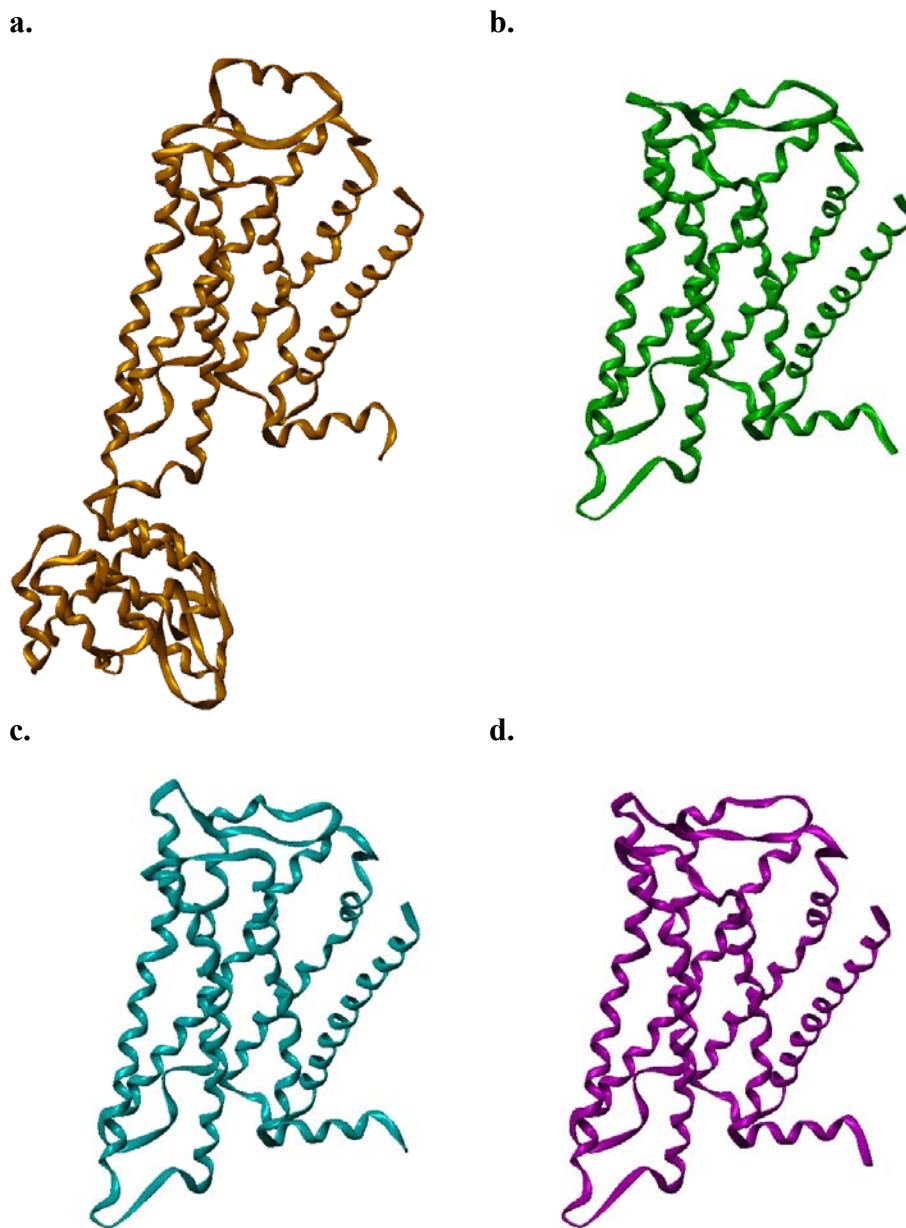


Figure 17. Opioid receptor models based on the β_2 -adrenergic receptor 2RH1 crystal structure. (a) The β_2 -adrenergic receptor (with lysozyme) template; (b) B-KOR; (c) B-DOR; (d) B-MOR models. The N- and C-termini have been truncated on all models.

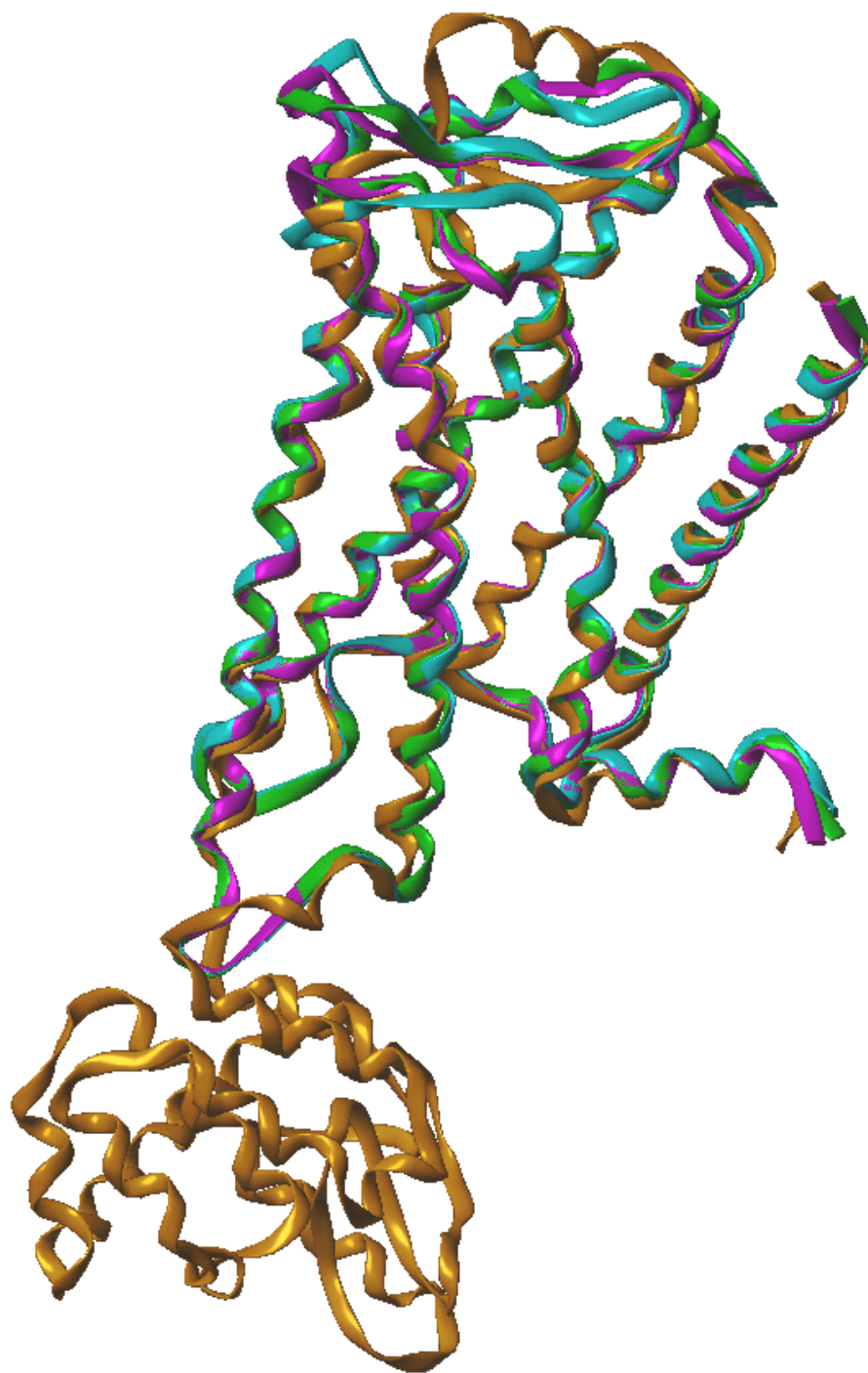


Figure 18. Superimposed β_2 -adrenergic receptor 2RH1 crystal structure and opioids receptor models. The β_2 -adrenergic receptor 2RH1 template (yellow); B-KOR (green); B-DOR (cyan); B-MOR (magenta).

3.3. MODELLER Models

3.3.1. Experimental

Models of the KOR, DOR and MOR were also constructed using the program MODELLER^{79,80} (version 9v3, Andrej Sali, Departments of Biopharmaceutical Sciences and Pharmaceutical Chemistry, and California Institute for Quantitative Biomedical Research, Mission Bay Byers Hall, University of California San Francisco, San Francisco, CA). One hundred models of the KOR were generated by MODELLER using the A chain of inactive bovine rhodopsin crystal structure (PDB ID = 1U19) as the template in which the N- and C-termini had been truncated and the ligand removed. The alignment used to create the input alignment file in PIR format for MODELLER was the Bissantz-opioid receptors alignment used previously (see Figure 2). After generation of 100 models of the KOR, the receptors were energy-minimized using the Tripos force field incorporating Gasteiger-Hückel charges with a distance-dependent dielectric constant = 4 and a nonbonded cutoff = 8 Å to a gradient of 0.05 kcal/(mol × Å). Following minimization, salvinorin A, salvinorin B and the kappa antagonist 5-guanidinylnaltrindole (GNTI) were docked in each of the 100 KOR models generated by MODELLER using the program GOLD⁸¹ (Genetic Optimization of Ligand Docking, version 3.1, Cambridge Crystallographic Data Centre, Cambridge, UK). Ten docking runs were performed for each ligand. The best-ranking solutions as determined by GOLD score for each ligand docked in each of the 100 receptors were visually inspected. Receptor number 36 of the 100 MODELLER-generated KORs was chosen as the best

overall KOR model based on GOLD scores and consistency with experimental biochemical studies. The model of the KOR chosen (number 36) is shown in Figure 19.

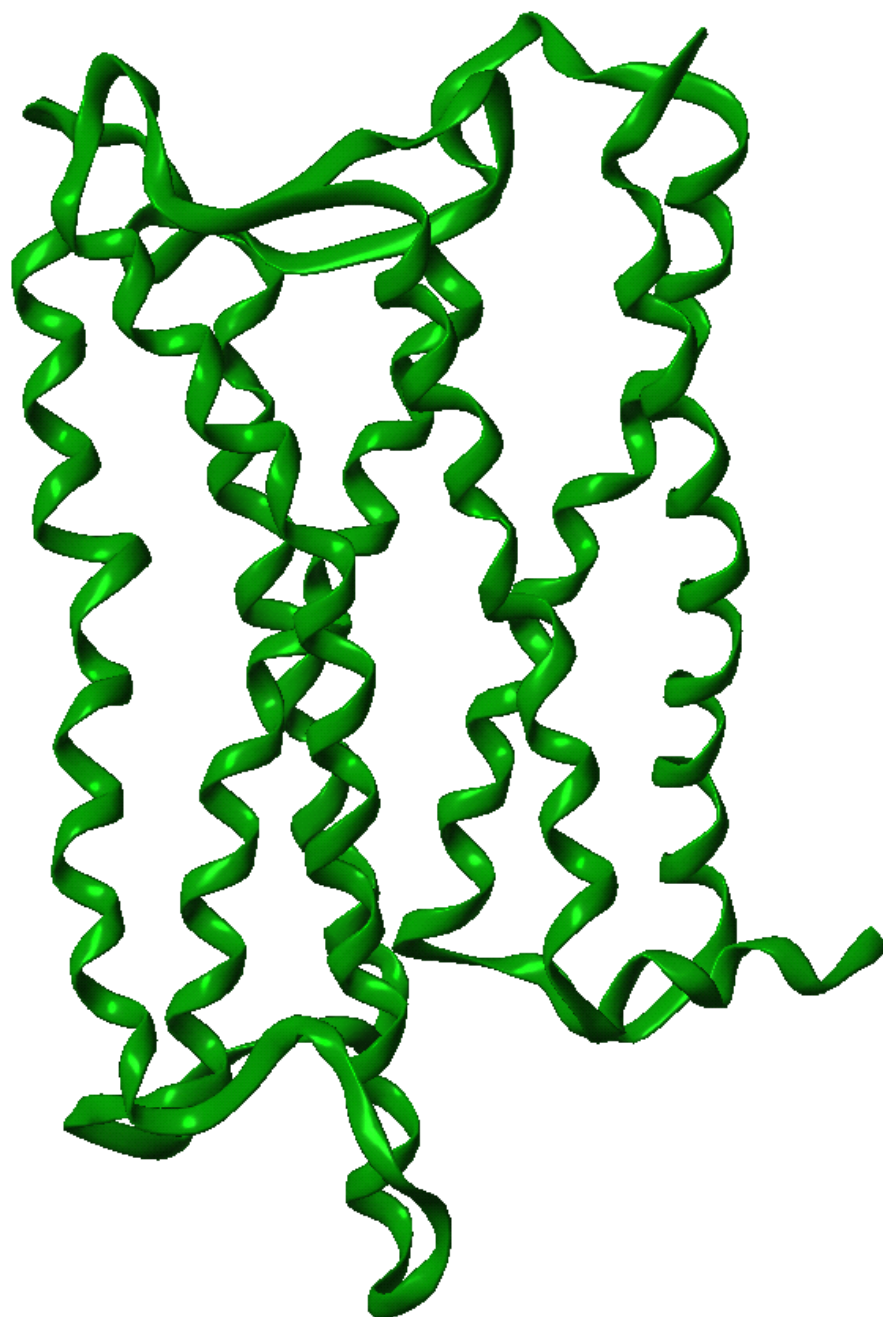


Figure 19. KOR model number 36 of the MODELLER-generated receptors. The N- and C-termini have been truncated.

3.4. Determining Best Models for Ligand Docking

3.4.1. Experimental

In order to determine which set of homology models to use for docking ligands a study was undertaken to compare the KOR, DOR and MOR models based on the inactive form of bovine rhodopsin (IR-KOR, IR-DOR and IR-MOR), the light-activated rhodopsin (AR-KOR, AR-DOR and AR-MOR) and the β_2 -adrenergic (B-KOR, B-DOR and B-MOR) receptors. The following compounds were selected for docking in the nine receptor models (see Table 5). Work was performed on an HP wx9400 workstation using SYBYL (version 7.3). Each compound was constructed using SYBYL's sketching utility followed by energy minimization applying Gasteiger-Hückel charges with a distance dielectric constant of 4.0 D/Å. Each compound was docked twenty times into each of the nine receptors using the program GOLD (version 4.0). The top-ranking GOLD Scores from each run were used in the comparison (see Table 6). The GOLD Score is made up of four components: 1) protein-ligand hydrogen bond energy (external H-bond); 2) protein-ligand van der Waals (vdw) energy (external vdw); 3) ligand internal vdw energy (internal vdw) and 4) ligand torsional strain energy (internal torsion). The GOLD fitness score is the negative sum of the four energy terms, with the external vdw term being multiplied by a factor of 1.375. This is a correction to encourage protein-ligand hydrophobic interactions. A larger positive GOLD Score indicates higher affinity of the ligand for the receptor. Negative scores usually indicate severe ligand-protein clashes.

Table 5. Compounds docked into the nine models of opioid receptors and their K_i values. Selective compounds are highlighted.

Ligand	Type	K_i (nM) at δ	K_i (nM) at κ	K_i (nM) at μ	Reference
BW373U86	agonist	0.01	17	26	82
SIOM ^a	agonist	1.7	>1000	33	83
BNTX ^b	antagonist	6.2	48	26	84
naltrindole	antagonist	0.2	10.1	6.3	38
TRK-820	agonist	1200	3.5	53	39
bremazocine	agonist	0.2	0.03	0.9	38
5'-GNTI ^c	antagonist	70	0.18	36.9	85
norBNI ^d	antagonist	5.7	0.2	21	38
fentanyl	agonist	152.7	84.8	0.7	38
morphine	agonist	140	46.9	1.1	38
GL-06 ^e	antagonist	306.3	67.02	0.41	86
GL-09 ^e	antagonist	135.2	36.93	0.56	86
etorphine	agonist	1.5	0.2	0.3	38
naloxone	antagonist	67.5	2.5	1.4	38

^aSIOM = 7-spiroindanyloxymorphone, ^bBNTX = benzyldenaltrexone, ^c5'-GNTI = guanidinylnaltrindole, ^dnorBNI = norbinaltorphimine, ^erefers to compounds 6 and 9 from a paper by G. Li, et.al.(see reference in table).

Table 6. Top-ranking GOLD Scores. The highest GOLD Score for each compound at any of the nine receptors is shown in bold type. IR- = inactive rhodopsin-based DOR, KOR or MOR. AR- = active rhodopsin-based DOR, KOR or MOR. B- = β_2 -adrenergic-based DOR, KOR or MOR.

Compound	IR-DOR	IR-KOR	IR-MOR
BW373U86	13.11	20.47	12.31
SIOM	18.25	32.11	-18.26
BNTX	20.51	16.07	16.94
naltrindole	29.68	32.00	-12.22
TRK-820	-8.74	13.22	16.63
bremazocine	18.69	21.88	-4.88
5'-GNTI	-136.47	-87.29	-126.16
norBNI	-322.17	-61.87	-76.76
fentanyl	14.87	23.82	23.23
morphine	34.93	26.80	30.96
GL-06	-5.24	-59.03	-0.97

GL-09	-40.36	-61.04	11.82
etorphine	-2.15	0.87	-5.77
naloxone	38.23	21.63	13.43

Compound	AR-DOR	AR-KOR	AR-MOR
BW373U86	31.68	45.32	29.30
SIOM	-50.75	19.31	-32.93
BNTX	-51.29	54.02	27.20
naltrindole	31.36	45.47	26.13
TRK-820	9.86	33.78	30.48
bremazocine	2.65	36.71	43.69
5'-GNTI	-140.47	-70.84	-99.16
norBNI	-382.57	-157.64	-500.23
fentanyl	20.62	40.08	37.64
morphine	25.89	47.33	41.44
GL-06	26.02	45.73	32.34
GL-09	-61.29	28.02	-31.50
etorphine	-85.95	22.94	26.73
naloxone	23.67	52.73	49.27

Compound	B-DOR	B-KOR	B-MOR
BW373U86	27.22	18.45	-14.38
SIOM	-6.73	-53.70	2.69
BNTX	36.74	-37.64	-23.20
naltrindole	29.30	-8.24	-6.76
TRK-820	42.99	16.84	-14.88
bremazocine	-12.67	-0.64	-7.20
5'-GNTI	-131.74	-118.11	-135.00
norBNI	-83.93	-277.87	-135.66
fentanyl	37.24	34.97	28.47
morphine	4.83	18.26	13.44
GL-06	-0.12	-17.50	-39.79
GL-09	-1.40	-32.37	-26.59
etorphine	-77.43	-80.30	-25.36
naloxone	10.48	22.31	11.06

3.4.2. Results

From the data it can be seen that the receptors based on the light-activated rhodopsin showed the highest GOLD scores for all but three compounds. The beta

adrenergic-based receptors showed the most clashing of docked compounds (negative GOLD Scores) and lowest overall scores. The GOLD Scores did not correlate well with the selectivity of the test compounds. If, instead of using the top-ranked GOLD Score, the GOLD Score corresponding to the docked position most like the postulated models in the literature is chosen the outcome is similar with AR-MOR and AR-KOR showing the highest scores. Based on this docking study, it was decided to use the light-activated rhodopsin-based kappa opioid receptor model (AR-KOR) for subsequent docking of the salvinorin A analogs rather than the inactive rhodopsin-based (IR-KOR) or the beta adrenergic-based (B-KOR) kappa opioid receptor models. With salvinorin A and many analogs being agonists this is consistent with the light-activated bovine rhodopsin-based model giving the best results.

4. Comparative Molecular Field Analysis (CoMFA)

4.1. Introduction

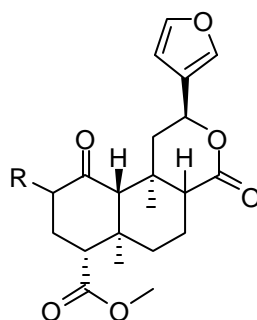
Comparative Molecular Field Analysis (CoMFA) was used to try to relate the binding mode of a large number of salvinorin A analogs to the K_i data in a meaningful way that may help answer the question of selectivity. CoMFA, a three-dimensional quantitative structure-activity relationship (3D-QSAR) methodology, may be used to rationalize and predict ligand-receptor interactions when used in conjunction with homology modeling. In CoMFA, a 3D-QSAR model is constructed by correlating regions of the steric and electrostatic fields with experimentally obtained affinity data for a set of ligands (the training set or TSET). Information contained in the model can then be used for the design and prediction of binding affinities of new ligands (the prediction set or PSET) for the target receptor. Salvinorin A analogs are well-suited for a CoMFA study because the core of the molecule does not vary and is conformationally constrained due to its polycyclic structure, much like the steroid system presented in the initial description of the method.⁸⁷

The quality and nature of the data used to construct the CoMFA model is of prime importance in obtaining an accurate, predictive model. Binding affinity data can vary from lab to lab depending on the assay methods, radioligand and cell lines employed. The choice of radiolabeled ligand can dramatically affect the values obtained^{88,89}, as can the level of gene expression which results in differing receptor densities in cloned cell

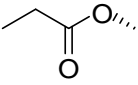
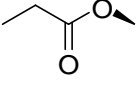
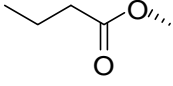
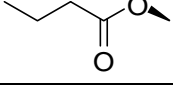
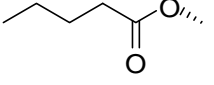
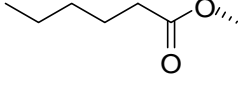
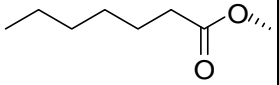
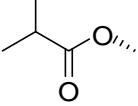
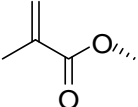
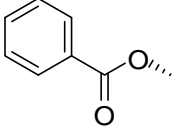
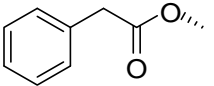
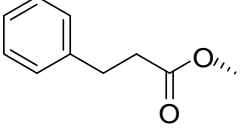
lines.⁹⁰ Therefore pooling of data for a CoMFA study is generally discouraged. In this study, K_i data was taken from a compilation of 280 known salvinorin analogs from several independent labs.^{42,43,45,47-49,91-107} Occasionally, K_i values determined for the same compound would vary greatly. Only those compounds with an exact K_i were used (i.e. estimated values such as those reported as $>10,000$ were not considered). The alignment of compounds is a critical factor in obtaining a good CoMFA model. Therefore, several alignment methods were tested.

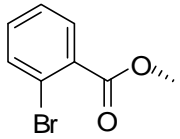
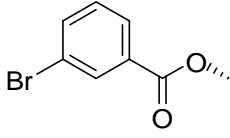
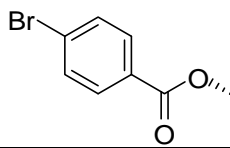
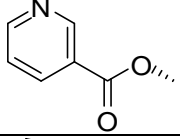
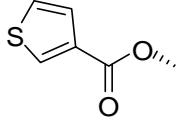
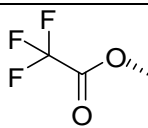
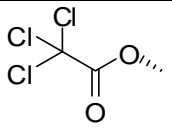
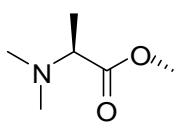
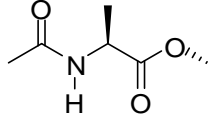
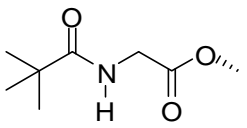
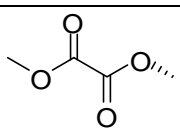
Initial CoMFA models of all analogs taken as a whole gave very poor results with no correlation, indicating that the nature and/or quality of the data may be adversely influencing the results. Therefore, the data was divided into subsets by laboratory, radioligand used, or by substituted position. The analogs used in this study varied at the C-2 and C-4 positions and included furan analogs and C-8 epimers (see Figure 1). The compounds available for this study are shown in Tables 7, 8, 9 and 10.

Table 7. C-2 position analogs.

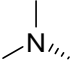
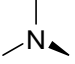
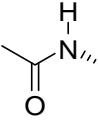
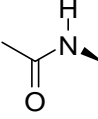
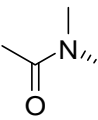
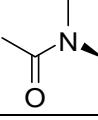
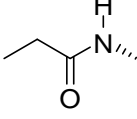
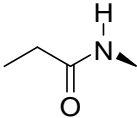
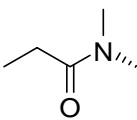
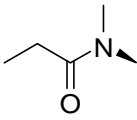
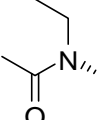


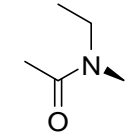
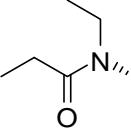
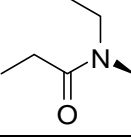

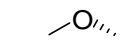
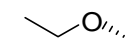
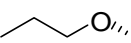
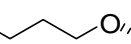
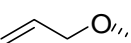
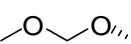
Cpd.	R	C-8 Configuration	$K_i \pm \text{S.E.M.}, \text{ nM}$ (Radioligand) ^a	Reference
1		beta	0.75 ± 0.62 (U) 1.0 ± 0.1 (D) 1.3 ± 0.5 (D) 1.9 ± 0.2 (IO) 2.4 ± 0.4 (D) 4 ± 1 (U) 4.4 (Und.) 5 ± 1 (U) 18.74 ± 3.38 (B)	105 104 47, 95, 96 37, 93, 98 49, 108 42 100 99 92
2	HO...	beta	65.9 ± 8.6 (D) 111 ± 12 (D) 155 ± 23 (D) 280 ± 20 (IO) 8672 (Und.)	104 94 47, 48, 95 37, 44 43
3		alpha	38 ± 2 (IO) 77 ± 4 (D) 140 ± 9 (D) 163 ± 50 (U) 300 (IO)	93 47, 94, 96 48 42 45
4	HO...	alpha	43 ± 5 (D) 304 ± 46 (D)	47, 94 49
5		beta	424 ± 16 (D)	48
6		beta	18 ± 2 (U) 51.18 ± 5.42 (Und.)	42 43

7		beta	1.8 ± 0.1 (IO) 7.2 ± 0.5 (D) 32.63 ± 15.7 (B)	45 47, 48, 95 43, 92
8		beta	641 ± 122 (D)	48
9		beta	4 ± 1 (IO) 4.9 ± 0.6 (D)	98 47, 48, 95
10		beta	665 ± 100 (D)	48
11		beta	15 ± 2 (IO)	98
12		beta	70 ± 4 (IO)	98
13		beta	3199 ± 961.2 (B)	92
14		beta	19 ± 2 (IO)	45, 93
15		beta	42 ± 1 (IO)	45, 93
16		beta	90 ± 2 (IO)	37, 45, 93
17		beta	290 ± 40 (IO)	98
18		beta	180 ± 10 (IO)	98

19		beta	90 ± 7 (IO)	37, 98
20		beta	70 ± 7 (IO)	37, 98
21		beta	740 ± 40 (IO)	37, 98
22		beta	1930 ± 50 (IO)	45, 93
23		beta	260 ± 20 (IO)	37, 98
24		beta	211 ± 37 (U)	99
25		beta	375 ± 42 (U)	99
26		beta	197 ± 19 (D)	47
27		beta	176 ± 5.5 (D)	47
28		beta	90 ± 10 (IO)	98
29		beta	430 ± 10 (IO)	45, 93

30		beta	3.2 ± 0.2 (D)	47, 95
31		beta	83.0 ± 8.5 (D)	47, 95
32		beta	462 ± 20 (D)	47, 95
33		beta	120 ± 4 (IO)	45, 93
34		beta	93 ± 3 (IO) 282 ± 13 (D)	45, 93 47
35		beta	64 ± 2 (IO)	45, 93
36		beta	223 ± 123 (D)	48
37		beta	328 ± 40 (D)	48
38		beta	65.2 ± 24.6 (D)	48
39		beta	28.9 ± 1.0 (D)	47, 48, 95
40		beta	17.6 ± 3.1 (D)	48
41		beta	2.3 ± 0.6 (D)	47, 48

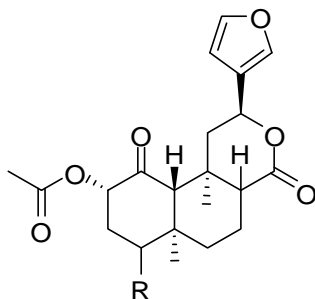
42		beta	168 ± 10 (D)	48
43		beta	90.9 ± 2.5 (D)	47, 48, 95
44		beta	30 ± 2 (IO) 86 ± 22 (U) 149 ± 1 (D)	37 99 48
45		beta	332 ± 41 (D)	48
46		beta	3.2 ± 0.1 (D)	48
47		beta	16.5 ± 1.1 (D)	47, 48
48		beta	374 ± 19 (D)	48
49		beta	117 ± 63 (D)	48
50		beta	1.6 ± 0.1 (D)	48
51		beta	6.9 ± 1.1 (D)	47, 48
52		beta	27.6 ± 1.8 (D)	48

53		beta	240 ± 17 (D)	48
54		beta	38.1 ± 1.9 (D)	48
55		beta	376 ± 36 (D)	48
56	HS \dots	beta	11.2 (Und.) 12.27 ± 1.44 (Und.) 54.5 ± 25.7 (U)	100 43 105
57		beta	7.50 ± 1.03 (Und.) 7.9 (Und.) 8 ± 1 (U) 18.4 ± 7.9 (U)	43 100 99 105
58	Cl \dots	beta	607.6 ± 102.7 (Und.)	43
59	Cl \blacktriangleleft	beta	608 ± 103 (U)	99
60	Br \blacktriangleleft	beta	261 ± 67 (U)	99
61		beta	220 ± 12 (D)	47, 48, 95
62		beta	7.9 ± 0.3 (D)	47, 48, 95
63		beta	28.7 ± 3.0 (D)	47, 95
64		beta	35.8 ± 5.1 (D)	47, 95
65		beta	60.1 ± 5.1 (D)	47, 95
66		beta	0.4 ± 0.02 (D) 0.60 ± 0.07 (D)	47, 94 108

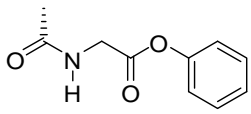
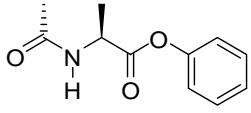
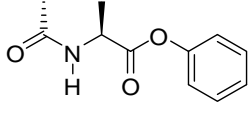
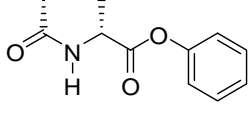
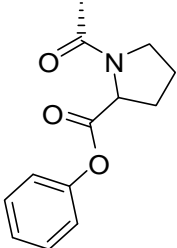
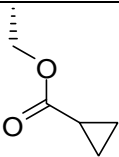
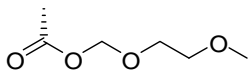
67		alpha	30 ± 3 (D)	47, 94
68		beta	75.7 ± 5.9 (D)	47, 95
69		beta	2.3 ± 0.1 (IO)	45, 93
70		beta	227 ± 32 (D)	47
71		beta	60 ± 6 (IO)	98
72		beta	50 ± 5 (IO)	98
73		beta	546 ± 140 (U)	105
74		beta	151 ± 53 (U)	105

a) **D** = [³H] Diprenorphine (antagonist), **IO** = [¹²⁵I] IOXY (antagonist) 6 beta-Iodo-3,14-dihydroxy-17-cyclopropylmethyl-4,5 alpha-epoxymorphinan (IOXY), **U** = [³H] U69,593 (agonist), **B** = [³H] Bremazocine (agonist), **Und.** = Undetermined

Table 8. C-4 position analogs.

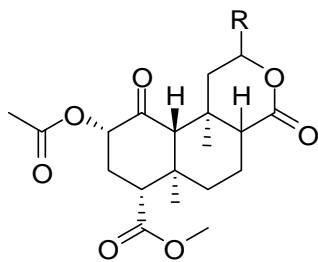


Cpd.	R	C-8 Configuration	$K_i \pm \text{S.E.M.}, \text{nM}$ (Radioligand) ^a	Reference
75		beta	43.4 ± 4.93 (D) 347 ± 53 (U) 1000 ± 269 (D)	106 42 48
76		alpha	769 ± 180 (D)	48
77		alpha	17.3 (D) 48.6 ± 4.4 (D)	47 96, 106
78		beta	28.5 ± 0.9 (D) 365 ± 26 (D)	96 47
79		beta	201 ± 26 (D) 679 ± 112 (D)	96 47
80		beta	99.6 ± 15.9 (D)	96
81		alpha	110 ± 15 (D)	96
82		beta	1392 ± 218 (D)	48
83		alpha	475 ± 41 (D)	96
84		beta	470 ± 92 (D)	47, 96

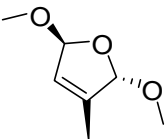
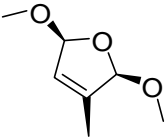
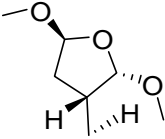
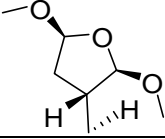
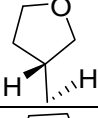
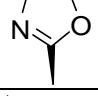
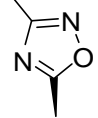
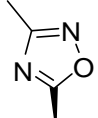
85		alpha	1147 ± 721 (D)	47
86		beta	19.3 (D)	47
87		alpha	18.1 (D)	47
88		beta	14.2 ± 0.8 (D) 26.9 ± 1.8 (D)	47 96
89		beta	210 ± 32 (D)	47, 96
90		beta	221 ± 19.1 (D)	106
91		beta	613 ± 54.1 (D)	106

a) See footnote Table 1.

Table 9. Furan analogs.

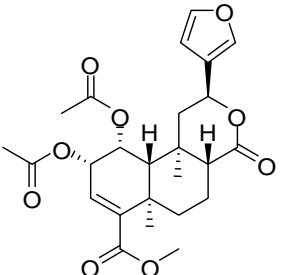
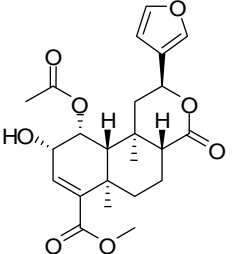
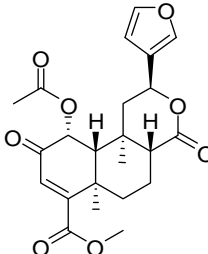
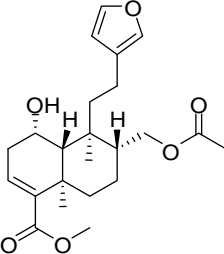
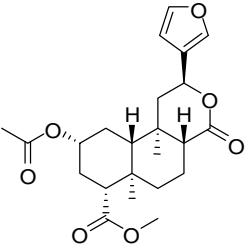


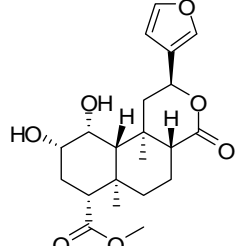
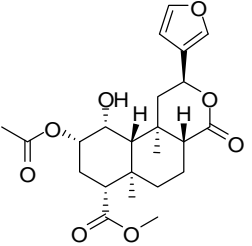
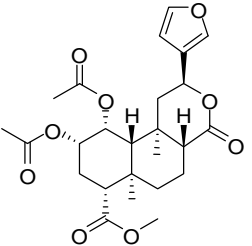
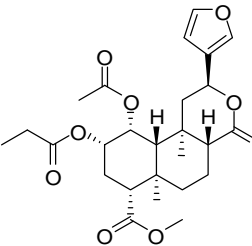
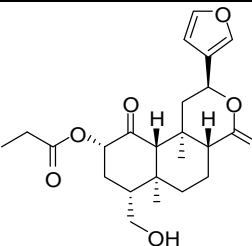
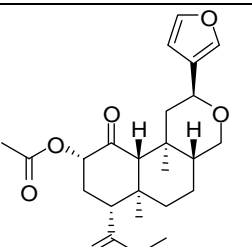
Cpd.	R	C-8 Configuration	$K_i \pm \text{S.E.M.}, \text{ nM}$ (Radioligand) ^a	Reference
92		beta	390 ± 30 (IO)	44
93		beta	7020 ± 750 (IO)	44
94		beta	840 ± 90 (IO)	97
95		beta	410 ± 30 (IO)	97
96		beta	1620 ± 110 (IO)	97
97		beta	8530 ± 550 (IO)	97
98		beta	3.0 ± 0.2 (IO)	44

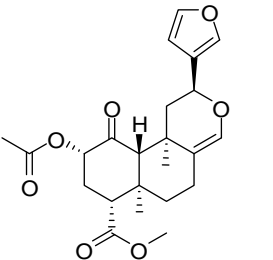
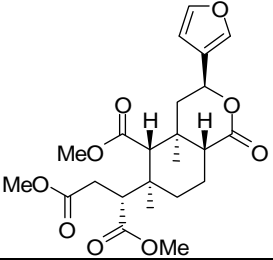
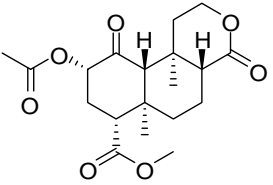
99		beta	420 ± 20 (IO)	44
100		beta	180 ± 20 (IO)	44
101		beta	25 ± 1 (IO)	44
102		beta	125 ± 4 (IO)	44
103		beta	3.7 ± 0.2 (IO)	44
104		beta	300 ± 20 (IO)	44
105		beta	56 ± 3 (IO)	44
106		alpha	990 ± 60 (IO)	44

a) See footnote Table 1.

Table 10. Miscellaneous analogs.

Cpd.	Structure	$K_i \pm \text{S.E.M.}, \text{ nM}$ (Radioligand) ^a	Reference
107		1022 ± 262 (U) 5378 ± 2595 (Und.)	42 43
108		76070 ± 47668 (Und.)	43
109		418 ± 117 (D)	104
110		230 (U) 230 ± 21 (D)	101 104
111		18 ± 2 (U) 20.13 ± 3.30 (Und.)	42 43

112		3190 ± 150 (IO)	93
113		1125 ± 365 (U)	42, 43
114		650 (IO) 14196 ± 2604 (Und.)	45 43
115		650 ± 30 (IO)	93
116		347 ± 53 (U)	42
117		6 ± 1 (U) 5.62 ± 0.68 (Und.)	42 43

118		6 ± 2 (U) 13.71 ± 3.58 (Und.)	42 43
119		2900 ± 400 (U)	101
120		3400 ± 150 (IO)	44

a) See footnote Table 1.

4.2. Experimental Methods

CoMFA studies were performed using SYBYL software (version 7.3, Tripos Associates, St. Louis, MO) on an HP xw9400 workstation running Red Hat Enterprise Linux 4. The hKOR model used here was built based on the coordinates of activated bovine rhodopsin crystal as previously described.^{29,33,34} Compounds were constructed using the crystal structure of Salvinorin A⁵, Cambridge Structural Database (CSD) code = BUJJIZ, as the template and then energy-minimized using the Tripos Force Field (Gasteiger-Hückel charges; distance-dependent dielectric constant = 4.0; default parameters elsewhere). Because the alignment is critical to a good CoMFA model outcome, several alignment methods were tested for use. Alignment methods included

the Fit Atoms function within SYBYL with salvinorin A as the template, SYBYL module GALAHAD, SYBYL module Surflex-Sim and FlexS¹⁰⁹ (version 1.20.3, BioSolveIT GmbH, Sankt Augustin, Germany). The Fit Atoms alignment uses a point-by-point rigid alignment of a molecule to the template. In this case, three atoms (C-2, C-4, and C-5) in the salvinorin A core and the corresponding three atoms in the molecule to be aligned were chosen. GALAHAD uses a two-stage alignment to generate a pharmacophore hypothesis and the aligned molecules. The first stage uses an advanced genetic algorithm and aligns the molecules in torsional space; the conformers generated are then aligned in Cartesian space. The first stage is a flexible alignment, while in the second stage the molecules are treated as rigid. Because a common template molecule could not be constructed that would include all molecules in the database, a number of structures were dropped from the GALAHAD alignment during the run and a complete database of salvinorin analogs could not be generated. Therefore, the GALAHAD alignment was not used to generate the final CoMFA alignments. Surflex-Sim uses a morphological similarity algorithm to generate alignments.¹¹⁰ Morphological similarity measures the distance to the molecule surface from observation points in space on a uniform grid. Minimum distances from each point are measured to the vdW surface, a H-bond acceptor or negatively charged atom, and a H-bond donor or positively charged atom. The input molecule is fragmented and each fragment conformationally searched and aligned to the target molecule to maximize the morphological similarity to the target. Remaining molecule fragments are then added iteratively using the positioned fragments as a guide. FlexS predicts the conformation and orientation of a ligand molecule relative to a

reference molecule which is treated as rigid. Therefore, the reference molecule used should be a high affinity compound and represent the bound conformation. The molecule to be superimposed is partitioned into fragments. An anchor fragment is placed first and the remaining fragments are added iteratively allowing conformational flexibility at each step.¹⁰⁹ To explore the effect of ligand superimposition on the resulting statistical models, three methods of alignment were employed in each of the following two studies. The first alignment used was generated by selecting the docked solution which most resembled the postulated model of Salvinorin A in the KOR^{29,33,34} (Figure 21) by first looking for the best interaction of the furan ring with Q115(2.60) and Y320(7.43) and second, inspecting for the best interactions of the rest of the molecule with receptor residues. The result in most cases was the first-ranked solution for each ligand. The second alignment method (using the same data set) was performed with FlexS (version 1.20.3, BioSolveIT GmbH, Sankt Augustin, Germany). The FlexS template (Compound **9**) used for this study is shown in Figure 20. Compound **9** was used as the template for this alignment because it is the longest C-2 chain which still retains high affinity. The third alignment method, a manual realignment of the docked poses in the receptor-docked alignment, was performed by aligning all docked poses from the first alignment method to salvinorin A using the SYBYL Fit Atoms method.

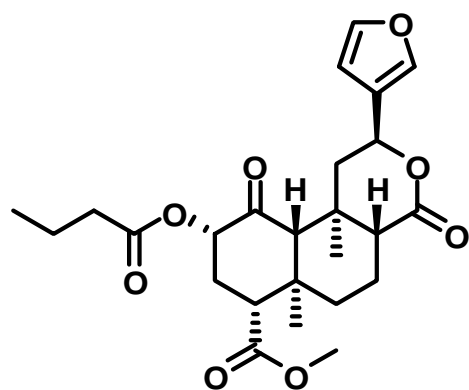


Figure 20. FlexS template molecule (Compound 9).

In the 3D-QSAR analysis, all aligned training set (TSET) molecules are placed in a cubic lattice (grid) which is divided into hundreds (or thousands) of points at a regular spacing. In this CoMFA study, the default grid spacing of 2.0 Å was used unless region focusing was employed. In some cases, further statistical improvement could be made using the advanced CoMFA technique of region focusing.¹¹¹ Region focusing divides the lattice grid into multiple grids with a smaller lattice spacing and then performs a CoMFA analysis on each of these smaller grids. Grids below a determined q^2 cutoff are eliminated and another CoMFA analysis is performed on the remaining grids as a whole resulting in enhancement of those lattice points and, in some cases, an improved statistical outcome.

Lennard-Jones 6-12 and Coulomb potentials were used to calculate the steric and electrostatic interaction fields, respectively. An sp^3 -hybridized carbon atom with a charge of +1 was used as the probe atom. The standard default settings were used, except for the steric and electrostatic cutoff values which were each varied by increments of 5 kcal/mol from 10-50 kcal/mol to obtain the highest value of q^2 for each dataset alignment. All K_i data were converted to pK_i ($-\log K_i$). The pK_i represents the dependent variable while the CoMFA field potentials at each grid point represent the independent variables in the partial least squares (PLS) regression analyses. The standard “leave-one-out” (LOO) cross-validation method was used to obtain the predictive correlation coefficient q^2 and the optimal number of principal components (PCs). The optimal number of PCs corresponds to the smallest error of prediction and the highest q^2 . The PLS analysis was then repeated with no validation using the optimal number of PCs to

generate the CoMFA model. The r^2 statistic and the standard error of estimate (SEE) were obtained from this model. The r^2 is a measure of the amount of variation in the dependent variable that can be ascribed to variation in the independent variables. The r^2_{pred} was obtained from the linear regression of the experimental vs. predicted pK_i values of the prediction set (PSET). A column filter of 3 or 4 kcal/mol was applied to improve efficiency and reduce noise in the field data. The filter procedure excludes those columns whose grid point potentials vary below the set cutoff. In the first model, region focusing¹¹¹ was used to improve the model statistics.

Experimentation with CoMFA parameters such as grid spacing (varying from 2.0Å to 0.75Å) while changing the default field setting from TriposStd to indicator gave no significant improvement for the standard CoMFA analyses. Therefore, the standard default settings were used except for the electrostatic and steric field cutoff values. It was found that significant improvement could be made in the CoMFA models by adjusting these two parameters. Initial attempts were made to arrive at a CoMFA model by pooling all salvinorin A analogs with an exact K_i . However, a suitable model with good statistical meaning could not be generated using this approach. Therefore, it was decided to focus on C-2 analogs only. The C-2 analogs contained the largest number and diversity of R groups. The C-4 analogs were omitted primarily because they exhibited either very high or very low affinity with few compounds falling mid-range. The C-2 analogs were used further subdivided into two groups based on the radioligand used in the binding assay.

In this work, two independent CoMFA studies were undertaken, one in which [¹²⁵I]IOXY (6β-iodo-3,14-dihydroxy-17-cyclopropylmethyl-4,5α-epoxymorphinan) was used as the assay radioligand (Model 1) and a second in which [³H]diprenorphine was the assay radioligand (Model 2). Both radioligands are non-selective opioid antagonists. Compounds that are protonated at physiological pH (e.g. amines) and compounds with a $K_i > 1,000$ nM were not included in the dataset. Protonated compounds would, perhaps, form an ion-pair interaction with D138(3.32) of transmembrane helix 3 (TM3) or E209(XL2.49) of the extracellular loop 2 (EL2) which may result in a significant difference in the binding mode compared to that of Salvinorin A. MOPAC charges (AM1) were then applied to each aligned dataset before initiating the CoMFA analyses. Training set compounds were chosen randomly with the only criterion being that they cover a wide range of K_i values and include a variety of functional groups. Docking of the salvinorin compounds was performed using GOLD (version 4.0, Cambridge Crystallographic Data Center, Cambridge, UK). Twenty docking runs were performed for each compound in the dataset.

4.3. Results and Discussion

It should be noted that affinity data obtained using [³H]U69,593 and [¹²⁵I]IOXY as the radioligand used rKOR and the data obtained using [³H]diprenorphine and [³H]bremazocine used hKOR. However, upon careful comparison of the rKOR and hKOR models it was observed that the non-conserved residues were generally not in the

binding pocket area of the receptor. Therefore, it was assumed that the K_i would not be significantly affected by receptor type. In cases where there were multiple K_i values given for a compound, the K_i used was chosen taking into account probable structure-affinity relationship trends.

In the postulated model of Salvinorin A docked in the hKOR as previously described⁷² (see Figure 21), the oxygen of the furan ring may form a hydrogen bond with both Q115(2.60) and Y320(7.43). A hydrogen bond interaction with these two residues is supported by site-directed mutagenesis studies^{33,34,88} in which KOR mutants Q115A, Y320A and Y320F all showed a substantial decrease in the binding affinity of salvinorin A as compared to wild type KOR. An additional hydrogen bond may possibly exist between Y312(7.35) and the methoxy oxygen of the C-4 position methyl ester, although the KOR mutants Y312A and Y312F showed only a modest decrease^{34,88} in the binding affinity of salvinorin A (4.5-fold decrease for the KOR Y312A mutant).¹¹² In addition, there is a hydrophobic interaction between Y313(7.36) and the methyl group of the C-2 position acetoxymoiety of Salvinorin A which is supported by site-directed mutagenesis studies^{34,88} in which there are substantial losses of affinity for the KOR Y313A mutant but little or no loss for the Y313F mutant indicating a hydrophobic interaction rather than a hydrogen bond interaction. Chimeric studies^{29,88,89} also indicate the importance of residues in TM2 and TM7 in the binding of salvinorin A to the KOR. In addition, substituted cysteine accessibility method (SCAM) studies^{29,33,34} indicate that these residues are accessible in the binding pocket. Other models of salvinorin A docked in the KOR have also been postulated by Kane, et al.^{112,113} based on mutagenesis data and

Singh, et al.¹¹⁴, that are consistent with their pharmacophoric model obtained using a 3D-QSAR method.

In the proposed binding model of Salvinorin A, (see Figure 21), a hydrophobic binding pocket consisting of Y312(7.35)¹¹⁵, Y313(7.36) and I316(7.39) surrounds the C-2 functional group of Salvinorin A. E209(XL2.49) is positioned behind and does not interact with Salvinorin A although subsequent research shown here postulates its interaction with amine analogs.

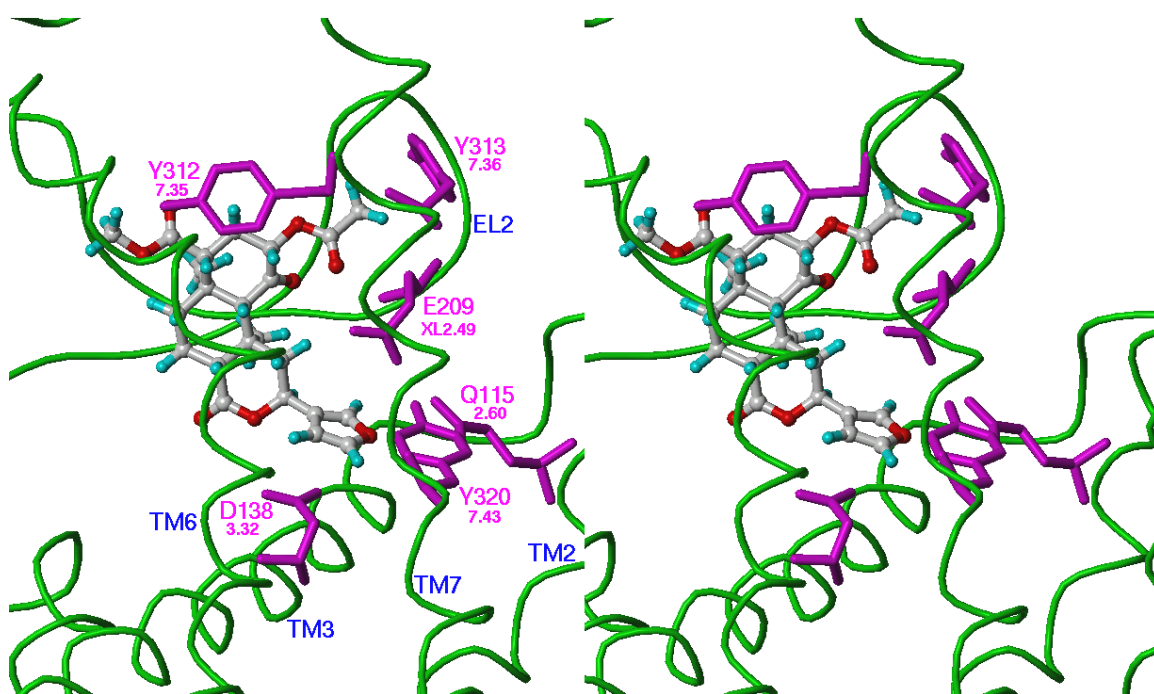


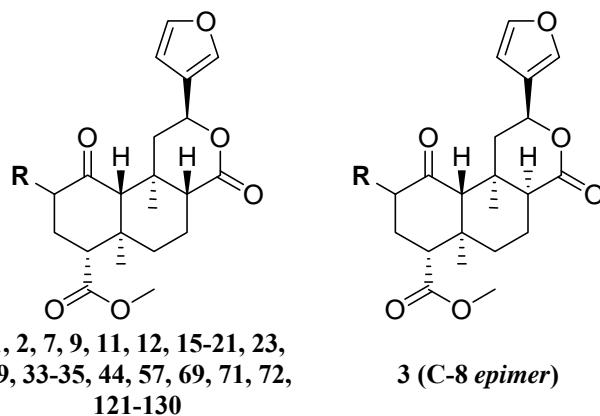
Figure 21. Stereo view of salvinorin A docked in the kappa opioid receptor. Salvinorin A is shown in ball-and-stick and colored according to atom type (grey = carbon, red = oxygen). Residues are colored magenta.

One can make the assumption that the C-2 position analogs would bind in much the same way as Salvinorin A since the core of the molecule, in most cases, remains identical. If this is the case, then methods such as FlexS or a manual fit, which produce a “tight” alignment of molecules (low RMSD values for those atoms in the common core structure), might be expected to result in a good CoMFA model. However, it was found that the receptor-docked alignment, in which many of the molecules’ docked position and/or orientation deviated from Salvinorin A (some by as much as 4.5 Å), was found to be superior to FlexS and the Fit Atoms realignment. In fact, in previous work (data not shown), several alignment methods available in the SYBYL package were evaluated including manual atom fitting, GALAHAD, database align and Surfex-Sim which resulted in well-aligned molecules but gave poor CoMFA statistics. Salvinorin A analogs may thus bind in a similar, but non-identical manner to the parent. Accordingly, a receptor-docked alignment may paint a better picture for predictive purposes.¹¹⁶ To further explore CoMFA models based on docked ligand conformation, a realignment of the docked poses was performed based on the “ligand’s point of view”. In this procedure, a rigid realignment of the docked solutions was performed using atoms of the core ring system. This realignment resulted in the core of the molecules being very well aligned but exhibited the poorest CoMFA statistics of the three types of alignments: FlexS, receptor-docked or realigned. In the FlexS alignment the assumption is made that all analogs bind in an identical manner to a high-affinity compound (Compound 9). The receptor-docked alignment allows for conformational diversity of the C-2 position

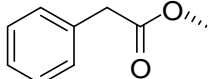
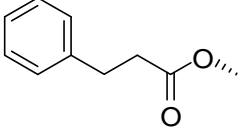
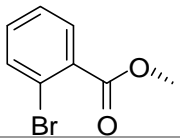
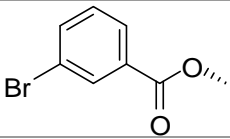
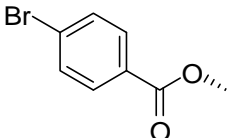
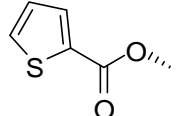
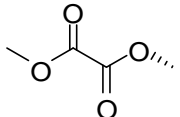
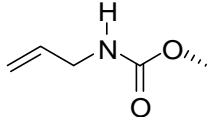
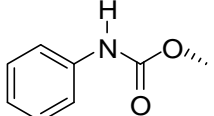
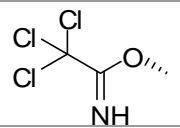
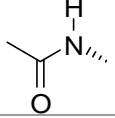
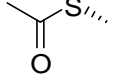
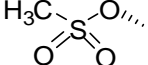
functional group and the core of the molecules to bind in a non-identical manner. The realignment method takes out the translational component that was due to the docking.

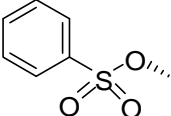
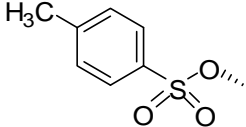
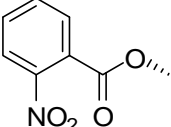
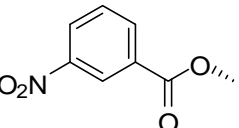
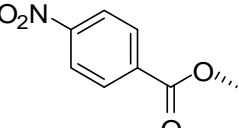
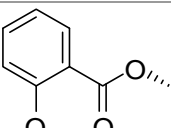
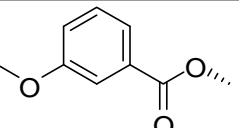
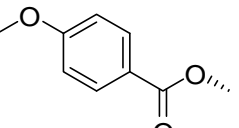
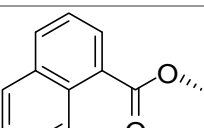
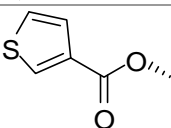
Model 1 consists of a dataset of 34 salvinorin A analogs in which [¹²⁵I]IOXY was used as the assay radioligand for the determination of affinity. This dataset was divided into a TSET of 23 compounds and a PSET of 11 compounds (Table 11). The three alignments employed are shown in Figure 22b (receptor-docked method), Figure 22c (FlexS method) and Figure 22d (realigned method). Although FlexS results in a “tighter” alignment of the molecules, this alignment gave statistically poorer results (see Table 14) with a $q^2 = 0.311$ as compared to the model based on the receptor-docked alignment with a region-focused $q^2 = 0.592$ for the identical training and predicted sets. Region focusing did not improve the FlexS model statistics in this case. The realigned set of molecules, which had the ‘tightest’ fit resulted in a $q^2 = 0.526$ after region focusing but a poor $r^2 = 0.767$ (see Table 16). Predicted pK_i values were also poor for the FlexS alignment and realignment resulting in six of the 34 compounds in the FlexS set and eight of the 34 compounds in the realigned set having a residual value (experimental pK_i – predicted pK_i) greater than the desired range of ± 0.50 pK_i unit (see Tables 13 and 15), whereas all values fell within the desired range for the receptor-docked alignment (see Table 11). It is hypothesized that the receptor-docked alignment paints a “truer” picture of the binding pocket of the receptor, resulting in a more accurate CoMFA contour map reflecting the residues surrounding the molecule in its docked position.

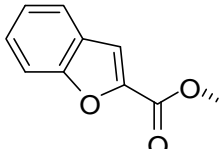
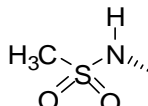
Table 11. Model 1 dataset of 34 compounds using [¹²⁵I] IOXY as the assay radioligand (receptor-docked alignment).



Cpd.	R	K _i (nM)	Ref.	Set ^a	pK _i ^b				
					exp.	-RF	-RF resi.	+RF	+RF resi.
1		1.9	37	T	8.72	8.66	0.06	8.71	0.01
2		280	37	T	6.55	6.41	0.14	6.42	0.13
3		38	93	T	7.42	7.34	0.08	7.37	0.05
7		1.8	98	T	8.74	8.58	0.16	8.61	0.14
9		4	98	T	8.40	8.39	0.01	8.39	0.01
11		15	98	P	7.82	7.99	-0.17	8.06	-0.24
12		70	98	T	7.15	7.18	-0.03	7.18	-0.03
15		42	93	T	7.38	7.44	-0.06	7.45	-0.07
16		90	37	T	7.05	7.00	0.05	6.99	0.06

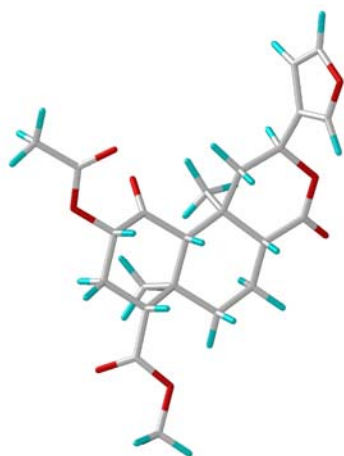
17		290	98	P	6.54	6.29	0.25	6.22	0.34
18		180	98	P	6.74	6.88	-0.14	6.96	-0.22
19		90	37	T	7.05	7.11	-0.05	7.14	-0.09
20		70	37	P	7.15	6.73	0.42	6.79	0.36
21		740	37	T	6.13	6.04	0.09	6.10	0.03
23		260	37	T	6.59	6.63	-0.04	6.58	0.01
29		430	93	P	6.37	6.34	0.03	6.50	-0.13
33		120	93	T	6.92	6.95	-0.03	6.95	-0.03
34		93	93	P	7.03	7.21	-0.18	7.26	-0.23
35		64	93	T	7.19	7.19	0.00	7.21	-0.02
44		30	37	T	7.52	7.86	-0.34	7.54	-0.02
57		5.7	37	P	8.24	7.86	0.38	7.88	0.36
69		2.3	93	T	8.64	8.74	-0.10	8.73	-0.09

71		60	98	T	7.22	7.34	-0.12	7.26	-0.04
72		50	98	T	7.30	7.30	0.00	7.28	0.02
121		900	37	T	6.05	6.09	-0.04	6.10	-0.05
122		800	37	P	6.10	6.53	-0.43	6.51	-0.41
123		570	37	P	6.24	5.90	0.34	6.01	0.23
124		230	37	T	6.64	6.61	0.03	6.59	0.05
125		550	37	P	6.26	6.31	-0.05	6.24	0.02
126		540	37	T	6.27	6.26	0.01	6.31	-0.04
127		410	37	T	6.39	6.42	-0.03	6.37	0.02
128		80	37	P	7.10	7.18	-0.08	7.34	-0.24

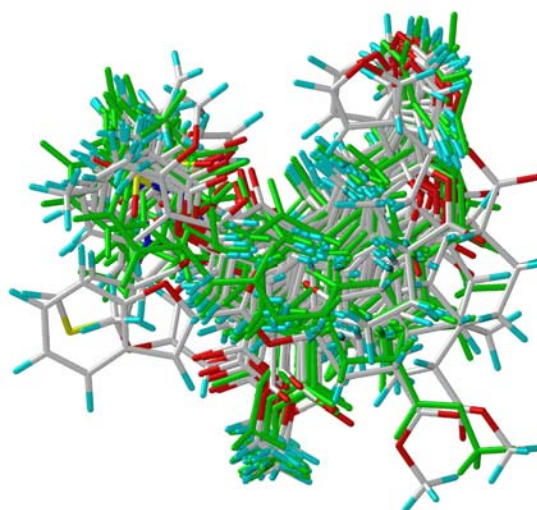
129		70	37	T	7.15	7.10	0.05	7.13	0.02
130		260	37	T	6.59	6.69	-0.10	6.62	-0.03

^a T = training set, P = predicted set. ^bexp. = experimentally-determined value, -RF = predicted value without region focusing, -RF resi. = residual (experimental value - predicted value) without region focusing, +RF = predicted value with region focusing, +RF resi. = residual (experimental value - predicted value) with region focusing.

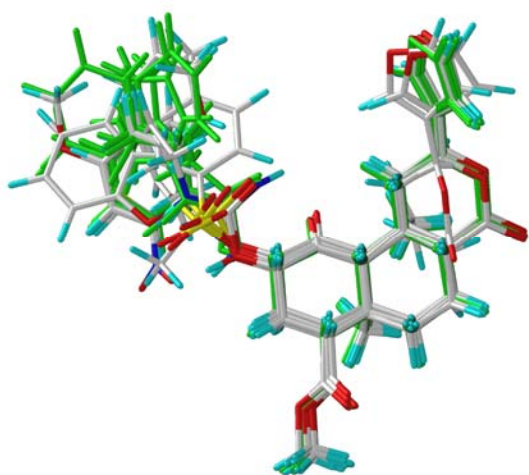
a.



b.



c.



d.

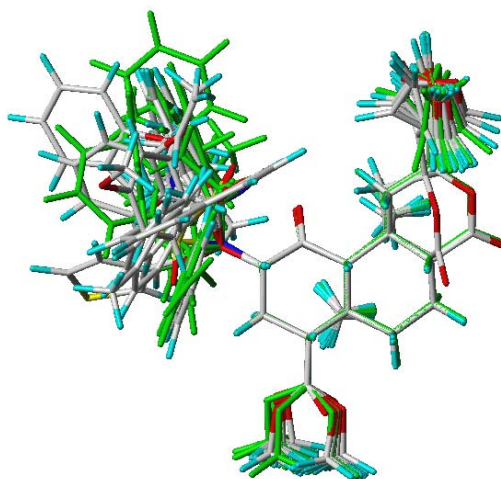


Figure 22. Model 1 dataset alignments. Salvinorin A for reference (a); receptor-docked alignment (b); FlexS alignment (c); realignment (d). Training set compounds are colored by atom type, prediction set compounds are green.

Model 1 CoMFA statistics (receptor-docked alignment) are shown in Table 12. A predictive q^2 for this model (0.592) was obtained after region focusing indicating the robustness of the model. The linear regression plots for Model 1 training and predicted datasets are shown in Figure 23. The region-focused CoMFA contour maps are shown in Figure 24.

Table 12. Model 1 CoMFA statistics for the receptor-docked alignment.

Parameter	Initial	Region Focused
Steric cutoff (kcal/mol)	25	25
Electrostatic cutoff (kcal/mol)	35	35
Column filtering (kcal/mol)	3	4
Components	6	6
q^2	0.491	0.592
r^2	0.991	0.994
Standard Error of Estimate (SEE)	0.090	0.071
F-test value	282.658	464.818
r^2_{pred}	0.841	0.833
Steric contribution %	0.343	0.393
Electrostatic contribution %	0.657	0.607

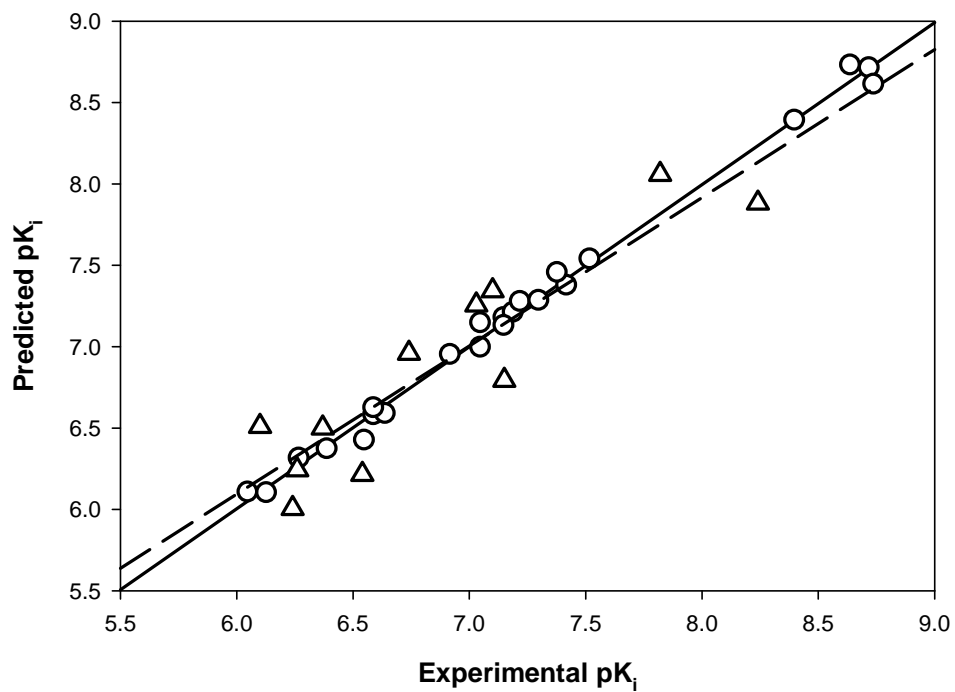
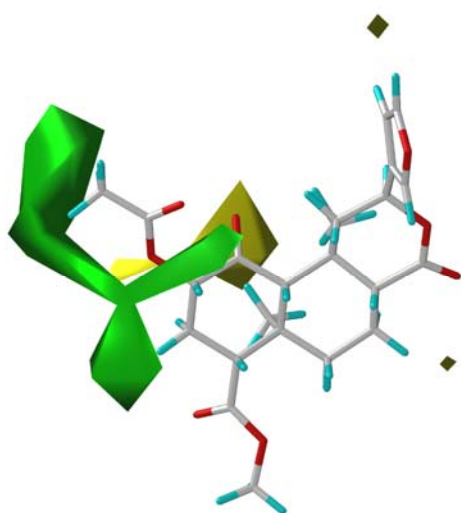


Figure 23. Model 1 linear regression plots. Open circles with a solid regression line indicate the training set and open triangles with a dashed regression line refer to the prediction set.

a.



b.

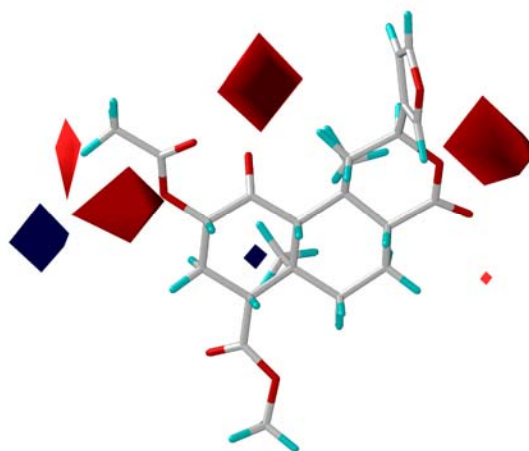
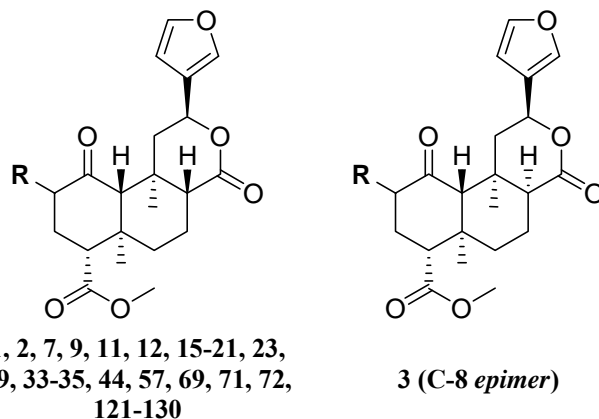


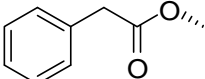
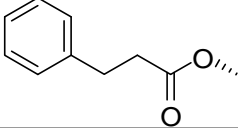
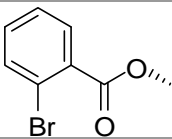
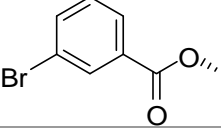
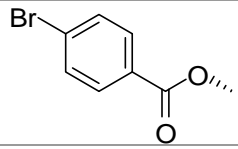
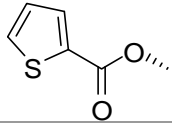
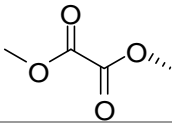
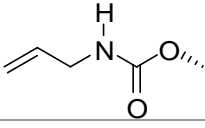
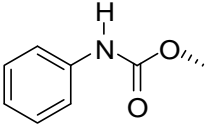
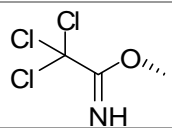
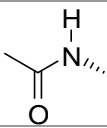
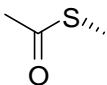
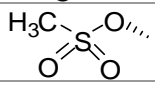
Figure 24. Model 1 CoMFA contour maps. In the steric map (a), green contours show regions where bulk is tolerated and yellow contours where bulk is not tolerated. In the electrostatic map (b), blue contours represent regions where positive charge enhances affinity and red contours represent where negative charge enhances affinity.

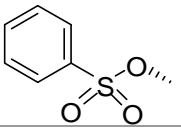
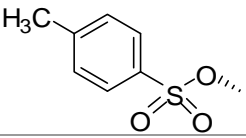
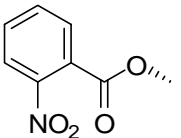
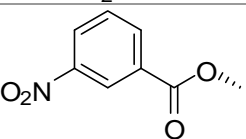
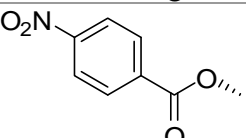
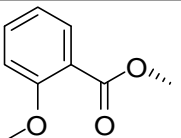
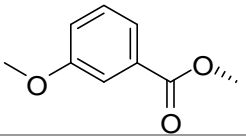
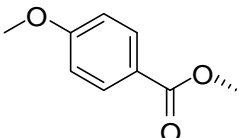
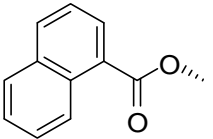
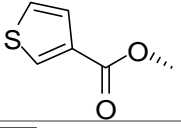
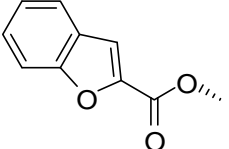
Both the TSET and PSET show a strong correlation in the linear regression plots. A region of bulk tolerance (green) can be seen around the C-2 position (Figure 24a) extending approximately three carbons in length from the carbonyl carbon. The binding affinity data indicates that affinity decreases sharply for esters with chain lengths larger than four carbons in length at the C-2 position. This bulk tolerance region falls within a hydrophobic pocket formed from Y312(7.35), Y313(7.36), and I316(7.39), which, on inspection would not be expected to accommodate long chain lengths of greater than four carbons. A region of bulk intolerance can be seen behind the C-1 position and in the receptor, this is the region occupied by extracellular loop 2 (EL2) near the disulfide bridge linking the EL2 with transmembrane helix 3 (TM3). In the electrostatic contour map (Figure 24b) several areas where electronegativity enhances affinity (red) are positioned around the ester and carbonyl oxygens of the molecule. A small area in which electropositive atoms on the ligand enhance affinity (blue) can be seen on the beta (above the plane of the paper) side of the C-2 position ester group. In the receptor, this blue region is found to fall near the negatively charged carboxylate moiety of E297(6.58) on TM6.

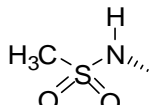
Table 13. Model 1 dataset of 34 compounds using [¹²⁵I] IOXY as the assay radioligand (FlexS alignment).



Cpd.	R	K _i (nM)	Ref.	Set ^a	pK _i ^b		
					exp.	pred.	resi.
1		1.9	37	T	8.72	8.19	<u>0.54</u>
2		280	37	T	6.55	6.39	0.16
3		38	93	T	7.42	7.40	0.02
7		1.8	98	T	8.74	8.55	0.19
9		4	98	T	8.40	7.91	0.49
11		15	98	P	7.82	7.44	0.38
12		70	98	T	7.15	7.25	-0.10
15		42	93	T	7.38	7.49	-0.11
16		90	37	T	7.05	6.69	0.36

17		290	98	P	6.54	7.83	<u>-1.29</u>
18		180	98	P	6.74	7.03	-0.29
19		90	37	T	7.05	6.67	0.38
20		70	37	P	7.15	6.67	0.48
21		740	37	T	6.13	6.47	-0.34
23		260	37	T	6.59	6.91	-0.32
29		430	93	P	6.37	7.34	<u>-0.97</u>
33		120	93	T	6.92	6.92	0.00
34		93	93	P	7.03	6.52	<u>0.51</u>
35		64	93	T	7.19	7.40	-0.21
44		30	37	T	7.52	8.14	<u>-0.62</u>
57		5.7	37	P	8.24	8.14	0.11
69		2.3	93	T	8.64	8.75	-0.11

71		60	98	T	7.22	7.32	-0.10
72		50	98	T	7.30	7.55	-0.25
121		900	37	T	6.05	6.15	-0.10
122		800	37	P	6.10	7.62	<u>-1.52</u>
123		570	37	P	6.24	6.68	-0.44
124		230	37	T	6.64	6.66	-0.02
125		550	37	P	6.26	6.47	-0.21
126		540	37	T	6.27	6.34	-0.07
127		410	37	T	6.39	6.25	0.14
128		80	37	P	7.10	6.86	0.24
129		70	37	T	7.15	7.23	-0.08

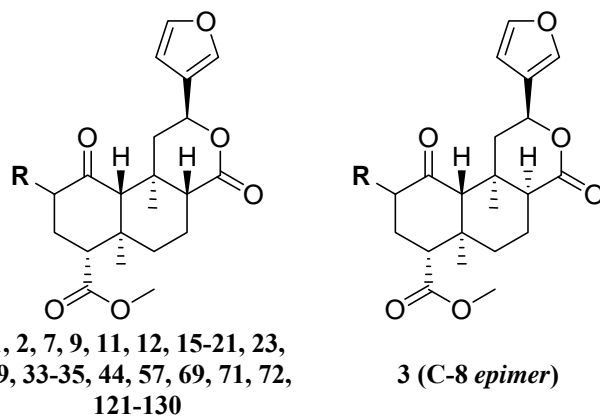
130		260	37	T	6.59	6.45	0.14
-----	---	-----	----	---	------	------	------

^a T = training set, P = predicted set. ^b exp. = experimentally-determined value, pred.= predicted value, resi. = residual (experimental value - predicted value). Outliers (residual > ±0.50 pK_i unit) are underlined.

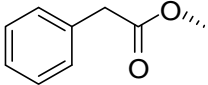
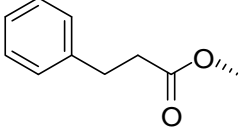
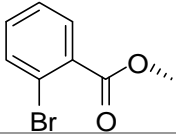
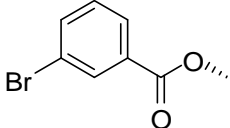
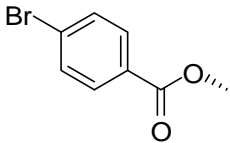
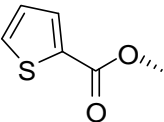
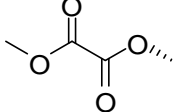
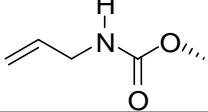
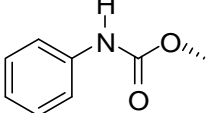
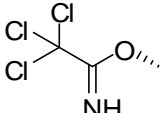
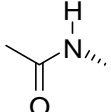
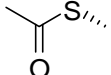
Table 14. Model 1 CoMFA statistics for the FlexS alignment.

Parameter	Value
Steric cutoff (kcal/mol)	50
Electrostatic cutoff (kcal/mol)	5
Column filtering (kcal/mol)	3
Components	3
q^2	0.311
r^2	0.881
Standard Error of Estimate (SEE)	0.296
F-test value	46.922
Steric contribution %	0.418
Electrostatic contribution %	0.582

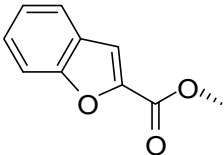
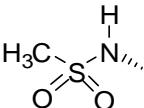
Table 15. Model 1 dataset of 34 compounds using [¹²⁵I] IOXY as the assay radioligand (realignment).



Cpd.	R	K _i (nM)	Ref.	Set ^a	pK _i ^b				
					exp.	-RF	-RF resi.	+RF	+RF resi.
1		1.9	37	T	8.72	7.94	<u>0.78</u>	8.00	<u>0.72</u>
2		280	37	T	6.55	6.98	-0.43	6.74	-0.19
3		38	93	T	7.42	7.70	-0.28	7.71	-0.29
7		1.8	98	T	8.74	7.96	<u>0.78</u>	8.10	<u>0.64</u>
9		4	98	T	8.40	7.95	0.45	8.07	0.33
11		15	98	P	7.82	7.79	0.03	7.84	-0.02
12		70	98	T	7.15	7.75	<u>-0.60</u>	7.74	<u>-0.59</u>
15		42	93	T	7.38	7.67	-0.29	7.47	-0.09
16		90	37	T	7.05	6.74	0.31	7.05	0.00

17		290	98	P	6.54	6.37	0.17	6.45	0.09
18		180	98	P	6.74	7.36	<u>-0.62</u>	7.47	<u>-0.73</u>
19		90	37	T	7.05	6.81	0.24	7.01	0.04
20		70	37	P	7.15	6.46	<u>0.69</u>	6.74	0.41
21		740	37	T	6.13	5.84	0.29	6.18	-0.05
23		260	37	T	6.59	6.47	0.12	6.65	-0.06
29		430	93	P	6.37	6.98	<u>-0.61</u>	7.39	<u>-1.02</u>
33		120	93	T	6.92	7.06	-0.14	6.96	-0.04
34		93	93	P	7.03	7.35	-0.32	7.30	-0.27
35		64	93	T	7.19	7.44	-0.25	7.19	0.00
44		30	37	T	7.52	8.04	<u>-0.52</u>	8.04	<u>-0.52</u>
57		5.7	37	P	8.24	7.57	<u>0.67</u>	7.26	<u>0.98</u>

69		2.3	93	T	8.64	8.42	0.22	8.71	-0.07
71		60	98	T	7.22	7.23	-0.01	7.18	0.04
72		50	98	T	7.30	7.69	-0.39	7.30	0.00
121		900	37	T	6.05	5.95	0.10	6.18	-0.13
122		800	37	P	6.10	6.31	-0.21	6.43	-0.33
123		570	37	P	6.24	5.96	0.28	6.11	0.13
124		230	37	T	6.64	6.63	0.01	6.52	0.12
125		550	37	P	6.26	6.77	<u>-0.51</u>	6.99	<u>-0.73</u>
126		540	37	T	6.27	6.34	-0.07	5.85	0.42
127		410	37	T	6.39	6.81	-0.42	6.52	-0.13
128		80	37	P	7.10	6.75	0.35	7.02	0.08

129		70	37	T	7.15	7.04	0.11	7.45	-0.30
130		260	37	T	6.59	6.63	-0.04	6.45	0.14

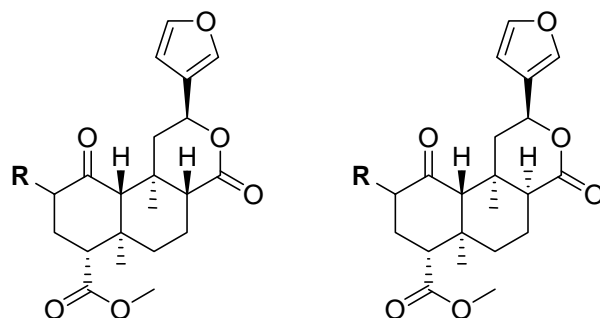
^a T = training set, P = predicted set. ^bexp. = experimentally-determined value, -RF = predicted value without region focusing, -RF resi. = residual (experimental value - predicted value) without region focusing, +RF = predicted value with region focusing, +RF resi. = residual (experimental value - predicted value) with region focusing. Outliers (residual > ±0.50 pK_i unit) are underlined.

Table 16. Model 1 CoMFA statistics for the realignment.

Parameter	Initial	Region Focused
Steric cutoff (kcal/mol)	25	25
Electrostatic cutoff (kcal/mol)	30	30
Column filtering (kcal/mol)	3	3
Components	2	2
q ²	0.402	0.526
r ²	0.777	0.767
Standard Error of Estimate (SEE)	0.395	0.404
F-test value	34.832	35.504
Steric contribution %	0.472	0.485
Electrostatic contribution %	0.528	0.566

Model 2 consists of 48 compounds in which [³H]diprenorphine was used as the assay radioligand (see Table 17). Of these, 35 compounds were chosen for the TSET with the remaining 13 compounds comprising the PSET. In this set of compounds, region focusing did not enhance the statistics of the model with the receptor-docked alignment, but did enhance the statistics of the FlexS-aligned compounds and the realignment of docked compounds. Prediction of pK_i values for the FlexS alignment, however, were very poor, resulting in eleven outliers (pK_i > ± 0.5 units from the experimental value) out of the 48 compounds. The q² for the FlexS region-focused model was 0.502, whereas for the receptor-docked alignment (no region focusing) q² = 0.646. The realigned dataset, after region focusing, showed poor CoMFA statistics with q² = 0.320 and resulted in six outliers out of the 48 compounds in the dataset. These alignments are shown in Figure 25 and the statistics for the receptor-docked model are reported in Table 18. The linear regression plot for Model 2 is shown in Figure 26. The CoMFA contour maps are shown in Figure 27.

Table 17. Model 2 dataset using [³H]diprenorphine as the assay radioligand (receptor-docked alignment).

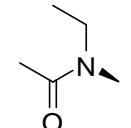
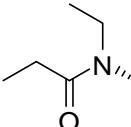
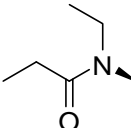
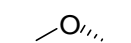
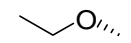
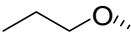
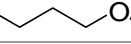
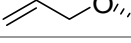
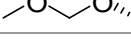
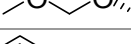
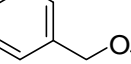
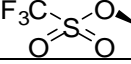
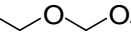
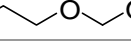
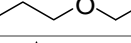
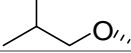
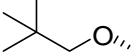
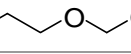
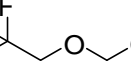
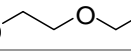
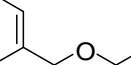


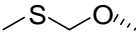
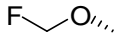
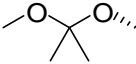
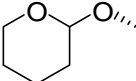
1, 2, 5, 7-10, 27, 30-32, 34,
44-55, 61-66, 68, 70, 131-
143

3, 4, 67 (*C-8 epimer*)

Cpd.	R	K _i (nM)	Ref.	Set ^a	pK _i ^b		
					exp.	pred.	resi.
1		2.4	108	T	8.62	8.39	0.23
2		155	48	T	6.81	6.70	0.11
3		77	47	T	7.11	7.13	-0.02
4		304	49	T	6.52	6.48	0.04
5		424	48	T	6.37	6.47	-0.10
7		7.2	48	T	8.14	8.14	0.00
8		641	48	P	6.19	6.09	0.10
9		4.9	48	P	8.31	7.82	0.49
10		665	48	T	6.18	6.13	0.05
27		176	47	P	6.75	6.47	0.28

30		3.2	47	T	8.49	8.64	-0.15
31		83	47	T	7.08	6.99	0.09
32		462	47	T	6.34	6.30	0.04
34		282	47	P	6.55	6.83	-0.28
44		149	48	T	6.83	6.99	-0.16
45		332	48	P	6.48	6.88	-0.40
46		3.2	48	T	8.49	8.42	0.07
47		16.5	48	T	7.78	7.73	0.05
48		374	48	T	6.43	6.52	-0.09
49		117	48	T	6.93	6.95	-0.02
50		1.6	48	T	8.80	8.87	-0.07
51		6.9	48	T	8.16	8.17	-0.01
52		27.6	48	T	7.56	7.45	0.11

53		240	48	T	6.62	6.64	-0.02
54		38.1	48	T	7.42	7.58	-0.16
55		376	48	P	6.42	6.72	-0.30
61		220	48	P	6.66	6.92	-0.26
62		7.9	48	T	8.10	8.16	-0.06
63		28.7	48	P	7.54	7.72	-0.18
64		35.8	47	T	7.45	7.36	0.09
65		60.1	47	P	7.22	7.64	-0.42
66		0.6	108	T	9.22	9.26	-0.04
67		30	47	P	7.52	7.32	0.20
68		75.7	108	T	7.12	7.14	-0.02
70		227	47	T	6.64	6.75	-0.11
131		0.32	108	T	9.49	9.33	0.16
132		2.2	108	P	8.66	8.20	0.46
133		5.3	108	T	8.28	8.23	0.05
134		1.6	108	T	8.80	8.87	-0.07
135		35	108	T	7.46	7.49	-0.03
136		1.9	108	T	8.72	8.84	-0.12
137		31	108	P	7.51	7.54	-0.03
138		141	108	T	6.85	6.79	0.06
139		147	108	T	6.83	6.82	0.01

140		13	108	P	7.89	8.22	-0.33
141		50	108	T	7.30	7.42	-0.12
142		72	108	T	7.14	7.02	0.12
143		4	108	T	8.40	8.33	0.07

^aT = training set, P = predicted set. ^bexp. = experimentally-determined value, pred. = predicted value, resi. = residual (experimental value – predicted value).

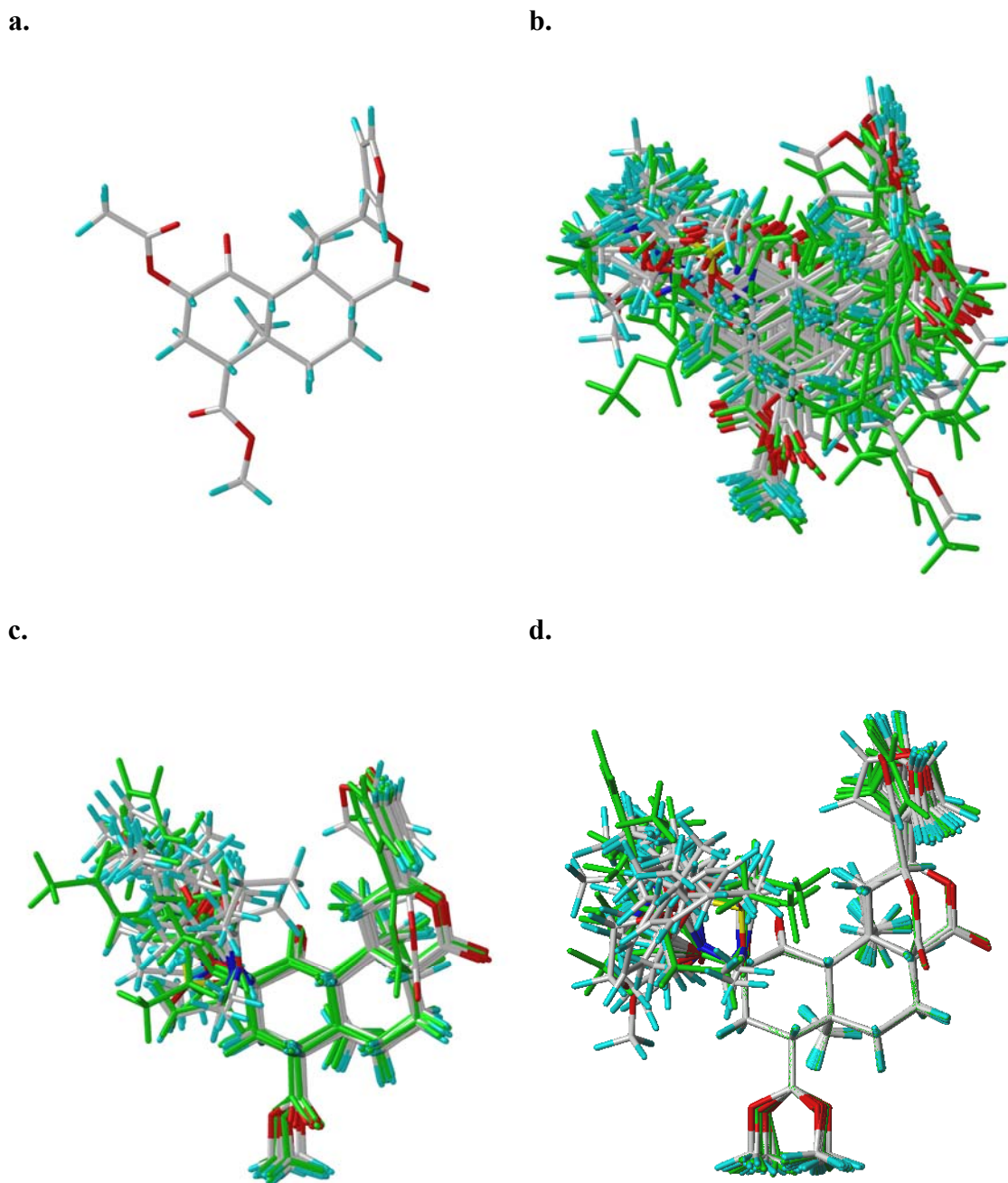


Figure 25. Model 2 dataset alignments. Salvinorin A (a) extracted for reference; receptor-docked alignment (b); FlexS alignment (c) and realignment (d). PSET compounds are green and TSET compounds are colored by atom type.

Table 18. Model 2 CoMFA statistics for the receptor-docked alignment.

Parameter	Value
Steric cutoff (kcal/mol)	35
Electrostatic cutoff (kcal/mol)	30
Column filtering (kcal/mol)	3
Components	6
q^2	0.646
r^2	0.989
Standard Error of Estimate (SEE)	0.105
F-test value	427.463
r^2_{pred}	0.828
Steric contribution %	0.350
Electrostatic contribution %	0.650

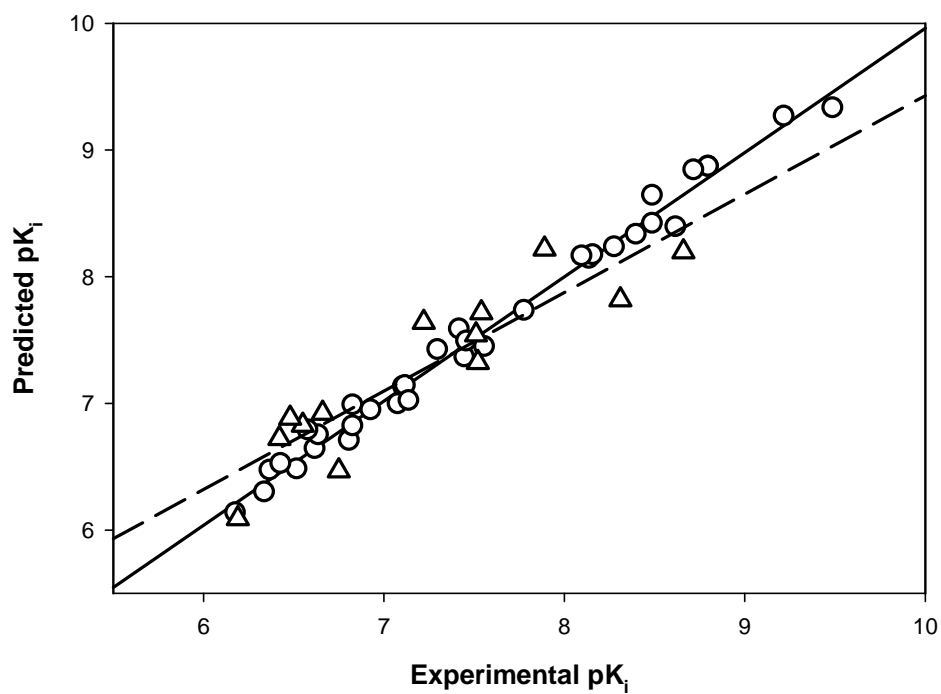
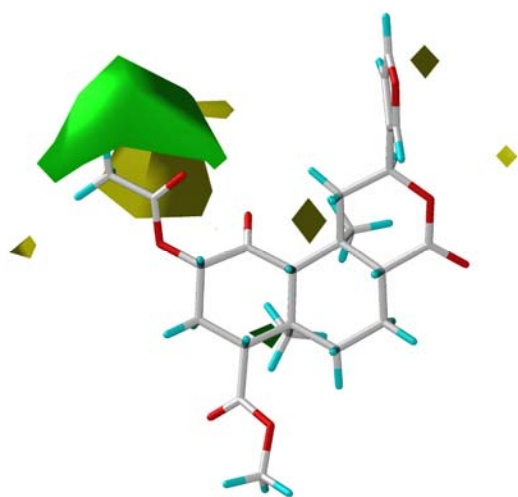


Figure 26. Model 2 linear regression plots. Open circles and a solid line represent the training set regression. Open triangles and a dashed line show the prediction set regression.

a.



b.

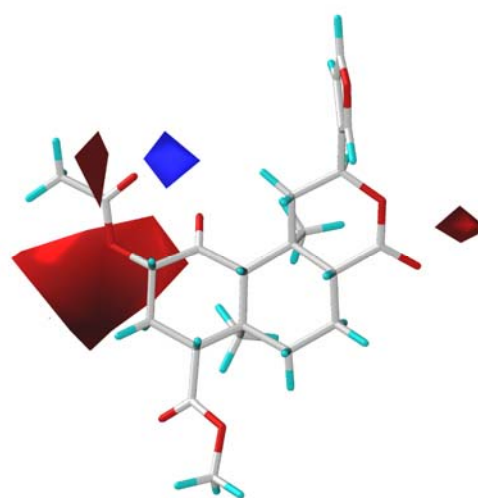


Figure 27. Model 2 CoMFA contour maps. (a). Green regions show bulk tolerance and yellow regions, bulk intolerance. (b). Red regions indicate enhanced affinity with electronegativity and blue, where electropositivity will enhance affinity.

It should be noted that at least half of the statistical outliers in the FlexS alignments (3 out of 6 for Model 1 and 7 out of 11 for Model 2) were compounds which did not superimpose well in the corresponding receptor-docked alignments. This supports the hypothesis that these compounds might bind in an orientation that differs from that of salvinorin A.

As in Model 1, there is a region of bulk tolerance around the C-2 ester group and a region of bulk intolerance behind it (Figure 27a). In Figure 27b, regions of enhanced affinity with electronegativity (red) are seen near the oxygens of the C-2 position ester group and the C-1 carbonyl. The largest electronegative contour falls within H-bonding distance of H304(7.27) near the extracellular region of TM7. There is a particularly interesting region of where an electropositive moiety enhances affinity (blue) near the C-2 position carbonyl oxygen atom on the beta side of the molecule. This region of electropositivity falls near E209(XL2.49), which may explain the high affinity of some amine containing analogs⁴⁸ not included in these models (*vide infra*). Docking studies of these amines place the positively charged amine group in a position to interact with E209(XL2.49). An example of the highest-affinity amine (see Figure 28), with a reported K_i of 2.3 nM⁴⁸, is shown docked in the KOR (see Figure 29).

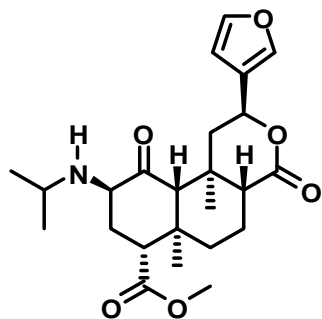


Figure 28. The β -N-isopropylamine analog of salvinorin A.

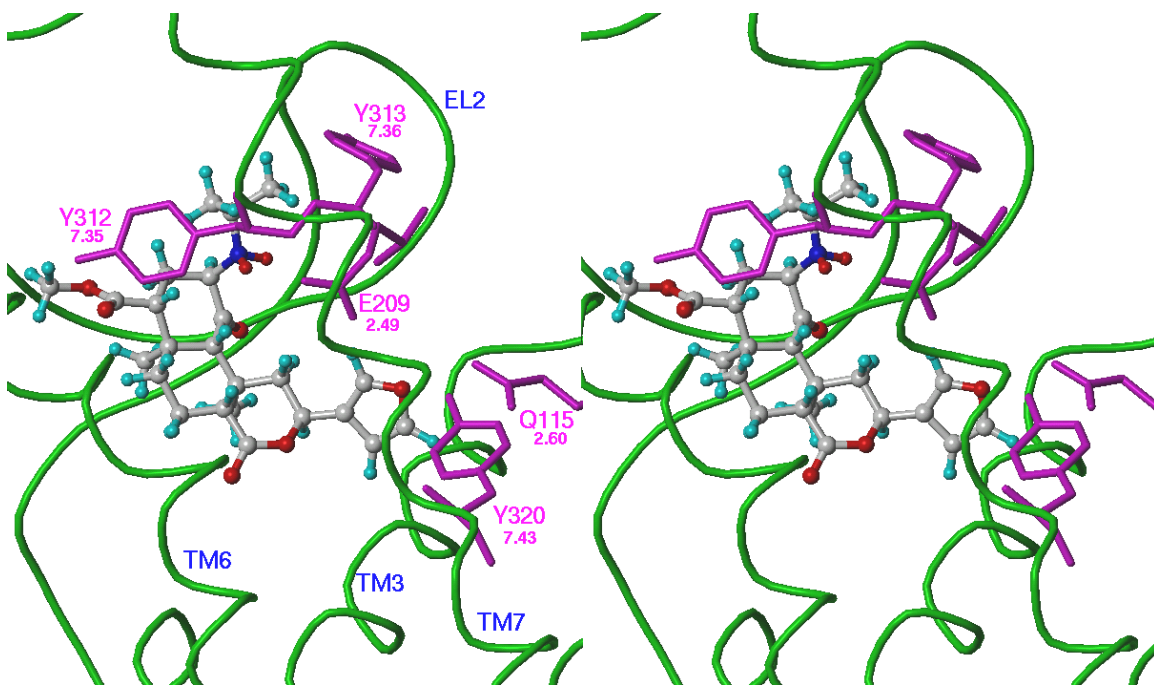
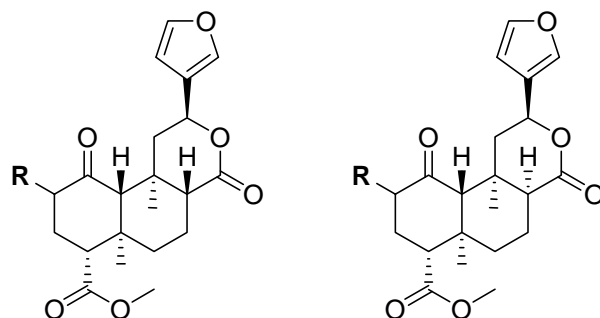


Figure 29. Stereo view of the β -*N*-isopropylamine analog of salvinorin A docked in the KOR.

The docked position of this amine is very similar to our proposed model of the Salvinorin A–KOR complex (see Figure 16). In addition to the furan oxygen having potential hydrogen bond interactions with both Q115(2.60) and Y320(7.43) and the hydrogen bonding interaction between Y312(7.35) and the C-4 position methyl ester oxygen, there is a hydrophobic interaction of the methyl groups of the isopropyl substituent with the aromatic rings of both Y312(7.35) and Y313(7.36) and an ionic interaction between the positively charged nitrogen and the negatively charged sidechain of E209(XL2.49). It should also be noted that this is the beta epimer (i.e. the *R* configuration at the C-2 position). The alpha (i.e. *S*) epimers do not interact as well with the residues mentioned here (data not shown), which may explain the lower affinity of the alpha isomers in this series of amine analogs, whereas the trend shown by the esters, ethers and amides is just the opposite with the alpha epimer having the higher affinity. The α -*N*-isopropylamine analog has a reported K_i of 17.6 nM .⁴⁸

Table 19. Model 2 dataset using [³H] diprenorphine as the assay radioligand (FlexS alignment).

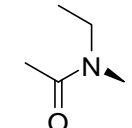
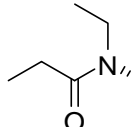
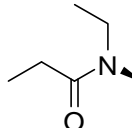
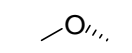
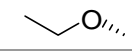
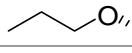
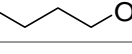
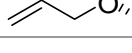
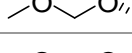
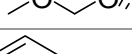
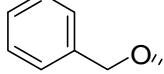
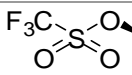
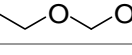
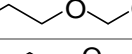
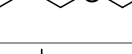
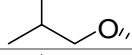
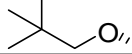
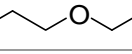
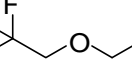
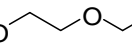
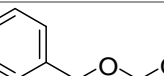


1, 2, 5, 7-10, 27, 30-32, 34,
44-55, 61-66, 68, 70, 131-
143

3, 4, 67 (C-8 epimer)

Cpd.	R	K _i (nM)	Ref.	Set ^a	pK _i ^b				
					exp.	-RF	-RF resi.	+RF	+RF resi.
1		2.4	108	T	8.62	8.43	0.19	8.48	0.14
2		155	48	T	6.81	6.66	0.15	6.89	-0.08
3		77	47	T	7.11	7.23	-0.12	7.10	0.01
4		304	49	T	6.52	6.63	-0.11	6.72	-0.20
5		424	48	T	6.37	6.18	0.19	6.23	0.14
7		7.2	48	T	8.14	7.98	0.16	8.07	0.07
8		641	48	P	6.19	7.46	<u>-1.27</u>	7.85	<u>-1.66</u>
9		4.9	48	P	8.31	7.48	<u>0.83</u>	7.63	<u>0.68</u>
10		665	48	T	6.18	6.00	0.18	6.35	-0.17
27		176	47	P	6.75	6.57	0.18	6.33	0.42

30		3.2	47	T	8.49	8.39	0.10	8.53	-0.04
31		83	47	T	7.08	7.40	-0.32	7.36	-0.28
32		462	47	T	6.34	5.96	0.38	6.14	0.20
34		282	47	P	6.55	6.73	-0.18	7.08	<u>-0.53</u>
44		149	48	T	6.83	6.70	0.13	6.58	0.25
45		332	48	P	6.48	6.41	0.07	6.53	-0.05
46		3.2	48	T	8.49	8.71	-0.22	8.71	-0.22
47		16.5	48	T	7.78	7.74	0.04	7.68	0.10
48		374	48	T	6.43	6.74	-0.31	6.68	-0.25
49		117	48	T	6.93	7.02	-0.09	6.97	-0.04
50		1.6	48	T	8.80	8.89	-0.09	8.80	0.00
51		6.9	48	T	8.16	8.23	-0.07	7.94	0.22
52		27.6	48	T	7.56	7.60	-0.04	7.85	-0.29

53		240	48	T	6.62	6.56	0.06	6.61	0.01
54		38.1	48	T	7.42	7.29	0.13	7.06	0.36
55		376	48	P	6.42	7.82	<u>-1.40</u>	7.51	<u>-1.09</u>
61		220	48	P	6.66	8.19	<u>-1.53</u>	8.28	<u>-1.62</u>
62		7.9	48	T	8.10	8.11	-0.01	8.09	0.01
63		28.7	48	P	7.54	8.29	<u>-0.75</u>	8.33	<u>-0.79</u>
64		35.8	47	T	7.45	7.88	-0.43	8.00	<u>-0.55</u>
65		60.1	47	P	7.22	8.25	<u>-1.03</u>	8.16	<u>-0.94</u>
66		0.6	108	T	9.22	8.80	0.42	8.95	0.27
67		30	47	P	7.52	8.45	<u>-0.93</u>	8.66	<u>-1.14</u>
68		75.7	108	T	7.12	7.06	-0.06	6.97	0.15
70		227	47	T	6.64	6.92	-0.28	6.53	0.11
131		0.32	108	T	9.49	9.16	0.33	9.20	0.29
132		2.2	108	P	8.66	8.19	0.47	7.99	<u>0.67</u>
133		5.3	108	T	8.28	8.36	-0.08	8.24	0.04
134		1.6	108	T	8.80	8.87	-0.07	8.86	-0.06
135		35	108	T	7.46	7.61	-0.15	7.61	-0.15
136		1.9	108	T	8.72	8.63	0.09	8.67	0.05
137		31	108	P	7.51	7.37	0.14	7.24	0.27
138		141	108	T	6.85	7.00	-0.15	6.80	0.05
139		147	108	T	6.83	6.75	0.08	6.64	0.19

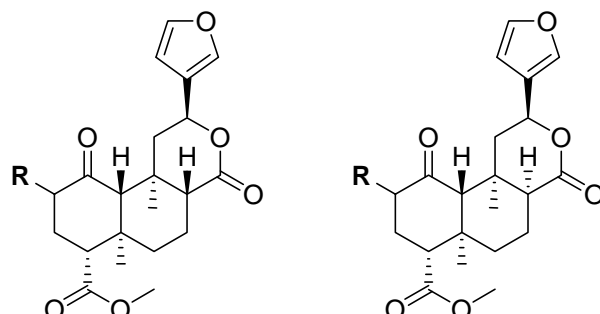
140		13	108	P	7.89	8.45	<u>-0.56</u>	8.47	<u>-0.58</u>
141		50	108	T	7.30	7.56	-0.26	7.62	-0.32
142		72	108	T	7.14	7.15	-0.01	7.27	-0.13
143		4	108	T	8.40	8.32	0.08	8.29	0.11

^a T = training set, P = predicted set. ^bexp. = experimentally-determined value, -RF = predicted value without region focusing, -RF resi. = residual (experimental value - predicted value) without region focusing, +RF = predicted value with region focusing, +RF resi. = residual (experimental value - predicted value) with region focusing. Outliers (residual > ±0.50 pK_i unit) are underlined.

Table 20. Model 2 CoMFA statistics for the FlexS alignment.

Parameter	Initial	Region Focused
Steric cutoff (kcal/mol)	25	25
Electrostatic cutoff (kcal/mol)	30	30
Column filtering (kcal/mol)	3	3
Components	6	6
q^2	0.455	0.504
r^2	0.953	0.951
Standard Error of Estimate (SEE)	0.218	0.222
F-test value	94.506	90.909
Steric contribution %	0.407	0.421
Electrostatic contribution %	0.593	0.579

Table 21. Model 2 dataset using [³H] diprenorphine as the assay radioligand (realignment).

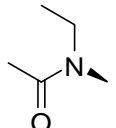
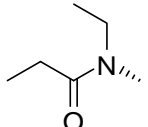
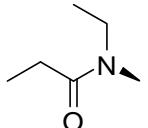
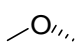
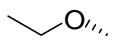
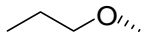
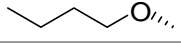



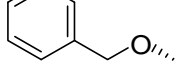
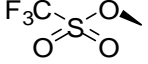
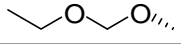
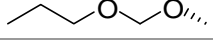
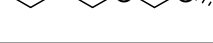
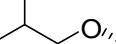
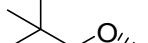
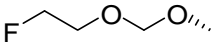
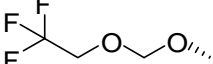
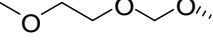
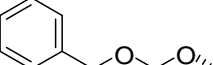


1, 2, 5, 7-10, 27, 30-32, 34,
44-55, 61-66, 68, 70, 131-
143

3, 4, 67 (C-8 epimer)

Cpd.	R	K _i (nM)	Ref.	Set ^a	pK _i ^b				
					exp.	-RF	-RF resi.	+RF	+RF resi.
1		2.4	108	T	8.62	8.05	<u>0.57</u>	8.17	0.45
2		155	48	T	6.81	6.80	0.01	6.93	-0.12
3		77	47	T	7.11	7.37	-0.26	7.09	0.02
4		304	49	T	6.52	6.49	0.03	6.72	-0.20
5		424	48	T	6.37	6.55	-0.18	6.67	-0.30
7		7.2	48	T	8.14	7.51	<u>0.63</u>	7.70	0.44
8		641	48	P	6.19	6.35	-0.16	6.44	-0.25
9		4.9	48	P	8.31	7.58	<u>0.73</u>	7.92	0.39
10		665	48	T	6.18	6.64	-0.46	6.59	-0.41
27		176	47	P	6.75	7.01	-0.26	7.26	<u>-0.51</u>

30		3.2	47	T	8.49	8.12	0.37	8.27	0.22
31		83	47	T	7.08	7.43	-0.35	7.42	-0.34
32		462	47	T	6.34	7.54	<u>-1.21</u>	7.18	<u>-0.84</u>
34		282	47	P	6.55	7.35	<u>-0.80</u>	7.48	<u>-0.93</u>
44		149	48	T	6.83	7.20	-0.37	6.76	0.07
45		332	48	P	6.48	6.50	-0.02	6.53	-0.05
46		3.2	48	T	8.49	8.08	0.41	8.09	0.40
47		16.5	48	T	7.78	7.67	0.11	7.75	0.03
48		374	48	T	6.43	6.55	-0.13	6.33	0.10
49		117	48	T	6.93	6.81	0.12	6.86	0.07
50		1.6	48	T	8.80	8.83	-0.03	8.56	0.24
51		6.9	48	T	8.16	7.57	<u>0.59</u>	7.50	<u>0.66</u>
52		27.6	48	T	7.56	7.57	-0.01	7.69	-0.13

53		240	48	T	6.62	6.63	-0.01	6.71	-0.09
54		38.1	48	T	7.42	7.69	-0.27	7.53	-0.11
55		376	48	P	6.42	6.70	-0.28	6.76	-0.34
61		220	48	P	6.66	7.50	<u>-0.84</u>	7.63	<u>-0.97</u>
62		7.9	48	T	8.10	8.03	0.07	8.24	-0.14
63		28.7	48	P	7.54	7.50	0.04	7.51	0.03
64		35.8	47	T	7.45	7.49	-0.04	7.83	-0.38
65		60.1	47	P	7.22	7.41	-0.19	7.40	-0.18
66		0.6	108	T	9.22	9.63	-0.41	9.67	-0.45
67		30	47	P	7.52	7.44	0.08	7.36	0.16
68		75.7	108	T	7.12	7.02	0.10	7.03	0.09
70		227	47	T	6.64	6.88	-0.22	6.70	-0.06
131		0.32	108	T	9.49	9.31	0.18	9.42	0.07
132		2.2	108	P	8.66	8.95	-0.29	8.70	-0.04
133		5.3	108	T	8.28	8.50	-0.22	8.46	-0.18
134		1.6	108	T	8.80	8.38	0.42	8.35	0.45
135		35	108	T	7.46	7.08	0.38	7.29	0.17
136		1.9	108	T	8.72	8.81	-0.09	8.81	-0.09
137		31	108	P	7.51	7.46	0.05	7.47	0.04
138		141	108	T	6.85	6.54	0.31	6.39	0.46
139		147	108	T	6.83	6.39	0.44	6.54	0.29

140		13	108	P	7.89	7.92	-0.03	7.82	0.07
141		50	108	T	7.30	7.63	-0.33	7.88	<u>-0.58</u>
142		72	108	T	7.14	7.24	-0.10	7.03	0.11
143		4	108	T	8.40	8.48	-0.08	8.31	0.09

^a T = training set, P = predicted set. ^bexp. = experimentally-determined value, -RF = predicted value without region focusing, -RF resi. = residual (experimental value - predicted value) without region focusing, +RF = predicted value with region focusing, +RF resi. = residual (experimental value - predicted value) with region focusing. Outliers (residual > ±0.50 pK_i unit) are underlined.

Table 22. Model 2 CoMFA statistics for the realignment.

Parameter	Initial	Region Focused
Steric cutoff (kcal/mol)	30	30
Electrostatic cutoff (kcal/mol)	30	30
Column filtering (kcal/mol)	2	2
Components	3	3
q ²	0.210	0.320
r ²	0.814	0.873
Standard Error of Estimate (SEE)	0.413	0.347
F-test value	53.334	45.274
Steric contribution %	0.527	0.527
Electrostatic contribution %	0.473	0.473

5. Conclusions

Salvinorin A is an extraordinarily selective kappa opioid receptor agonist that is devoid of a basic nitrogen common to all known opioids, yet has high affinity. Structure-affinity relationships indicate that most of the important functional groups reside on the A ring. Therefore, a fragment of salvinorin A including the A ring and its functional groups was synthesized. This fragment was found not to bind to the kappa, delta or mu opioid receptors. With this information, it is apparent that the B, C and D rings contribute to the stability of the molecule in the binding pocket of the KOR. Salvinorin A has a total of eight H-bond acceptor oxygen atoms. SAFIR studies indicate that not all of these oxygen atoms are essential for binding. Binding free energy calculations also support the indication that not all functionalities are involved in binding.

In order to try and shed some light on the selectivity of salvinorin A, computational studies were undertaken. Homology models of the kappa, delta and mu opioid receptors were constructed based on two different inactive crystal structures of bovine rhodopsin, the light-activated crystal structure of bovine rhodopsin and the β_2 adrenergic receptor. A set of selective opioid ligands were then docked into these receptor models in order to determine the best models for further docking studies. It was found that the models based on the light-activated bovine rhodopsin crystal structure gave the best results, specifically the AR-KOR model. A database of salvinorin A analogs were docked into this model.

Because Salvinorin A and its analogs have a constrained polycyclic ring core and only differ in the functional groups attached at the C-2 and C-4 positions (much like steroids), it was thought that these analogs would be ideal for a comparative molecular field analysis study. The information obtained may then help to clarify the binding mode and selectivity of salvinorin A and analogs and serve to predict new high-affinity analogs.

In the CoMFA study, two models of C-2 position salvinorin A analogs bound to the KOR were presented whose similar contour maps coincided with the presence of complementary amino acid sidechains in the binding pocket. These models also demonstrated significant predictive ability. Model 1 analogs used [¹²⁵I]IOXY as the radioligand in the binding affinity assay while Model 2 analogs used [³H]diprenorphine. The alignment that was found to produce the most statistically significant model was a receptor-docked alignment when compared to a FlexS alignment and a Fit Atoms realignment method. The latter two alignment methods gave poor statistical results, yet were the most closely aligned sets of structures. This indicated that salvinorin A analogs may be binding differently from one another despite their similarity in structure. The receptor-docked alignment also supported our postulated model of salvinorin A in the KOR. Region focusing enhanced Model 1 but not Model 2. The contour maps revealed a region of bulk tolerance allowing for approximately a three-carbon chain from the ester carbonyl carbon. The expected enhancement of affinity with increasing electronegativity was seen around the C-2 position ester oxygens and the C-1 position carbonyl oxygen. An area of enhanced affinity corresponding to increased electropositivity on the beta side of the molecule correlated well with our postulated docked position of amine analogs in

the KOR and may explain the trend for C-2 position beta-isomer amines to have a higher affinity than the corresponding alpha-isomer amines in the series. Further mutagenesis studies on the key interacting residues could be carried out to support or refute the postulated docked model of the amines.

List of References

List of References

1. Valdes, L. J., III Salvia divinorum and the unique diterpene hallucinogen, Salvinorin (divinorin) A. *J. Psychoactive Drugs* **1994**, *26*, 277-283.
2. Valdes, L. J., III; Diaz, J. L.; Paul, A. G. Ethnopharmacology of ska Maria Pastora (Salvia divinorum, Epling and Jativa-M.). *J. Ethnopharmacol.* **1983**, *7*, 287-312.
3. Siebert, D. J. Salvia divinorum and salvinorin A: new pharmacologic findings. *J. Ethnopharmacol.* **1994**, *43*, 53-56.
4. Babu, K. M.; McCurdy, C. R.; Boyer, E. W. Opioid receptors and legal highs: Salvia divinorum and Kratom. *Clin. Toxicol. (Phila)* **2008**, *46*, 146-152.
5. Ortega, A. Salvinorin, a new trans-neoclerodane diterpene from Salvia divinorum (Labiatae). *J. Chem. Soc. :Perkins Trans. I* **1982**, 2505-2508.
6. Valdes III, L. J. Divinorin A, a psychotropic terpenoid, and divinorin B from the hallucinogenic Mexican mint Salvia divinorum. *J. Org. Chem.* **1984**, *49*, 4716-4720.
7. Roth, B. L.; Baner, K.; Westkaemper, R.; Siebert, D.; Rice, K. C.; Steinberg, S.; Ernsberger, P.; Rothman, R. B. Salvinorin A: a potent naturally occurring nonnitrogenous kappa opioid selective agonist. *Proc. Natl. Acad. Sci. U. S. A.* **2002**, *99*, 11934-11939.
8. McCurdy, C. R.; Sufka, K. J.; Smith, G. H.; Warnick, J. E.; Nieto, M. J. Antinociceptive profile of salvinorin A, a structurally unique kappa opioid receptor agonist. *Pharmacol. Biochem. Behav.* **2006**, *83*, 109-113.
9. McCurdy, C. R.; Scully, S. S. Analgesic substances derived from natural products (natureceuticals). *Life Sci.* **2005**, *78*, 476-484.
10. Fantegrossi, W. E.; Kugle, K. M.; Valdes, L. J., III; Koreeda, M.; Woods, J. H. Kappa-opioid receptor-mediated effects of the plant-derived hallucinogen, salvinorin A, on inverted screen performance in the mouse. *Behav. Pharmacol.* **2005**, *16*, 627-633.
11. Carlezon, W. A., Jr.; Beguin, C.; Dinieri, J. A.; Baumann, M. H.; Richards, M. R.; Todtenkopf, M. S.; Rothman, R. B.; Ma, Z.; Lee, D. Y.; Cohen, B. M.

- Depressive-like effects of the kappa-opioid receptor agonist salvinorin A on behavior and neurochemistry in rats. *J. Pharmacol. Exp. Ther.* **2006**, *316*, 440-447.
12. Eguchi, M. Recent advances in selective opioid receptor agonists and antagonists. *Med. Res. Rev.* **2004**, *24*, 182-212.
 13. Braenden, O. J.; Eddy, N. B.; Halbach, H. Synthetic substances with morphine-like effect; relationship between chemical structure and analgesic action. *Bull. World Health Organ.* **1955**, *13*, 937-998.
 14. John, T. F.; French, L. G.; Erlichman, J. S. The antinociceptive effect of salvinorin A in mice. *Eur. J. Pharmacol.* **2006**, *545*, 129-133.
 15. Beckett, A. H.; Casy, A. F. Synthetic analgesics: stereochemical considerations. *J. Pharm. Pharmacol.* **1954**, *6*, 986-1001.
 16. Pert, C. B.; Snyder, S. H. Opiate receptor: demonstration in nervous tissue. *Science* **1973**, *179*, 1011-1014.
 17. Martin, W. R.; Eades, C. G.; Thompson, J. A.; Huppler, R. E.; Gilbert, P. E. The effects of morphine- and nalorphine- like drugs in the nondependent and morphine-dependent chronic spinal dog. *J. Pharmacol. Exp. Ther.* **1976**, *197*, 517-532.
 18. Lord, J. A.; Waterfield, A. A.; Hughes, J.; Kosterlitz, H. W. Endogenous opioid peptides: multiple agonists and receptors. *Nature* **1977**, *267*, 495-499.
 19. Hughes, J.; Smith, T. W.; Kosterlitz, H. W.; Fothergill, L. A.; Morgan, B. A.; Morris, H. R. Identification of two related pentapeptides from the brain with potent opiate agonist activity. *Nature* **1975**, *258*, 577-580.
 20. Cox, B. M.; Goldstein, A.; Hi, C. H. Opioid activity of a peptide, beta-lipotropin-(61-91), derived from beta-lipotropin. *Proc. Natl. Acad. Sci. U. S. A* **1976**, *73*, 1821-1823.
 21. Goldstein, A.; Tachibana, S.; Lowney, L. I.; Hunkapiller, M.; Hood, L. Dynorphin-(1-13), an extraordinarily potent opioid peptide. *Proc. Natl. Acad. Sci. U. S. A.* **1979**, *76*, 6666-6670.
 22. Zadina, J. E.; Hackler, L.; Ge, L. J.; Kastin, A. J. A potent and selective endogenous agonist for the mu-opiate receptor. *Nature* **1997**, *386*, 499-502.

23. Mollereau, C.; Parmentier, M.; Mailleux, P.; Butour, J. L.; Moisand, C.; Chalon, P.; Caput, D.; Vassart, G.; Meunier, J. C. ORL1, a novel member of the opioid receptor family. Cloning, functional expression and localization. *FEBS Lett.* **1994**, *341*, 33-38.
24. Bunzow, J. R.; Saez, C.; Mortrud, M.; Bouvier, C.; Williams, J. T.; Low, M.; Grandy, D. K. Molecular cloning and tissue distribution of a putative member of the rat opioid receptor gene family that is not a mu, delta or kappa opioid receptor type. *FEBS Lett.* **1994**, *347*, 284-288.
25. Meunier, J. C.; Mollereau, C.; Toll, L.; Suaudeau, C.; Moisand, C.; Alvinerie, P.; Butour, J. L.; Guillemot, J. C.; Ferrara, P.; Monsarrat, B.; . Isolation and structure of the endogenous agonist of opioid receptor-like ORL1 receptor. *Nature* **1995**, *377*, 532-535.
26. Reinscheid, R. K.; Nothacker, H. P.; Bourson, A.; Ardati, A.; Henningsen, R. A.; Bunzow, J. R.; Grandy, D. K.; Langen, H.; Monsma, F. J., Jr.; Civelli, O. Orphanin FQ: a neuropeptide that activates an opioidlike G protein-coupled receptor. *Science* **1995**, *270*, 792-794.
27. Waldhoer, M.; Bartlett, S. E.; Whistler, J. L. Opioid receptors. *Annu. Rev. Biochem.* **2004**, *73*, 953-990.
28. Palczewski, K.; Kumasaka, T.; Hori, T.; Behnke, C. A.; Motoshima, H.; Fox, B. A.; Le, T., I; Teller, D. C.; Okada, T.; Stenkamp, R. E.; Yamamoto, M.; Miyano, M. Crystal structure of rhodopsin: A G protein-coupled receptor. *Science* **2000**, *289*, 739-745.
29. Henderson, R.; Baldwin, J. M.; Ceska, T. A.; Zemlin, F.; Beckmann, E.; Downing, K. H. Model for the structure of bacteriorhodopsin based on high-resolution electron cryo-microscopy. *J. Mol. Biol.* **1990**, *213*, 899-929.
30. Metzger, T. G.; Paterlini, M. G.; Portoghese, P. S.; Ferguson, D. M. An analysis of the conserved residues between halobacterial retinal proteins and G-protein coupled receptors: implications for GPCR modeling. *J. Chem. Inf. Comput. Sci.* **1996**, *36*, 857-861.
31. Pebay-Peyroula, E.; Rummel, G.; Rosenbusch, J. P.; Landau, E. M. X-ray structure of bacteriorhodopsin at 2.5 angstroms from microcrystals grown in lipidic cubic phases. *Science* **1997**, *277*, 1676-1681.
32. Schertler, G. F.; Villa, C.; Henderson, R. Projection structure of rhodopsin. *Nature* **1993**, *362*, 770-772.

33. Subramanian, G.; Paterlini, M. G.; Portoghese, P. S.; Ferguson, D. M. Molecular docking reveals a novel binding site model for fentanyl at the mu-opioid receptor. *J. Med. Chem.* **2000**, *43*, 381-391.
34. Schwwyzer, R. ACTH: a short introductory review. *Ann. N. Y. Acad. Sci.* **1977**, *297*, 3-26.
35. Schwwyzer, R.; Eberle, A. On the molecular mechanism of alpha-MSH receptor interactions. *Front. Horm. Res.* **1977**, *4*, 18-25.
36. Befort, K.; Tabbara, L.; Kling, D.; Maigret, B.; Kieffer, B. L. Role of aromatic transmembrane residues of the delta-opioid receptor in ligand recognition. *J. Biol. Chem.* **1996**, *271*, 10161-10168.
37. Tidgewell, K.; Groer, C. E.; Harding, W. W.; Lozama, A.; Schmidt, M.; Marquam, A.; Hiemstra, J.; Partilla, J. S.; Dersch, C. M.; Rothman, R. B.; Bohn, L. M.; Prisinzano, T. E. Herkinorin analogues with differential beta-arrestin-2 interactions. *J. Med. Chem.* **2008**, *51*, 2421-2431.
38. Toll, L.; Berzetei-Gurske, I. P.; Polgar, W. E.; Brandt, S. R.; Adapa, I. D.; Rodriguez, L.; Schwartz, R. W.; Haggart, D.; O'Brien, A.; White, A.; Kennedy, J. M.; Craymer, K.; Farrington, L.; Auh, J. S. Standard binding and functional assays related to medications development division testing for potential cocaine and opiate narcotic treatment medications. *NIDA Res. Monogr.* **1998**, *178*, 440-466.
39. Seki, T.; Awamura, S.; Kimura, C.; Ide, S.; Sakano, K.; Minami, M.; Nagase, H.; Satoh, M. Pharmacological properties of TRK-820 on cloned mu-, delta- and kappa-opioid receptors and nociceptin receptor. *Eur. J. Pharmacol.* **1999**, *376*, 159-167.
40. Andrews, P. R.; Craik, D. J.; Martin, J. L. Functional group contributions to drug-receptor interactions. *J. Med. Chem.* **1984**, *27*, 1648-1657.
41. Page, M. I. Entropy, binding energy, and enzymatic catalysis. *Angew. Chem. Int. Ed. Eng.* **1977**, *16*, 449-459.
42. Munro, T. A.; Rizzacasa, M. A.; Roth, B. L.; Toth, B. A.; Yan, F. Studies toward the pharmacophore of salvinorin A, a potent kappa opioid receptor agonist. *J. Med. Chem.* **2005**, *48*, 345-348.
43. Yan, F.; Roth, B. L. Unpublished data supplied by the Roth Group. 2005. Case Western Reserve University, Cleveland, OH.

44. Simpson, D. S.; Katavic, P. L.; Lozama, A.; Harding, W. W.; Parrish, D.; Deschamps, J. R.; Dersch, C. M.; Partilla, J. S.; Rothman, R. B.; Navarro, H.; Prisinzano, T. E. Synthetic studies of neoclerodane diterpenes from *Salvia divinorum*: preparation and opioid receptor activity of salvinicin analogues. *J. Med. Chem.* **2007**, *50*, 3596-3603.
45. Prisinzano, T. E. Opioid receptor ligands and methods for their preparation. [US 2006/0058264 A1], **2006**.
46. Prisinzano, T. E.; Rothman, R. B. Salvinorin A analogs as probes in opioid pharmacology. *Chem. Rev.* **2008**, *108*, 1732-1743.
47. Beguin, C.; Carlezon, W. A., Jr.; Cohen, B.; He, M.; Lee, D. Y.; Richards, M. R. Salvinorin derivatives and uses thereof. [WO 2005/089745 A1], **2005**.
48. Beguin, C.; Richards, M. R.; Li, J. G.; Wang, Y.; Xu, W.; Liu-Chen, L. Y.; Carlezon, W. A., Jr.; Cohen, B. M. Synthesis and in vitro evaluation of salvinorin A analogues: effect of configuration at C(2) and substitution at C(18). *Bioorg. Med. Chem. Lett.* **2006**, *16*, 4679-4685.
49. Munro, T. A.; Duncan, K. K.; Staples, R. J.; Xu, W.; Liu-Chen, L. Y.; Beguin, C.; Carlezon, W. A., Jr.; Cohen, B. M. 8-epi-Salvinorin B: crystal structure and affinity at the kappa opioid receptor. *Beilstein. J. Org. Chem.* **2007**, *3*, 1.
50. Mori, K.; Tominaga, M.; Takigawa, T.; Matsui, M. A mild transesterification method. *Synthesis* **1973**, 790-791.
51. Ranu, B. C.; Dutta, P.; Sarkar, A. A simple and efficient procedure for transesterification catalyzed by indium triiodide. *J. Org. Chem.* **1998**, *63*, 6027-6028.
52. Tanyeli, C.; Turkut, E.; Akhmedov, I. M. Chemoenzymatic synthesis of α' - and α -acetoxylated cyclic ketones. *Tetrahedron: Asymmetry* **2004**, *15*, 1729-1733.
53. Lee, J. C.; Jin, Y. S.; Choi, J.-H. Synthesis of α -acetoxy and formyloxy ketones by thallium (III) promoted α -oxidation. *Chem. Commun.* **2001**, 956-957.
54. Fleischmann, K.; Scheunemann, K. H.; Schorlemmer, H. U.; Dickneite, G.; Blumbach, J.; Fischer, G. Immunomodulation by the new synthetic thiazole derivative tiprotimod. *Arzneim. -Forsch/Drug Res.* **1989**, *39*, 743-746.

55. Lauktien, G.; Volk, F. J.; Frahm, A. W. Diastereo- and enantioselective synthesis of *cis*-2-hydroxycyclohexanamine and corresponding ethers by asymmetric reductive amination. *Tetrahedron: Asymmetry* **1997**, *8*, 3457-3466.
56. House, H. O.; Czuba, L. J.; Gall, M.; Olmstead, H. D. The chemistry of carbanions. XVIII. Preparation of trimethylsilyl enol ethers. *J. Org. Chem.* **1969**, *34*, 2324-2336.
57. Yamamoto, Y.; Matui, C. Preparation of silyl enol ethers by the reaction of ketones with silylamines and methyl iodide. *Organometallics* **1997**, *16*, 2204-2206.
58. Rubottom, G. M.; Gruber, J. M. *m*-Chloroperbenzoic acid oxidation of 2-trimethylsilyloxy-1,3-dienes. Synthesis of α -hydroxy and α -acetoxy enones. *J. Org. Chem.* **1978**, *43*, 1599-1602.
59. Chenna, R.; Sugawara, H.; Koike, T.; Lopez, R.; Gibson, T. J.; Higgins, D. G.; Thompson, J. D. Multiple sequence alignment with the Clustal series of programs. *Nucleic Acids Res.* **2003**, *31*, 3497-3500.
60. Thompson, J. D.; Gibson, T. J.; Plewniak, F.; Jeanmougin, F.; Higgins, D. G. The CLUSTAL_X windows interface: flexible strategies for multiple sequence alignment aided by quality analysis tools. *Nucleic Acids Res.* **1997**, *25*, 4876-4882.
61. Henikoff, S.; Henikoff, J. G. Amino acid substitution matrices from protein blocks. *Proc. Natl. Acad. Sci. U. S. A.* **1992**, *89*, 10915-10919.
62. Bissantz, C.; Bernard, P.; Hibert, M.; Rognan, D. Protein-based virtual screening of chemical databases. II. Are homology models of G-Protein Coupled Receptors suitable targets? *Proteins* **2003**, *50*, 5-25.
63. Canutescu, A. A.; Shelenkov, A. A.; Dunbrack, R. L., Jr. A graph-theory algorithm for rapid protein side-chain prediction. *Protein Sci.* **2003**, *12*, 2001-2014.
64. Xu, W.; Sanz, A.; Pardo, L.; Liu-Chen, L. Y. Activation of the mu opioid receptor involves conformational rearrangements of multiple transmembrane domains. *Biochemistry* **2008**, *47*, 10576-10586.
65. Xu, W.; Campillo, M.; Pardo, L.; Kim de, R. J.; Liu-Chen, L. Y. The seventh transmembrane domains of the delta and kappa opioid receptors have different accessibility patterns and interhelical interactions. *Biochemistry* **2005**, *44*, 16014-16025.

66. Xu, W.; Li, J.; Chen, C.; Huang, P.; Weinstein, H.; Javitch, J. A.; Shi, L.; de Riel, J. K.; Liu-Chen, L. Y. Comparison of the amino acid residues in the sixth transmembrane domains accessible in the binding-site crevices of mu, delta, and kappa opioid receptors. *Biochemistry* **2001**, *40*, 8018-8029.
67. Xu, W.; Chen, C.; Huang, P.; Li, J.; de Riel, J. K.; Javitch, J. A.; Liu-Chen, L. Y. The conserved cysteine 7.38 residue is differentially accessible in the binding-site crevices of the mu, delta, and kappa opioid receptors. *Biochemistry* **2000**, *39*, 13904-13915.
68. Vortherms, T. A.; Mosier, P. D.; Westkaemper, R. B.; Roth, B. L. Differential helical orientations among related G protein-coupled receptors provide a novel mechanism for selectivity. Studies with salvinorin A and the kappa-opioid receptor. *J. Biol. Chem.* **2007**, *282*, 3146-3156.
69. Individual amino acid residues of the receptor are identified by the traditional residue identifier indicating the residue's position in the primary amino acid sequence, followed by the general Ballesteros-Weinstein GPCR residue identifier as a superscript. See Ballesteros, J. A.; Weinstein, H. *Methods Neurosci.* 1995, *25*, 366-428 and Xhaard, H. et al. *J. Struct. Biol.*, **2006**, *150*, 126-143.
70. Okada, T.; Sugihara, M.; Bondar, A. N.; Elstner, M.; Entel, P.; Buss, V. The retinal conformation and its environment in rhodopsin in light of a new 2.2 Å crystal structure. *J. Mol. Biol.* **2004**, *342*, 571-583.
71. Salom, D.; Lodowski, D. T.; Stenkamp, R. E.; Le, T., I; Golczak, M.; Jastrzebska, B.; Harris, T.; Ballesteros, J. A.; Palczewski, K. Crystal structure of a photoactivated deprotonated intermediate of rhodopsin. *Proc. Natl. Acad. Sci. U. S. A* **2006**, *103*, 16123-16128.
72. Yan, F.; Mosier, P. D.; Westkaemper, R. B.; Roth, B. L. Galpha-subunits differentially alter the conformation and agonist affinity of kappa-opioid receptors. *Biochemistry* **2008**, *47*, 1567-1578.
73. Yan, F.; Mosier, P. D.; Westkaemper, R. B.; Stewart, J.; Zjawiony, J. K.; Vortherms, T. A.; Sheffler, D. J.; Roth, B. L. Identification of the molecular mechanisms by which the diterpenoid salvinorin A binds to kappa-opioid receptors. *Biochemistry* **2005**, *44*, 8643-8651.
74. Personal communication with Philip D. Mosier, Ph.D., Virginia Commonwealth University, Richmond, VA. 2009.
75. Cherezov, V.; Rosenbaum, D. M.; Hanson, M. A.; Rasmussen, S. G.; Thian, F. S.; Kobilka, T. S.; Choi, H. J.; Kuhn, P.; Weis, W. I.; Kobilka, B. K.; Stevens,

- R. C. High-resolution crystal structure of an engineered human beta2-adrenergic G protein-coupled receptor. *Science* **2007**, *318*, 1258-1265.
76. Zhang, L.; DeHaven, R. N.; Goodman, M. NMR and modeling studies of a synthetic extracellular loop II of the kappa opioid receptor in a DPC micelle. *Biochemistry* **2002**, *41*, 61-68.
77. Shi, L.; Liapakis, G.; Xu, R.; Guarnieri, F.; Ballesteros, J. A.; Javitch, J. A. Beta2 adrenergic receptor activation. Modulation of the proline kink in transmembrane 6 by a rotamer toggle switch. *J. Biol. Chem.* **2002**, *277*, 40989-40996.
78. Laskowski, R. A.; MacArthur, M. W.; Moss, D. S.; Thornton, J. M. PROCHECK: a program to check the stereochemical quality of protein structures. *J. Appl. Cryst.* **1993**, *26*, 283-291.
79. Marti-Renom, M. A.; Stuart, A. C.; Fiser, A.; Sanchez, R.; Melo, F.; Sali, A. Comparative protein structure modeling of genes and genomes. *Annu. Rev. Biophys. Biomol. Struct.* **2000**, *29*, 291-325.
80. Sali, A.; Blundell, T. L. Comparative protein modelling by satisfaction of spatial restraints. *J. Mol. Biol.* **1993**, *234*, 779-815.
81. Jones, G.; Willett, P.; Glen, R. C.; Leach, A. R.; Taylor, R. Development and validation of a genetic algorithm for flexible docking. *J. Mol. Biol.* **1997**, *267*, 727-748.
82. Raynor, K.; Kong, H.; Law, S.; Heerding, J.; Tallent, M.; Livingston, F.; Hines, J.; Reisine, T. Molecular biology of opioid receptors. *NIDA Res. Monogr.* **1996**, *161*, 83-103.
83. Raynor, K.; Kong, H.; Chen, Y.; Yasuda, K.; Yu, L.; Bell, G. I.; Reisine, T. Pharmacological characterization of the cloned kappa-, delta-, and mu-opioid receptors. *Mol. Pharmacol.* **1994**, *45*, 330-334.
84. Palmer, R. B.; Uthagrove, A. L.; Nelson, W. L. (E)- and (Z)-7-arylidenealtrexones: synthesis and opioid receptor radioligand displacement assays. *J. Med. Chem.* **1997**, *40*, 749-753.
85. Jones, R. M.; Portoghese, P. S. 5'-Guanidinonaltrindole, a highly selective and potent kappa-opioid receptor antagonist. *Eur. J. Pharmacol.* **2000**, *396*, 49-52.
86. Li, G.; Aschenbach, L. C.; He, H.; Selley, D. E.; Zhang, Y. 14-O-Heterocyclic-substituted naltrexone derivatives as non-peptide mu opioid receptor

selective antagonists: Design, synthesis, and biological studies. *Bioorg. Med. Chem. Lett.* **2008**.

87. Cramer III, R. D.; Patterson, D. E.; Bunce, J. D. Comparative molecular field analysis (CoMFA). 1. Effect of shape on binding of steroids to carrier proteins. *J. Am. Chem. Soc.* **1988**, *110*, 5959-5967.
88. Hjorth, S. A.; Thirstrup, K.; Schwartz, T. W. Radioligand-dependent discrepancy in agonist affinities enhanced by mutations in the kappa-opioid receptor. *Mol. Pharmacol.* **1996**, *50*, 977-984.
89. Rosenkilde, M. M.; Cahir, M.; Gether, U.; Hjorth, S. A.; Schwartz, T. W. Mutation along transmembrane segment II of the NK-1 receptor affect substance P competition with non-peptide antagonists but not substance P binding. *J. Biol. Chem.* **1994**, *269*, 28160-28164.
90. Law, P. Y.; McGinn, T. M.; Wick, M. J.; Erikson, L. J.; Evans, C.; Loh, H. H. Analysis of delta-opioid receptor activities stably expressed in CHO cell lines: function of receptor density? *J. Pharmacol. Exp. Ther.* **1994**, *271*, 1686-1694.
91. Yan, F.; Roth, B. L. Salvinorin A: a novel and highly selective kappa-opioid receptor agonist. *Life Sci.* **2004**, *75*, 2615-2619.
92. Chavkin, C.; Sud, S.; Jin, W.; Stewart, J.; Zjawiony, J. K.; Siebert, D. J.; Toth, B. A.; Hufeisen, S. J.; Roth, B. L. Salvinorin A, an active component of the hallucinogenic sage *salvia divinorum* is a highly efficacious kappa-opioid receptor agonist: structural and functional considerations. *J. Pharmacol. Exp. Ther.* **2004**, *308*, 1197-1203.
93. Harding, W. W.; Tidgewell, K.; Byrd, N.; Cobb, H.; Dersch, C. M.; Butelman, E. R.; Rothman, R. B.; Prisinzano, T. E. Neoclerodane diterpenes as a novel scaffold for mu opioid receptor ligands. *J. Med. Chem.* **2005**, *48*, 4765-4771.
94. Lee, D. Y.; Karnati, V. V.; He, M.; Liu-Chen, L. Y.; Kondaveti, L.; Ma, Z.; Wang, Y.; Chen, Y.; Beguin, C.; Carlezon, W. A., Jr.; Cohen, B. Synthesis and in vitro pharmacological studies of new C(2) modified salvinorin A analogues. *Bioorg. Med. Chem. Lett.* **2005**, *15*, 3744-3747.
95. Beguin, C.; Richards, M. R.; Wang, Y.; Chen, Y.; Liu-Chen, L. Y.; Ma, Z.; Lee, D. Y.; Carlezon, W. A., Jr.; Cohen, B. M. Synthesis and in vitro pharmacological evaluation of salvinorin A analogues modified at C(2). *Bioorg. Med. Chem. Lett.* **2005**, *15*, 2761-2765.

96. Lee, D. Y.; He, M.; Kondaveti, L.; Liu-Chen, L. Y.; Ma, Z.; Wang, Y.; Chen, Y.; Li, J. G.; Beguin, C.; Carlezon, W. A., Jr.; Cohen, B. Synthesis and in vitro pharmacological studies of C(4) modified salvinorin A analogues. *Bioorg. Med. Chem. Lett.* **2005**, *15*, 4169-4173.
97. Harding, W. W.; Schmidt, M.; Tidgewell, K.; Kannan, P.; Holden, K. G.; Dersch, C. M.; Rothman, R. B.; Prisinzano, T. E. Synthetic studies of neoclerodane diterpenes from *Salvia divinorum*: selective modification of the furan ring. *Bioorg. Med. Chem. Lett.* **2006**, *16*, 3170-3174.
98. Tidgewell, K.; Harding, W. W.; Lozama, A.; Cobb, H.; Shah, K.; Kannan, P.; Dersch, C. M.; Parrish, D.; Deschamps, J. R.; Rothman, R. B.; Prisinzano, T. E. Synthesis of salvinorin A analogues as opioid receptor probes. *J. Nat. Prod.* **2006**, *69*, 914-918.
99. Stewart, D. J.; Fahmy, H.; Roth, B. L.; Yan, F.; Zjawiony, J. K. Bioisosteric modification of salvinorin A, a potent and selective kappa-opioid receptor agonist. *Arzneimittelforschung.* **2006**, *56*, 269-275.
100. Zjawiony, J. K.; Fahmy, H.; Stewart, D. J.; Roth, B. L. Agents with selective kappa-opioid receptor affinity. [WO 2006/012643 A2], **2006**.
101. Munro, T. A.; Goetchius, G. W.; Roth, B. L.; Vortherms, T. A.; Rizzacasa, M. A. Autoxidation of salvinorin A under basic conditions. *J. Org. Chem.* **2005**, *70*, 10057-10061.
102. Harding, W. W.; Tidgewell, K.; Schmidt, M.; Shah, K.; Dersch, C. M.; Snyder, J.; Parrish, D.; Deschamps, J. R.; Rothman, R. B.; Prisinzano, T. E. Salvinicins A and B, new neoclerodane diterpenes from *Salvia divinorum*. *Org. Lett.* **2005**, *7*, 3017-3020.
103. Harding, W. W.; Schmidt, M.; Tidgewell, K.; Kannan, P.; Holden, K. G.; Gilmour, B.; Navarro, H.; Rothman, R. B.; Prisinzano, T. E. Synthetic studies of neoclerodane diterpenes from *Salvia divinorum*: semisynthesis of salvinicins A and B and other chemical transformations of salvinorin A. *J. Nat. Prod.* **2006**, *69*, 107-112.
104. Lee, D. Y.; Ma, Z.; Liu-Chen, L. Y.; Wang, Y.; Chen, Y.; Carlezon, W. A., Jr.; Cohen, B. New neoclerodane diterpenoids isolated from the leaves of *Salvia divinorum* and their binding affinities for human kappa opioid receptors. *Bioorg. Med. Chem.* **2005**, *13*, 5635-5639.
105. Bikbulatov, R. V.; Yan, F.; Roth, B. L.; Zjawiony, J. K. Convenient synthesis and in vitro pharmacological activity of 2-thioanalogs of salvinorins A and B. *Bioorg. Med. Chem. Lett.* **2007**, *17*, 2229-2232.

106. Lee, D. Y.; He, M.; Liu-Chen, L. Y.; Wang, Y.; Li, J. G.; Xu, W.; Ma, Z.; Carlezon, W. A., Jr.; Cohen, B. Synthesis and in vitro pharmacological studies of new C(4)-modified salvinorin A analogues. *Bioorg. Med. Chem. Lett.* **2006**, *16*, 5498-5502.
107. Beguin, C.; Carlezon, W. A., Jr.; Cohen, B.; He, M.; Lee, D. Y.; Richards, M. R.; Liu-Chen, L. Y. Salvinorin derivatives and uses thereof. [US 2007/0213394 A1], **2007**.
108. Munro, T. A.; Duncan, K. K.; Xu, W.; Wang, Y.; Liu-Chen, L. Y.; Carlezon, W. A., Jr.; Cohen, B. M.; Beguin, C. Standard protecting groups create potent and selective kappa opioids: salvinorin B alkoxymethyl ethers. *Bioorg. Med. Chem.* **2008**, *16*, 1279-1286.
109. Lemmen, C.; Lengauer, T.; Klebe, G. FlexS: a method for fast flexible ligand superposition. *J. Med. Chem.* **1998**, *41*, 4502-4520.
110. Jain, A. N. Morphological similarity: a 3D molecular similarity method correlated with protein-ligand recognition. *J. Comput. Aided Mol. Des* **2000**, *14*, 199-213.
111. Cho, S. J.; Tropsha, A. Cross-validated R²-guided region selection for comparative molecular field analysis: a simple method to achieve consistent results. *J. Med. Chem.* **1995**, *38*, 1060-1066.
112. Kane, B. E.; Nieto, M. J.; McCurdy, C. R.; Ferguson, D. M. A unique binding epitope for salvinorin A, a non-nitrogenous kappa opioid receptor agonist. *FEBS J.* **2006**, *273*, 1966-1974.
113. Kane, B. E.; McCurdy, C. R.; Ferguson, D. M. Toward a structure-based model of salvinorin A recognition of the kappa-opioid receptor. *J. Med. Chem.* **2008**, *51*, 1824-1830.
114. Singh, N.; Cheve, G.; Ferguson, D. M.; McCurdy, C. R. A combined ligand-based and target-based drug design approach for G-protein coupled receptors: application to salvinorin A, a selective kappa opioid receptor agonist. *J. Comput. Aided Mol. Des.* **2006**, *20*, 471-493.
115. Individual amino acid residues of the receptor are identified by the traditional residue identifier indicating the residue's position in the primary amino acid sequence, followed by the general Ballesteros-Weinstein GPCR residue identifier as a superscript. See Ballesteros, J. A.; Weinstein, H. *Methods Neurosci.* **1995**, *25*, 366-428.

116. Clark, R. D. A ligand's-eye view of protein binding. *J. Comput. Aided Mol. Des* **2008**, 22, 507-521.

VITA

Donna L. McGovern was born March 17, 1952 in Escanaba, Michigan and is an American citizen. She graduated from Escanaba Area High School in 1970, Bay de Noc Community College with an Associate of Arts in 1972, Northern Michigan University with a Bachelor of Science in Chemistry in 1976 and Old Dominion University with a Master of Science in Organic Chemistry in 1978. She was employed as a Forensic Drug Chemist for the Commonwealth of Virginia 1979 – 1983 and as an Environmental Chemist for the Federal Government 1984 – 1991.